

Peter Söllner, B.Eng.

Determination of the *in situ* Block Size Distribution as a Parameter for the Rock Mass Characterization based on Measurements and Statistical Methods

MASTER THESIS

For the award of the academic degree

Diplom-Ingenieur

Master programme Geotechnics and Hydraulics

submitted to the
Graz University of Technology

Advisors:

O.Univ.-Prof. Dipl.-Ing. Dr.mont. Wulf Schubert

Institute for Rock Mechanics and Tunnelling
Graz University of Technology

Dipl.-Ing. Dr.techn. Markus Pötsch

3GSM GmbH
Graz, Austria

Dipl.-Ing. Alexander Kluckner

Institute for Rock Mechanics and Tunnelling
Graz University of Technology

Graz, August 2014

Statuary Declaration

I declare that I have authored this thesis independently, that I have not used other than the declared sources / resources, and that I have explicitly marked all material which has been quoted either literally or by content from the used sources. The text document uploaded to TUGRAZonline is identical to the present master thesis.

Graz, August 2014

Peter Söllner

Acknowledgements

At first, I would like to thank Professor Wulf Schubert who has seriously sparked my interest in rock mechanics and tunneling. His lectures delivered me expert insight into this issue and moreover, he sensitized me to critically question rock mechanical problems. He also enabled me to compose this thesis at the Institute for Rock Mechanics and Tunnelling.

I am deeply grateful to my advisors Alexander Kluckner and Markus Pötsch. They strongly supported me in this complex issue and always stood by my side in all matters. With their extensive and constructive discussions they made it feasible for me to develop my master thesis. Furthermore, I gained a close friendship with them. I hope our common interest can be pursued further and we will not allow ourselves to drift out of contact.

I sincerely thank my girlfriend Manuela Reischl who suffered strenuous times by establishing my thesis. She gave me crucial mental support and always reassured and motivated me in hard times. She even gave me the idea to complete my master studies at the Graz University of Technology.

At last, I will thank my parents Brunhilde and Dieter from the bottom of my heart. Without their strong trust in my studies and their essential financial help I would not have been able to fulfill my dreams of getting a civil engineer.

Abstract

The *in situ* block size is a key parameter for the geomechanical characterization of a rock mass describing its fracturing. It is directly related to the rock mass strength. The *in situ* block size is applied in several classification systems. For instance, the block volume and the joint condition factor have to be known for determining the Geological Strength Index (GSI). Moreover, the *in situ* block size is also an important factor in the field of blasting. It is required for choosing a blasting design for obtaining a desired post-blast particle size distribution.

The *in situ* block size is difficult to gather because the insight into a rock mass is not possible. Especially, in the design stage, a rock face is only exposed in a particular orientation, and thus, essential information related to other orientations is often not accessible. Due to the limited available information about the internals of a rock mass it is not possible to determine the *in situ* block size directly. Currently, the *in situ* block size is determined by calculations using oversimplified models, vague estimations or, due to the lack of relevant information, it is even not performed.

As remote measurement systems have become available for rock mass characterization, a more advanced application was provided recording the discontinuity properties on a sophisticated level. Measurements can be performed on outcrops as well as on tunnel faces and walls delivering the orientation, spacing and persistence of discontinuities. This thesis aims at examining the relationship between visible and measureable information at the rock surface and the *in situ* block size.

Three-dimensional rock mass model simulations with discontinuity systems were performed using the block model engine of the distinct element code 3DEC. The simulations were used to investigate the relationships between visible, two-dimensional information at the surface and the obstructed, three-dimensional block size distribution of the rock mass. For all investigations the joint set parameters, such as the spacing, the orientation and the persistence have been varied, in order to account for the natural variability of jointed rock masses.

Initially, a ratio for the minimally required size of the outcrop depending on the mean block area was established. Having a specific mean block area, the size of the outcrop has to be large enough in order to obtain reliable block area distributions.

Furthermore, the transformation factor T was introduced, describing the correlation between block volumes generated by persistent and corresponding non-persistent joint sets. Based on the approach by Cai *et al.* (2004), the equation for calculating the block

volume was further developed by replacing the term of persistence by the transformation factor T. Hence, quantitative estimations about the *in situ* block sizes, valid for three joint sets, are feasible leading to a more advanced characterization of rock mass. The investigations conclude with a comparison between the results of simulations with 3DEC, the calculated block volumes according to Cai *et al.* and the results achieved from the improved formulas including the transformation factor T. For all analyzed examples, the mean values and selected quantiles of the block size distributions using the transformation factor show a good agreement with the simulation results. It gives a comprehensive picture about the block size distribution in jointed rock masses with three non-persistent joint sets. Finally, the application of the method is illustrated on a tunnel face using 3D imaging technology.

Kurzfassung

In der geomechanischen Gebirgscharakterisierung stellt die Blockgröße einen Schlüsselparameter dar, mit dem die Zerlegung eines Gebirges beschrieben werden kann. Dieser Parameter wird in verschiedenen Gebirgsklassifizierungen angewendet, wie zum Beispiel, zur Ermittlung des *Geological Strength Index* (GSI). Dabei dienen das Blockvolumen und der *joint condition factor* als Eingangsparameter. Auch in der Sprengtechnik ist die Blockgröße ein entscheidender Faktor, um unter Berücksichtigung einer gewünschten Blockgrößenverteilung, eine effizientere Sprengplanung zu entwickeln. Die Blockgrößenverteilung im Gebirge kann allerdings messtechnisch nicht bestimmt werden. Aus diesem Grund wird sie häufig mit stark vereinfachten Methoden berechnet, grob abgeschätzt oder aufgrund fehlender Informationen erst gar nicht berücksichtigt. Vor allem in der Planungsphase eines Projektes, in welcher detaillierte Informationen noch nicht zur Verfügung stehen, kann die Blockgröße meist nur über die Auswertung von Felsaufschlüssen abgeschätzt werden.

Seit Fernerkundungssysteme für die Gebirgscharakterisierung erhältlich sind, ist es möglich, Eigenschaften von Trennflächen messtechnisch zu erfassen. Die Messungen können dabei sowohl an Aufschlüssen als auch an der Ortsbrust und der Tunnellaibung erfolgen. Diese Methode ermöglicht es, die Orientierungen, die Abstände und die Durchtrennungen von Trennflächenscharen relativ schnell und gefahrlos zu bestimmen.

Das Ziel dieser Masterarbeit ist es, den Zusammenhang zwischen sichtbaren und messbaren Informationen an Felsaufschlüssen und der Blockgrößenverteilung im Gebirge zu untersuchen. Dazu wurden mit dem Programm 3DEC dreidimensionale Gebirgsmodelle mit Kluftsystemen erzeugt und anschließend die Blockflächen am Aufschluss und die Blockgrößenverteilung des gesamten Modells ausgewertet. Die natürliche Variabilität der Klufteigenschaften wurde durch Variation der Modell- und Trennflächenparameter berücksichtigt.

Zunächst wurde die mittlere Blockfläche am Aufschluss mit der Größe der Aufschlussfläche ins Verhältnis gesetzt. Dabei konnte ein Grenzverhältnis identifiziert werden, unterhalb dessen die Aufschlussfläche groß genug ist, um zuverlässige Rückschlüsse auf die flächige Blockgrößenverteilung ziehen zu können.

Ferner wurde der Transformationsfaktor T eingeführt, welcher das Verhältnis zwischen den Blockvolumen mit vollständig durchtrennten und dazugehörigen nicht vollständig durchtrennten Trennflächenscharen beschreibt. Auf Grundlage des Ansatzes nach Cai *et al.* (2004), wurde die Formel zur Berechnung des Blockvolumens weiter entwickelt. Dazu

wurde der Term, der die Durchtrennung beschreibt, durch den Transformationsfaktor T ersetzt. Da damit mehrere Parameter als zuvor in die Rechnung mit einfließen, lassen sich zuverlässigere Aussagen über die Blockvolumen treffen.

Eine Bewertung der gewonnenen Ergebnisse erfolgte anhand weiterer Simulationen, bei denen die Ergebnisse aus 3DEC mit jenen nach Cai *et al.* und denen auf Basis der in dieser Arbeit vorgestellten Herangehensweise verglichen wurden. Es zeigte sich eine gute Übereinstimmung der berechneten Mittelwerte und Quantile der Blockvolumen nach der vorgestellten Methode mit den Ergebnissen aus den Simulationen. Auf diese Weise erhält man ein umfassenderes Bild über die Blockgrößenverteilung in Gebirgsabschnitten mit drei nicht vollständig durchtrennten Trennflächenscharen. Abgerundet wird die Arbeit mit der Bestimmung der charakteristischen Blockgrößen am Beispiel einer Ortsbrust, die durch eine 3D- Bildmesstechnik aufgenommen wurde.

Contents

1	Introduction	1
1.1	Research issue	1
1.2	Scope of work	3
1.2.1	Development of a numerical block model	3
1.2.2	Statistical analysis	4
1.3	Objectives	4
2	State of the art	5
2.1	Importance of block size in rock mechanics	5
2.2	Determination of block size	8
2.2.1	Measurement of joint set parameters	8
2.2.2	Estimation of block size	8
3	Preliminary work	11
3.1	Model composition in 3DEC	11
3.1.1	General information	11
3.1.2	Consideration of boundary blocks	12
3.1.3	Validation of the block model.....	13
3.1.4	Replication of calculation cases.....	14
3.2	Influence of 3DEC specific input of non-persistent joint sets on block size distributions	23
3.2.1	Influence of the input sequence of joint sets	23
3.2.2	Influence of selected origins of joint sets	27
4	Investigations	30
4.1	Minimally required outcrop area for determination of block sizes.....	30
4.2	Development of a calculation tool for mean block size estimation	40
4.3	Evaluation of analytic block size calculation	43
4.3.1	Evaluation of joint sets with different spacings.....	44
4.3.2	Evaluation of joint sets with different persistences.....	47
4.3.3	Evaluation of non-orthogonal joint sets.....	49
4.4	Determination of block size distribution from ShapeMetriX3D measurements	54
5	Conclusions	58

References	59
Appendix A	61

List of Figures

Figure 1.1: Illustrative example of a 3DEC rock mass model with three joint sets	3
Figure 2.1: Profiles of tunnel sections: tunnel supported with rock bolts only (left illustration) and a tunnel additionally supported with shotcrete (right illustration) (taken from (Palmström, 2001)).....	5
Figure 2.2: Quantification of Geological Strength Index (GSI chart from Cai <i>et al.</i> (2004)).	7
Figure 2.3: Convention of spacing and angles of respective joint sets (from Kim <i>et al.</i> (2007)).	9
Figure 3.1: Illustration of the general 3DEC model.....	12
Figure 3.2: Illustration of areal boundary blocks.....	12
Figure 3.3: 3DEC plot of the validation case.....	13
Figure 3.4: Examples of cumulative block volume size distributions – left: illustration with varying joint orientation and spacing; right: illustration with deterministic joint orientation and spacing.....	15
Figure 3.5: Results of replication test 1 (for model parameters see Table 3.3).	16
Figure 3.6: Results of replication test 2 (for model parameters see Table 3.3).	17
Figure 3.7: Results of replication test 3 (for model parameters see Table 3.3).	18
Figure 3.8: Results of replication test 4 (for model parameters see Table 3.3).	19
Figure 3.9: Assembly of replication test 1: the averaged mean block areas and the according standard deviations in dependence of the replication factor.....	20
Figure 3.10: Assembly of replication test 2: the averaged mean block areas and the according standard deviations in dependence of the replication factor.....	21
Figure 3.11: Assembly of replication test 3: the averaged mean block areas and the according standard deviations in dependence of the replication factor.....	21
Figure 3.12: Assembly of replication test 4: the averaged mean block areas and the according standard deviations in dependence of the replication factor.....	22
Figure 3.13: Input sequence – Results of the performed calculations, case 1 - 3.....	24
Figure 3.14: Input sequence – Results of the performed calculations, case 4 - 6.....	25

Figure 3.15: Input sequence – Assembly of the averaged mean block areas in dependence of the case number.....	26
Figure 3.16: Input sequence – Assembly of the averaged mean block volumes in dependence of the case number.....	26
Figure 3.17: Origin coordinates for simulations with origin variation.....	27
Figure 3.18: Joint set origin – Assembly of averaged mean block sizes in dependence of the case number.....	28
Figure 3.19: Cumulative block size distributions of origin testing.....	29
Figure 4.1: Sketch of a rock mass with two different outcrop areas.....	30
Figure 4.2: Illustration of the systematic minimization of the outcrop area.....	32
Figure 4.3: Cumulative block area distributions of test 7	33
Figure 4.4: Compilation of the maximal ratio $A_{\text{mean}}/A_{\text{out}}$	35
Figure 4.5: Examples of an outcrop at a limitation ratio of 0.25 (left illustration) and 1.00 (right illustration).	36
Figure 4.6: Outcrop area versus averaged mean area (test 14).	37
Figure 4.7: Quantiles versus A_{quantile} (test 14).	38
Figure 4.8: Evaluation diagram for minimally required outcrop area.....	39
Figure 4.9: Correlation between persistence factor and transformation factor – Fitted curves for mean values (blue), 25%- (orange), 50%- (red) and 75%-quantiles (green). ...	42
Figure 4.10: Cumulative block size distributions of evaluation test 1.....	45
Figure 4.11: Cumulative block size distributions of evaluation test 2.....	46
Figure 4.13: Cumulative block size distributions of evaluation test 3.....	47
Figure 4.14: Cumulative block size distributions of evaluation test 4.....	48
Figure 4.16: Cumulative block size distributions of evaluation test 5.....	50
Figure 4.17: Cumulative block size distributions of evaluation test 6.....	51
Figure 4.18: Cumulative block size distributions of evaluation test 7.....	52
Figure 4.19: Comparison of simulated and calculated block volumes of evaluation tests.	53
Figure 4.20: Illustration of analyzed joint sets of the investigated tunnel face (3D image provided by 3GSM GmbH (2014)).....	54

Figure 4.21: Lambert projection of investigated joint sets..... 55

Figure 4.22: Estimation of a potential GSI range (chart modified from Cai *et al.* (2004)). . 57

List of Tables

Table 1.1: Characteristic parameters of intact rock and discontinuities (modified from Giafferi <i>et al.</i> (2003)).....	2
Table 2.1: General categories of ground behaviors (taken from OEGG (2010)).....	6
Table 3.1: Model parameters for validation case.....	13
Table 3.2: Example results of the model validation case.....	13
Table 3.3: Model parameters for replication test	14
Table 3.4: Test runs with corresponding replications.....	14
Table 3.5: Model parameter for sequence testing.	23
Table 3.6: Sequences of joint sets.	23
Table 3.7: Model parameters for simulations with origin variation.	27
Table 3.8: Origin coordinates for simulations with origin variation.	28
Table 4.1: Concept of an evaluation scheme for block size determination.	31
Table 4.2: Considered rotation cases for the investigation of the minimally required outcrop area.	31
Table 4.3: Block area results of test 7.	34
Table 4.4: Block area results of test 14.	37
Table 4.5: Block volume results of test 14.	40
Table 4.6: Joint set parameters for evaluation test 1.....	44
Table 4.7: Comparison of simulated and calculated results of evaluation test 1.....	45
Table 4.8: Joint set parameters for evaluation test 2.....	46
Table 4.9: Comparison of simulated and calculated results of evaluation test 2	46
Table 4.12: Joint set parameters for evaluation test 3.....	47
Table 4.13: Comparison of simulated and calculated results of evaluation test 3.....	48
Table 4.14: Joint set parameters for evaluation test 4.....	48
Table 4.15: Comparison of simulated and calculated results of evaluation test 4	49

Table 4.18: Joint set parameters for evaluation test 5	49
Table 4.19: Comparison of simulated and calculated results of evaluation test 5	50
Table 4.20: Joint set parameters for evaluation test 6	51
Table 4.21: Comparison of simulated and calculated results of evaluation test 6	51
Table 4.22: Joint set parameters for evaluation test 7	52
Table 4.23: Comparison of simulated and calculated results of evaluation test 7	52
Table 4.24: Investigated mean orientations of the joint sets	54
Table 4.25: Normal joint set spacing of the investigated joints sets	55
Table 4.26: Proposed persistence factors of investigated joint sets	56
Table 4.27: Angles between investigated joint sets	56
Table 4.28: Calculated block volumes	56
Table 5.1: Test parameters for minimally required outcrop area	61
Table 5.2: Results of minimally required outcrop testing	63

List of Abbreviations

- bbBoundary blocks
BTBehavior Type
F-testFisher-test
FDForm of diagrams
GSIGeological Strength Index
ID indexInterval between Discontinuities Index
jset_iJoint set
NBCNatural Breakage Behavior
OEGGAustrian Society for Geomechanics
Q-systemRock Mass Quality System
RAMRandom Access Memory
RMRRock Mass Rating
RQDRock Quality Designation
RVERepresentative Volume Element
3DEC3-Dimensional Distinct Element Code
UDECUniversal Distinct Element Code

Symbols

$A_{b,i}$	Block area / areal block size [m^2]
A_{out}	Outcrop area [m^2]
$A_{b,mean}$	Average of all mean block areas [m^2]
dd	Dip direction in 3DEC
dip	Dip angle in 3DEC
γ_i	Average angle between two joint sets [°]
J_n	Factor for the number of joints [-]
J_c	Joint Condition Factor [-]
$minA_{b,mean}$	Minimum feasible mean block area [m^2]
$maxA_{b,mean}$	Maximum feasible mean block area [m^2]
num	Number of joints within a joint set in 3DEC
or	Joint set origin in 3DEC
p	Persistence in 3DEC
r	Replication factor
S_i	Average spacing of a joint set [m]
S	Average joint set spacing
sp	Average joint set spacing in 3DEC
σ	Standard deviation of block volumes/ block areas [m^3/ m^2]
$T_{25\%}$	Transformation factor for calculating the mean 25%-quantiles volume [-]
$T_{50\%}$	Transformation factor for calculating the mean 50%-quantiles volume [-]
$T_{75\%}$	Transformation factor for calculating the mean 75%-quantiles volume [-]
T_{mean}	Transformation factor for mean block volume calculation [-]
$V_{25\%}$	Average of all 25%-quantiles block volumes [m^3]
$V_{50\%}$	Average of all 50%-quantiles block volumes [m^3]
$V_{75\%}$	Average of all 75%-quantiles block volumes [m^3]
$V_{b,i}$	Block volume / volumetric block size [m^3]
$V_{b,mean}$	Average of all mean block volumes [m^3]

1 Introduction

1.1 Research issue

The field of civil engineering has a large diversity of disciplines. It is subdivided in specialized sections, dealing with construction problems in a wide range of duty, e.g. hydraulic engineering, environmental engineering, construction management and economics, surveying and also geotechnical engineering including rock mechanics and tunneling.

The profession of rock mechanical and tunneling engineers in general deals on the one hand with the characterization of the natural rock mass, on the other hand, the engineers have to design and to construct structures like tunnels for transportation, for mining of raw materials or to stabilize rock slopes against failure. The interpretation and the characterization of rock mass is important to evaluate existing rock slopes under consideration of rock movement and potential failure which can affect hazards on infrastructures, buildings or in the worst case on humans. In order to pretend or to minimize these risks or to improve the construction progress with respect to design and efficiency, one principal task of rock mechanic engineers and geologists is to gather reliable information of local rock mass conditions.

Reasonably characterizing a rock mass requires to determine a large number of properties and their measurable parameters. Due to the fact that the insight in a rock mass is mostly confined because only outcrops, tunnel walls or faces are visible, investigations on rock mass parameters are often cost-intensive and currently only feasible by borehole drillings, outcrop surveys, window mappings, scanlines, laser scanning or photogrammetry. Furthermore, the gained information barely describes the overall conditions *in situ* comprehensively because of the heterogeneity (different properties at different locations) and the anisotropy (different properties in different directions) of rock mass. Consequently, the detected parameters can merely describe the investigated areas but unfortunately offer uncertainties for the description of the whole rock mass in the project area. Therefore, it is desirable to find a new approach in order to reduce these uncertainties.

The rock mass parameters can be arranged in two different characteristics, see Table 1.1.

Table 1.1: Characteristic parameters of intact rock and discontinuities (modified from Giafferi *et al.* (2003)).

Characteristics of intact rock	Characteristics of discontinuities
Identification parameters <ul style="list-style-type: none"> • Common names • Petrography & mineralogy • Densities • Volume weights • Moisture content • Porosity • Degree of saturation • Permeability • Ultrasonic wave velocities, continuity index 	Identification parameters <ul style="list-style-type: none"> • Types and origin of discontinuities • Description of discontinuities: orientation, spacing, persistence, roughness, weathering, aperture, infill, water Characterization of joint systems <ul style="list-style-type: none"> • Directional joint set patterns • Statistical analysis of geometrical parameters of each set: orientation, spacing, persistence • Lumped jointed density indexes: RQD, ID, FD

This thesis examines the characteristics of discontinuities, in particular the characterization of joint systems with regard to a rock mass's block size distribution.

Block size distribution indicates the occurrence of a certain block volume or block area with the according relative frequency in a considered rock mass volume or rock face. It can be illustrated in cumulative distribution diagrams. "Discontinuities" summarizes bedding planes, faults, schistosity planes, fracture zones and lithological contact surfaces and have already been defined in literature in detail (Giafferi *et al.* (2003)).

A jointed rock mass with several sets of intersection planes form a series of finite blocks all of which having different sizes (block volumes). These volumes are statistically distributed and related to the fracturing of the rock mass. The distribution is called the volumetric block size distribution. It usually cannot be quantified by measurement techniques since insight into a rock mass is inhibited. The volumetric block size also referred to as the block volume (V_B) depends on the following major joint set parameters:

1. Orientation: angles of a joint set in space with respect to the north direction, including dip angle (dip) [$^{\circ}$], acute angle (inclination) between horizon (0°) and the joint plane dip vector, and the dip direction (dd) [$^{\circ}$], angle (clockwise) between the North (0°) and the azimuth of the joint plane dip vector.

2. Normal set spacing: measured distance (sp) [m] between two adjacent joints from a particular discontinuity set normal to their orientation.
3. Persistence: degree of transection or areal extent of joint planes in a rock mass (p)[-].

These data can be applied to rock mass classification systems, e.g. the Q-System (Barton, et al., 1974), the Rock Mass Rating (RMR) (Bieniawski, 1973) system. Also the Geological Strength Index (GSI) (Hoek, et al., 1995) which has similarities to classification systems, but is merely an index value, uses the block volume as an input parameter.

The knowledge of the block size is an important factor, which has a crucial influence on the calculation of a project, the estimation of construction progress, the selection of support measures, time requirement and even on hazards for the environment and humans. Therefore, strong efforts in research and investigation are necessary to obtain an improved method for estimating the block size distribution of a rock mass.

1.2 Scope of work

1.2.1 Development of a numerical block model

The first step to solve the problem is to develop a numerical block model. With the aid of 3DEC™, a numerical modeling code for advanced geotechnical analysis of soil, rock, and structural support in three dimensions” (Itasca Consulting Group, 2014), it is possible to create a blocky rock mass model including an arbitrary number of joint sets with defined joint set parameters. Furthermore, the code for 3DEC provides access to the required parameters, e.g. block volumes and block areas of the model for further processing. Afterwards, representative simulations are performed while varying the joint set parameters (orientation, spacing, and persistence), the model parameters (model dimensions) or even the dimensions of the outcrop. Figure 1.1 shows an example of a 3DEC model with three mutually orthogonal joint sets.

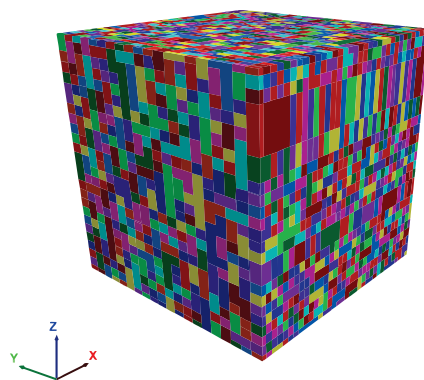


Figure 1.1: Illustrative example of a 3DEC rock mass model with three joint sets.

1.2.2 Statistical analysis

The next step is to set up an analysis tool which can handle the huge amount of 3DEC data output semi-automatically and additionally, is able to deliver significant analysis results of the simulation cases. With the aid of R (GNU R, 2014), an open source software environment for statistical computing and graphics, the statistical analysis of input data is performable on a sophisticated level. Thus, a program code is developed in R to enable the desired analysis, e.g. the cumulative block size probability distribution, etc.

1.3 Objectives

After completion of the preliminaries (development of a numerical model and performance of simulations), the results of the statistical analysis have to be investigated in detail. The principal aim is to find a correlation between the areal block size distribution (2D) and the volumetric block size distribution (3D) in the numerical rock mass model in order to improve the *in situ* block size estimation or even to quantify the block size distribution. Moreover, limitations should be outlined concerning the minimum required outcrop area in dependence from joint set parameters.

2 State of the art

2.1 Importance of block size in rock mechanics

A rock mass intersected by joint sets is divided into blocks. The block size can vary within the range of few cubic centimeters up to several cubic meters, depending on the number, the spacing and the persistence of joints, and is used to describe the fracturing of the rock mass (from e.g. predominantly disintegrated to massive). Hence, statements about “compressive strength, deformation modulus, shear strength, dilation, and conductivity” of a rock mass (Palmström, 2005) can be taken. Moreover, the block size represents an essential parameter for characterization and classification of rock masses.

For instance, if a rock mass is disintegrated, a systematic rock bolt pattern and shotcrete lining are required (right illustration in Figure 2.1), while a barely jointed or massive rock mass probably does not need systematic but specific application of bolts (left illustration in Figure 2.1).

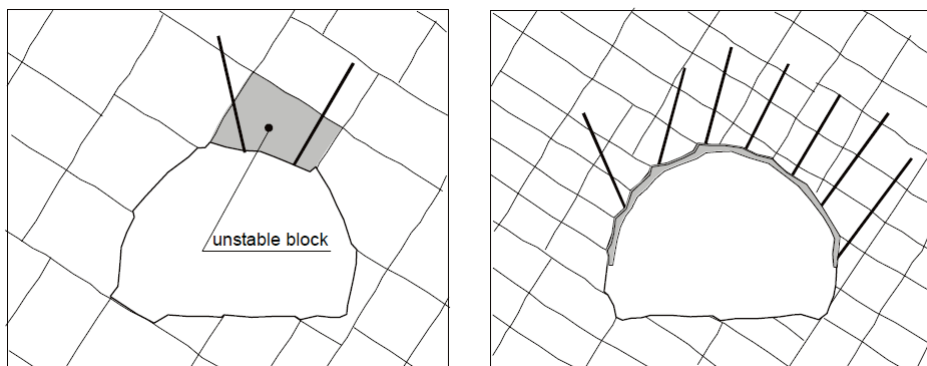


Figure 2.1: Profiles of tunnel sections: tunnel supported with rock bolts only (left illustration) and a tunnel additionally supported with shotcrete (right illustration) (taken from (Palmström, 2001)).

Among other rock parameters, the block size influences the type, amount and dimension of support measures. As already mentioned above, the block size is an essential parameter in classification systems. The following examples should merely give a short overview about the most applied methods.

The Austrian Society for Geomechanics (OEGG) proposed a guideline for rock mass classification where rock mass with “similar ground behaviors with respect to failure modes and displacement characteristics” (OEGG, (2010)) can be arranged into basic

categories of ground behavior types (BT). In Table 2.1 predefined categories of the ground behavior types are presented.

Table 2.1: General categories of ground behaviors (taken from OEGG (2010)).

Basic categories of Behaviour Types (BT)		Description of potential failure modes/mechanisms during excavation of the unsupported ground
1	Stable	Stable ground with the potential of small local gravity induced falling or sliding of blocks
2	Potential of discontinuity controlled block fall	Voluminous discontinuity controlled, gravity induced falling and sliding of blocks, occasional local shear failure on discontinuities
3	Shallow failure	Shallow stress induced failure in combination with discontinuity and gravity controlled failure
4	Voluminous stress induced failure	Stress induced failure involving large ground volumes and large deformation
5	Rock burst	Sudden and violent failure of the rock mass, caused by highly stressed brittle rocks and the rapid release of accumulated strain energy
6	Buckling	Buckling of rocks with a narrowly spaced discontinuity set, frequently associated with shear failure
7	Crown failure	Voluminous overbreaks in the crown with progressive shear failure
8	Ravelling ground	Ravelling of dry or moist, intensely fractured, poorly interlocked rocks or soil with low cohesion
9	Flowing ground	Flow of intensely fractured, poorly interlocked rocks or soil with high water content
10	Swelling ground	Time dependent volume increase of the ground caused by physical-chemical reaction of ground and water in combination with stress relief
11	Ground with frequently changing deformation characteristics	Combination of several behaviours with strong local variations of stresses and deformations over longer sections due to heterogeneous ground (i.e. in heterogeneous fault zones; block-in-matrix rock, tectonic melanges)

Another classification method is the Q - system according to Barton *et al.* (1974), where the block size is indirectly integrated with the ratio between Rock Quality Designation (RQD) and a factor for the number of joint sets (J_n).

The Rock Mass Rating (RMR) system (Bieniawski, 1973), an estimation for rock mass properties and required support measures, applies also the RQD and the joint spacing (S).

The original Geological Strength Index (GSI) introduced by Hoek *et al.* (1995) uses the

joint “surface quality” and the “interlocking of pieces” as input parameters for determination of the GSI. Cai *et al.* (2004) further developed the GSI chart by replacing the input parameters from Hoek *et al.* by the block volume (V_B) and the joint condition factor (J_c) to determine the rock mass strength. As both input parameters are known, the GSI can be received directly from the chart shown in the Figure 2.2.

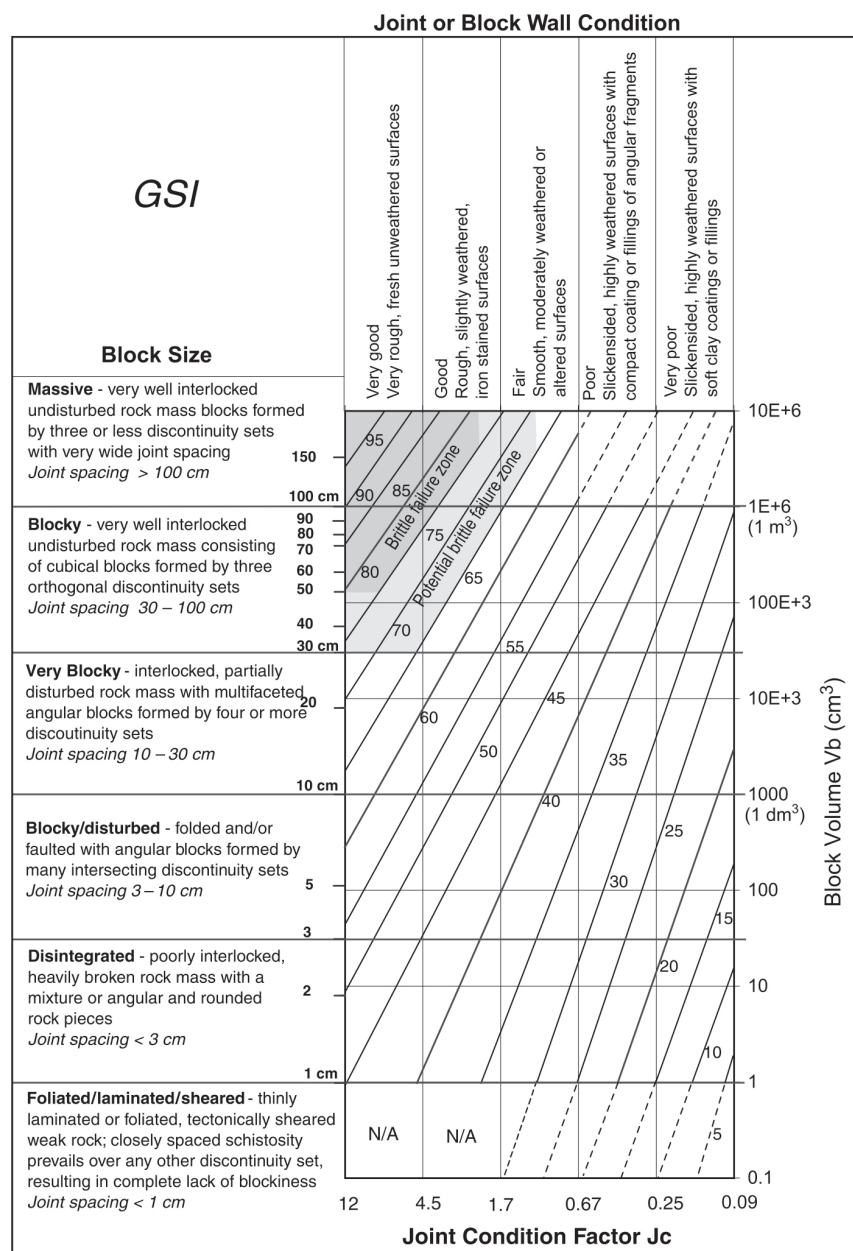


Figure 2.2: Quantification of Geological Strength Index (GSI chart from Cai *et al.* (2004)).

2.2 Determination of block size

2.2.1 Measurement of joint set parameters

The block size is governed by the joint set parameters. Therefore it is necessary to collect sufficient and representative information about the joint sets *in situ*. There are different approaches:

1. Measurements on drill cores (1-dimensional)
2. Measurements on rock surfaces (2-dimensional)
3. Photogrammetric measurements

The used method depends on current circumstances (e.g. progress of project) and the availability of measurements. For instance, in the design stage where an outcrop is not always visible, measurements on drill cores have to be applied to investigate the joint set parameters. During tunneling progress, more precise measurements are feasible on tunnel walls and faces. The parameters to be recorded have already been mentioned in Chapter 1.1 (see page 2).

2.2.2 Estimation of block size

In literature, several publications are available dealing with the determination of the block size, e.g. Elmouttie *et al.* (2012), Kim *et al.* (2007), Palmström (2005), Wang *et al.* (2003), etc. Unfortunately, there is still no satisfying, sufficient and easy to use tool to get reliable results.

Palmström (2005) introduced a formula to calculate the block volume (V_B) depending on the joint spacing and the angles between the joint sets. The formula is merely valid for three persistent joint sets and can be calculated as

$$V_B = \frac{S_1 \cdot S_2 \cdot S_3}{\sin \gamma_1 \cdot \sin \gamma_2 \cdot \sin \gamma_3}, \quad (1)$$

where S_i is the average joint spacing of one joint set and γ_i the average angle between two joint sets, respectively (see Figure 2.3).

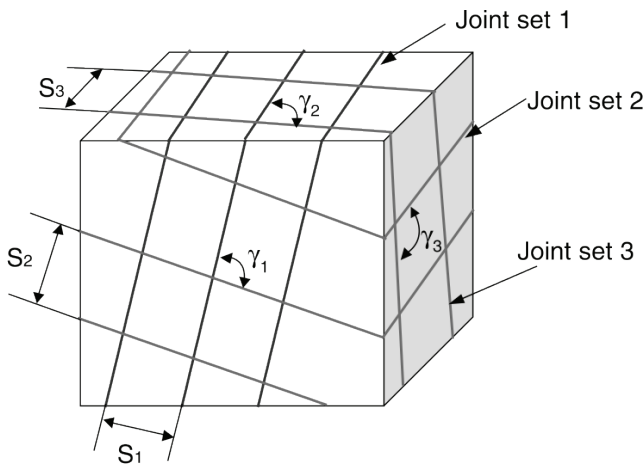


Figure 2.3: Convention of spacing and angles of respective joint sets (from Kim *et al.* (2007)).

As natural rock mass is almost always discontinuous, the above suggested formula is limited in its application because the persistence of joints is not considered.

Cai *et al.* (2004) extended the equation (1) by including the factor of persistence and is expressed as

$$V_B = \frac{S_1 \cdot S_2 \cdot S_3}{\sin \gamma_1 \cdot \sin \gamma_2 \cdot \sin \gamma_3 \cdot \sqrt[3]{p_1 \cdot p_2 \cdot p_3}} , \quad (2)$$

where p_i is the average joint persistence of one joint set. The proposed equation (2) is based on field experience and considers the influence of joint persistence on the block volume. However, the validity of the formula has not been proved in detail in the literature.

Kim *et al.* (2007) investigated the influence of joint persistence on the block size distribution, using the distinct element analysis tools UDEC and 3DEC. Firstly, they concluded, that their investigated block size distributions follow a lognormal distribution. Secondly, they compared the block sizes obtained from equation (2) with their numerical results and found “very good correlations” between them. In addition, they performed a statistical analysis by using the F-test and concluded that the joint spacing is the most significant parameter which defines the block size followed by the joint persistence with a moderate influence and the angle between the joint sets with minor influence.

Wang *et al.* (2003) presented a new software named “MAKEBLOCK” and is based on Monte Carlo simulations. With this tool it is possible to predict the ore size distribution in block caving. They found a good agreement between the simulated ore fracturing and the ore fractures *in situ*.

Elmouttie and Poropat (2012) presented “a new technique for estimating the *in situ* block size distribution in a jointed rock mass”. Their method is also based on Monte Carlo simulations, which should provide more realistic distributed joint sets compared to other methods. They compared their results with approaches by Kim *et al.* (2007) and Wang *et al.* (2003). However, they identified significant difference for rock mass with “small discontinuities” (joint sets with low persistence).

In the field of blasting technology, Moser *et al.* (2003) also wanted to predict the particle size distribution of blasted material depending on the rock mass condition. The authors wanted to set up a more efficient blasting design where “less fines” are produced. Performed laboratory tests on rock samples have shown that the natural breakage behavior (NBC) by blasting is preserved in particle sizes in the range of centimeters. By comparing the NBC and the blast fragmentation curve they are able to quantify the reduction potential of fines.

The investigations above should emphasize the importance to improve the determination of block size distribution. While the mentioned methods are partially complicated to comprehend or have still not been established in practice, this thesis should offer new approaches concerning a more advanced and reliable but practically applicable method for the determination of block size distribution.

3 Preliminary work

3.1 Model composition in 3DEC

3.1.1 General information

For generating a rock mass model with various joint sets the distinct element software 3DEC, developed by Itasca Consulting Group (2014), was used. With this program one is able to create a rock mass model with arbitrary geometric dimensions and an arbitrary number of joints sets with variable joint set parameters. However, the number of blocks created by different joint sets is limited by the capacity of the working computer. For instance, creating a model with 100,000 rigid blocks, 3DEC requires about 1000 MB available RAM minimum. Therefore it is recommended to roughly estimate the maximum number of blocks (blocks generated by continuous joint sets compared to the model dimension) beforehand in order to achieve results.

Initially, the rock mass model has to be generated. In this work, the y - direction is determined to be equal to North, being important for the joint set's orientation. The reference model has size of 10.0 m x 10.0 m x 10.0 m and contains three joints sets. The joint sets are defined by the dip angle (dip), the dip direction (dd), the average joint spacing (sp), the number of joints within a joint set (num), the origin of the joint set (or) and the persistence (p) of each joint set. Moreover, standard deviations can be added to the angles (dip, dd), and to the average spacing (sp). In Figure 3.1 the reference model in 3DEC is illustrated with its dimensions and the joints sets with respect to the orientation convention. The joint sets are assumed to be continuous and mutually orthogonal. A variation of parameters has not been applied.

Next, an output file including the desired values for further processing has to be designed. Since 3DEC is not able to export the values automatically, the development of a FISH code was necessary. FISH is an internal programming language in 3DEC, which allows users more advanced applications, deeper access to the computations, and higher control on the numerical processing. In this case, the FISH code delivers the block areas ($A_{b,i}$) of a defined outcrop area and the block volumes of the entire rock mass model ($V_{b,i}$) after the model generation in 3DEC and saves the data into a text file.

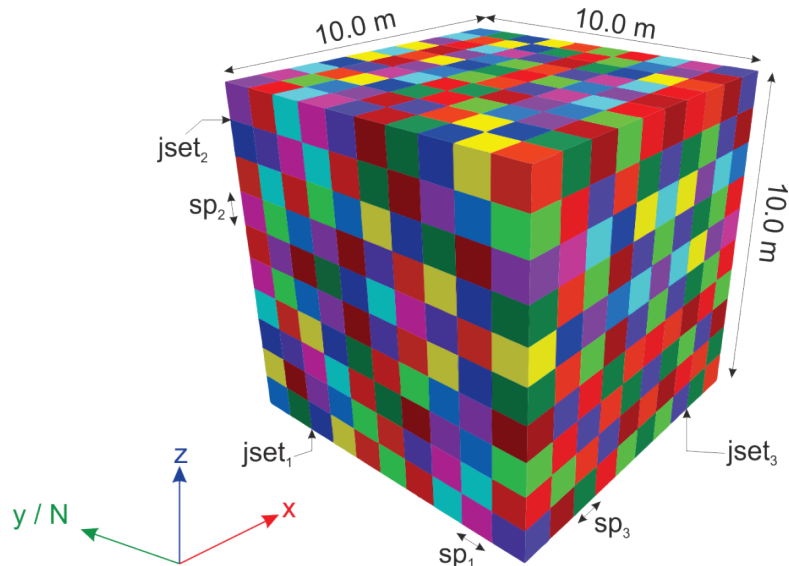


Figure 3.1: Illustration of the general 3DEC model.

3.1.2 Consideration of boundary blocks

Boundary blocks (bb) are blocks which are delineated by the frame of the outcrop area or by the constraints of the model (blocks with contact to free space). Figure 3.2 shows an example of a rock mass model with the definition of areal boundary blocks. The border of the outcrop area (black solid line) intersects the real block faces (red colored faces) and would create additional, artificial block faces. Thus, the number of block faces increases while the size of the block areas decreases, resulting in a misleading interpretation of the real block size distribution. Therefore, boundary blocks are disregarded and just relevant block areas (green colored faces) are considered in the analysis and written into the output file.

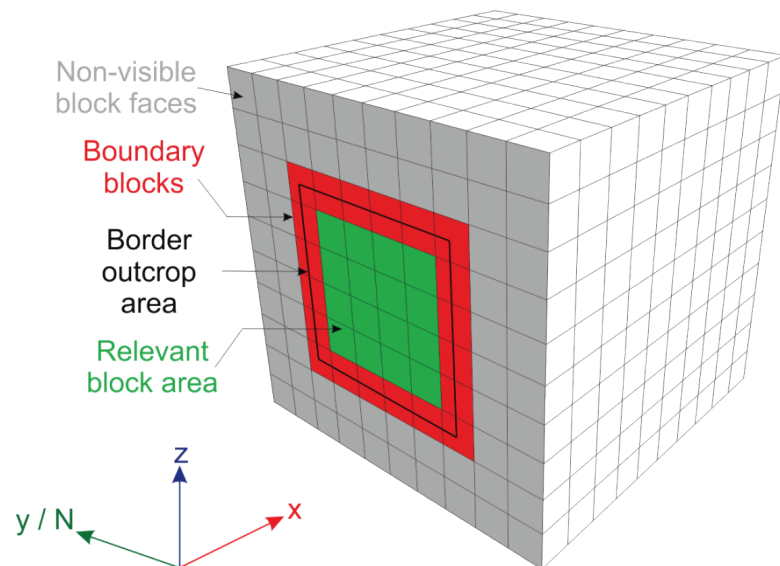


Figure 3.2: Illustration of areal boundary blocks.

3.1.3 Validation of the block model

After developing the model code, it was tested for correctness. Hence, a simple model was created in order to check manually whether the actual values (area and volume of blocks at the outcrop area) are written into the output file correctly. For a better traceability also the boundary blocks were readout. For this evaluation, the following model parameters were used:

Table 3.1: Model parameters for validation case.

model dimension	x[-5; 5]		y[-5; 5]		z[-5; 5]	
	dip direction [°]	dip angle [°]	spacing [m]	origin [x, y, z]	persistence [-]	
joint set ₁	0	90	3.0	0, 0, 0	1.0	
joint set ₂	0	0	3.0	0, 0, 0	1.0	
joint set ₃	90	90	3.0	0, 0, 0	1.0	

As can be seen in Table 3.2, the calculation of the validation case offers 16 block areas at the observation area. The sum of block areas corresponds with the whole model face. The highlighted numbers (red colored) should illustrate the agreement between the output file and the attributes of one chosen block in 3DEC (Figure 3.3). Hence, the proposed model set-up and the FISH code operate appropriately and can be applied for further investigations.

Table 3.2: Example results of the model validation case.

Block Index	V _{B,i} [m ³]	A _{B,i} [m ²]
11870	12	6
11043	18	9
10354	12	6
9611	18	9
8784	12	6
8053	8	4
7310	12	6
6621	8	4
5890	12	6
5063	18	9
4374	12	6
3631	18	9
2934	12	6
2239	8	4
1233	12	6
217	8	4
$\Sigma A_{B,i}$		100
Control	10.0 m x 10.0 m	100.0

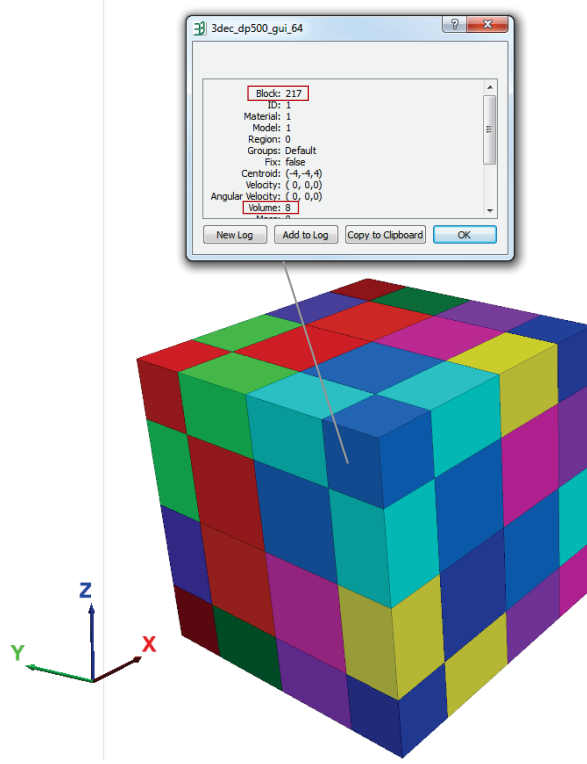


Figure 3.3: 3DEC plot of the validation case.

3.1.4 Replication of calculation cases

Another problem to deal with is the influence of the persistence (p). Persistence in 3DEC (2014) is defined as the probability that a block model lying in the path of a joint set is split, *i.e.* if $p = 0.8$ means, that 80 % of the block model will be split on average. Due to the fact, that for non-persistent joints ($p < 1.0$) 3DEC places the “joint gaps” randomly, leads to different block sizes for each new model simulation. Thus, it is required to repeat each simulation case several times in order to receive statistically representative results. A series of simulations were performed in order to examine the minimum required number of replications. The number of replications is introduced as the replication factor r . For the simulations four arbitrary parameter sets are used (Table 3.3). The parameter sets vary in the persistence, in the orientation and in the spacing in order to cover all possibilities and to ensure the representativeness. Test number 3 also considers deviations in the angles [$^{\circ}$] of the joint sets and represents one feasible example for non-orthogonal joint sets. Table 3.4 shows the performed test runs and calculations.

Table 3.3: Model parameters for replication test.

		model dimension	x[-5; 5]		y[-5; 5]		z[-5; 5]	
		test number	dip direction [$^{\circ}$]	dip angle [$^{\circ}$]	spacing [m]	origin [x, y, z]	persistence [-]	
1	joint set ₁	0	0	90	0.5	0, 0, 0	0.8	
	joint set ₂	0	0	0	0.6	0, 0, 0	0.8	
	joint set ₃	90	90	90	0.7	0, 0, 0	0.8	
2	joint set ₁	0	0	90	0.5	0, 0, 0	0.4	
	joint set ₂	0	0	0	0.6	0, 0, 0	0.4	
	joint set ₃	90	90	90	0.7	0, 0, 0	0.4	
3	joint set ₁	20 ± 5	70 ± 5	0.5	0, 0, 0	0.8		
	joint set ₂	0 ± 5	10 ± 5	0.6	0, 0, 0	0.8		
	joint set ₃	90 ± 0	90 ± 0	0.7	0, 0, 0	0.8		
4	joint set ₁	0	0	90	0.3	0, 0, 0	0.8	
	joint set ₂	0	0	0	0.4	0, 0, 0	0.8	
	joint set ₃	90	90	90	0.5	0, 0, 0	0.8	

Table 3.4: Test runs with corresponding replications.

test run	replication factor r					
1 st run	1	5	10	25	50	100
2 nd run	1	5	10	25	50	100

Figure 3.5 to Figure 3.8 illustrate the cumulative block area size distributions (solid lines; 1st run: orange, 2nd run: blue) for all performed replication tests (test number 1 - 4). The replication factor r (1, 5, 10, 25, 50 or 100) is depicted in each diagram. Also the minimum and maximum possible mean areas of the total number of replications are shown (vertically dashed lines; 1st run: orange, 2nd run: blue). The intention of performing two test runs was to prove that an insufficient replication leads to a significant deviation in the block size distributions.

Similar to the grain size distributions for soils and granular materials, the block size distributions are as well illustrated in cumulative distribution diagrams. The distributions of block sizes are assumed to obey a log-normal distribution, as shown by Kim *et al.* (2007), Song and Lee (2001) and Song *et al.* (2001).

Figure 3.4 demonstrates two examples of cumulative block size distributions. Although, the average joint set parameters are equal in both cases, an obvious difference is noticeable. The solid blue lines represent the empirical block size distributions and the solid red lines the corresponding theoretical log-normal distributions.

The log-normal distribution in the left illustration matches the block size distribution better than in the right illustration, due to the fact, that standard deviations are added to the joint set parameters in the left illustration. This case reflects the *in situ* conditions, where a certain irregularity (deviations in joint set parameters) can be found.

In the right block size distribution without any standard deviations in the joint set parameters, merely blocks are cut with certain sizes (less variation in block volumes) and thus, the empirical distributions appears steplike.

In the present study only the developed log-normal distributions are illustrated in order to avoid clutter in the figures. Nevertheless, further calculations always deal with the empirical values.

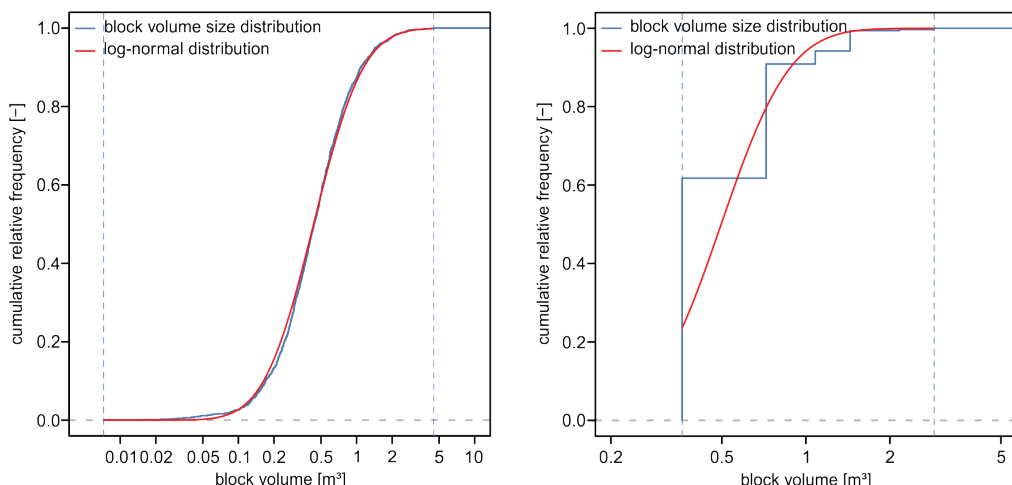


Figure 3.4: Examples of cumulative block volume size distributions – left: illustration with varying joint orientation and spacing; right: illustration with deterministic joint orientation and spacing.

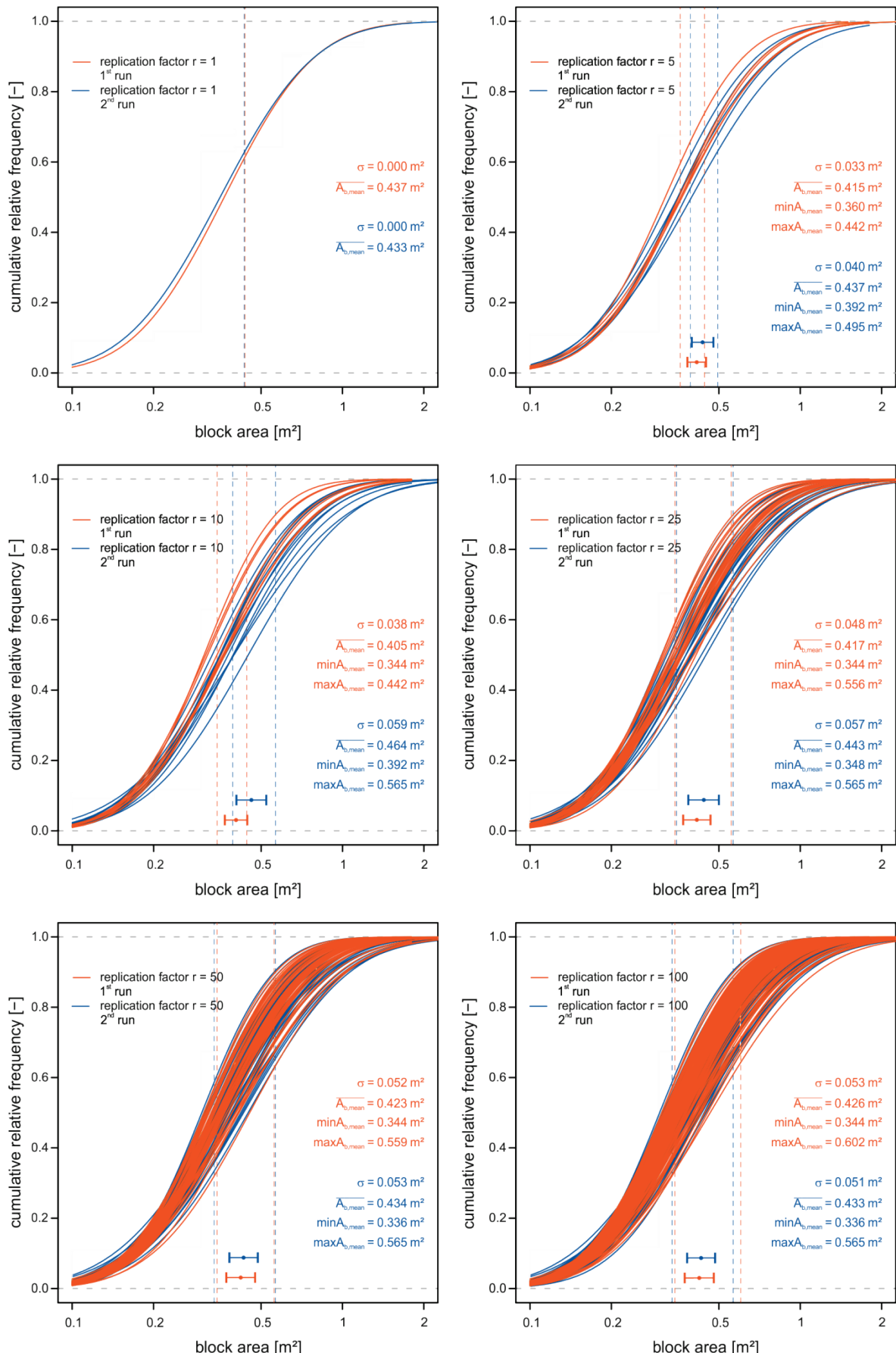


Figure 3.5: Results of replication test 1 (for model parameters see Table 3.3).

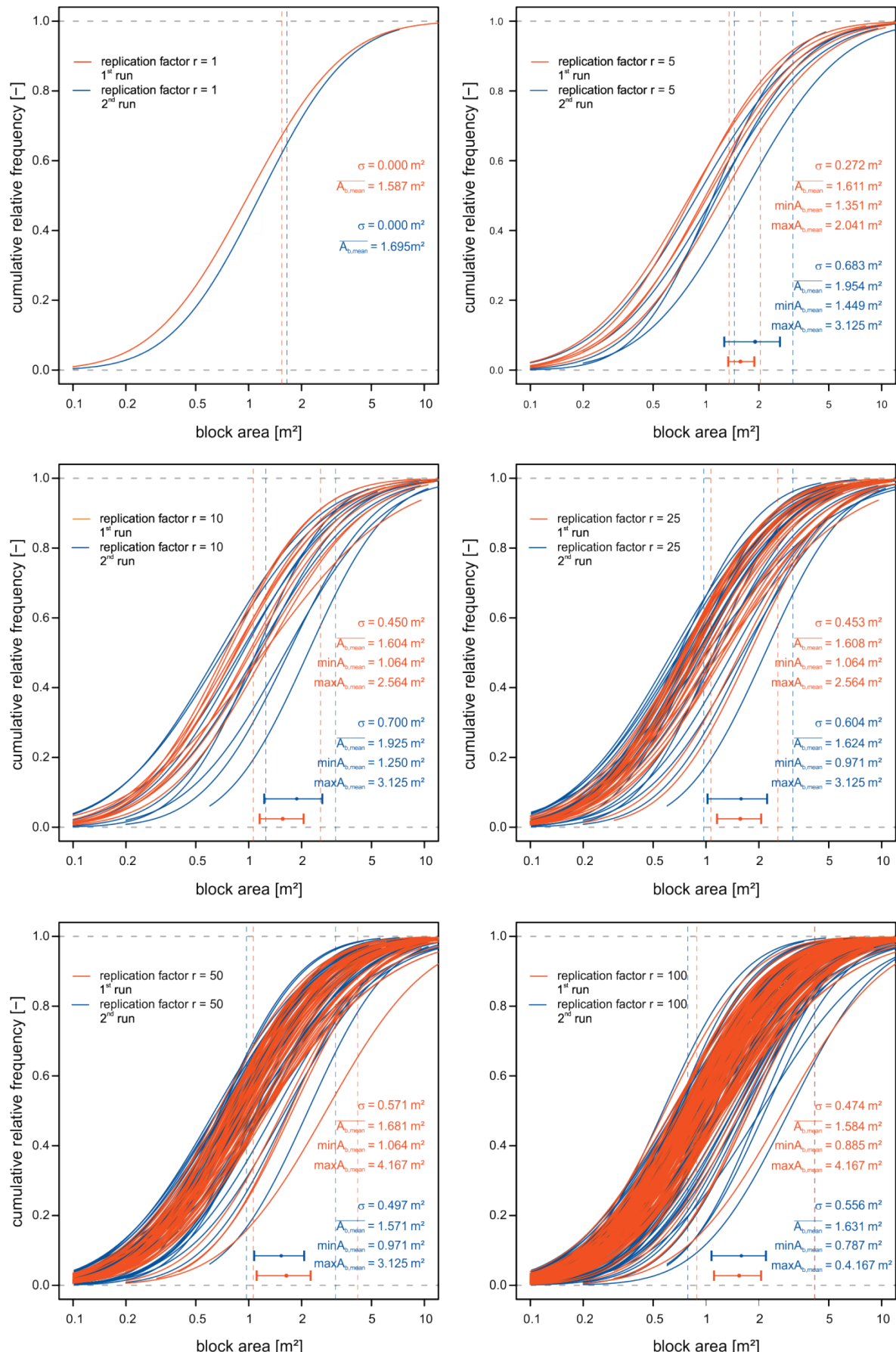


Figure 3.6: Results of replication test 2 (for model parameters see Table 3.3).

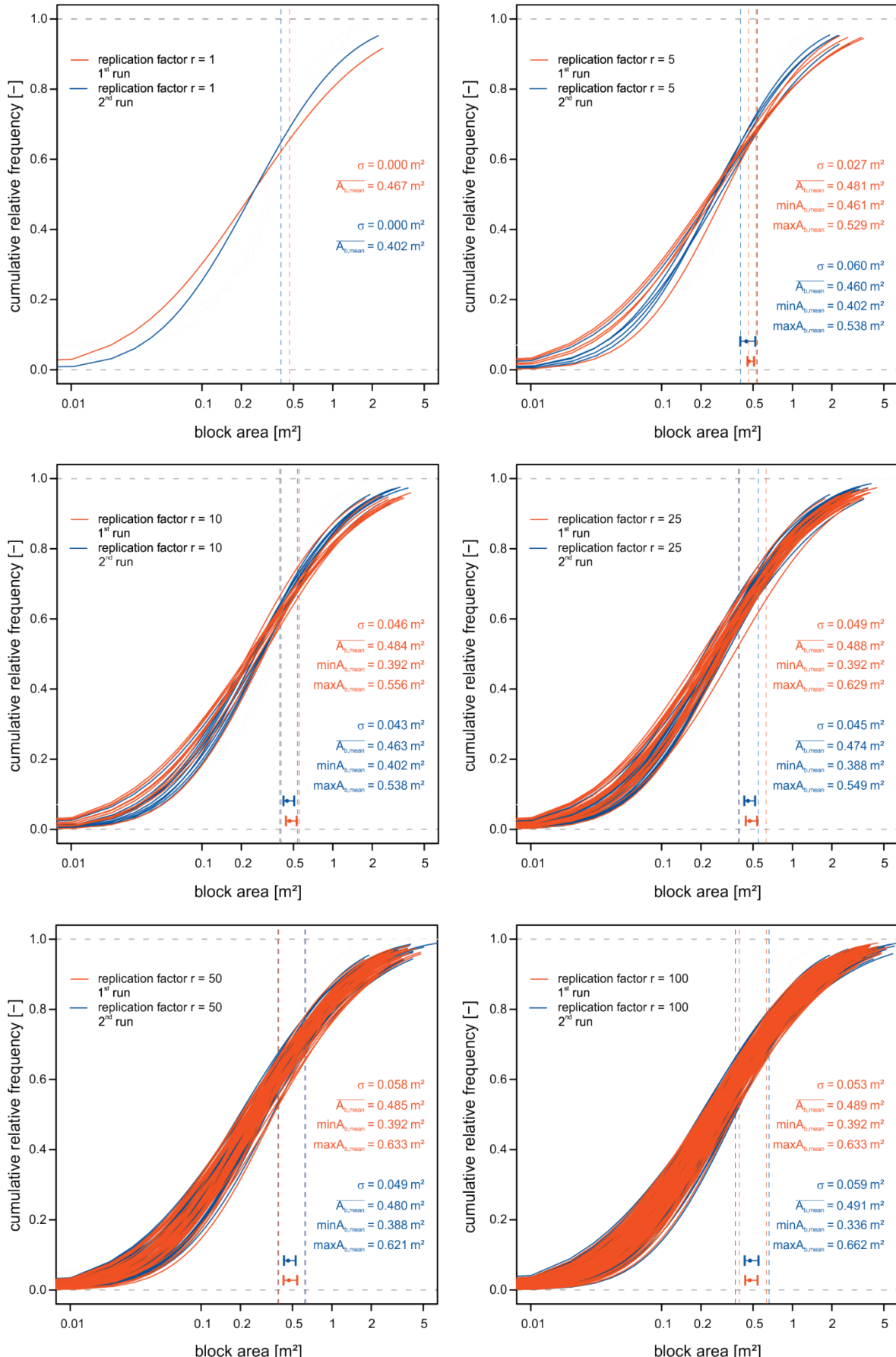


Figure 3.7: Results of replication test 3 (for model parameters see Table 3.3).

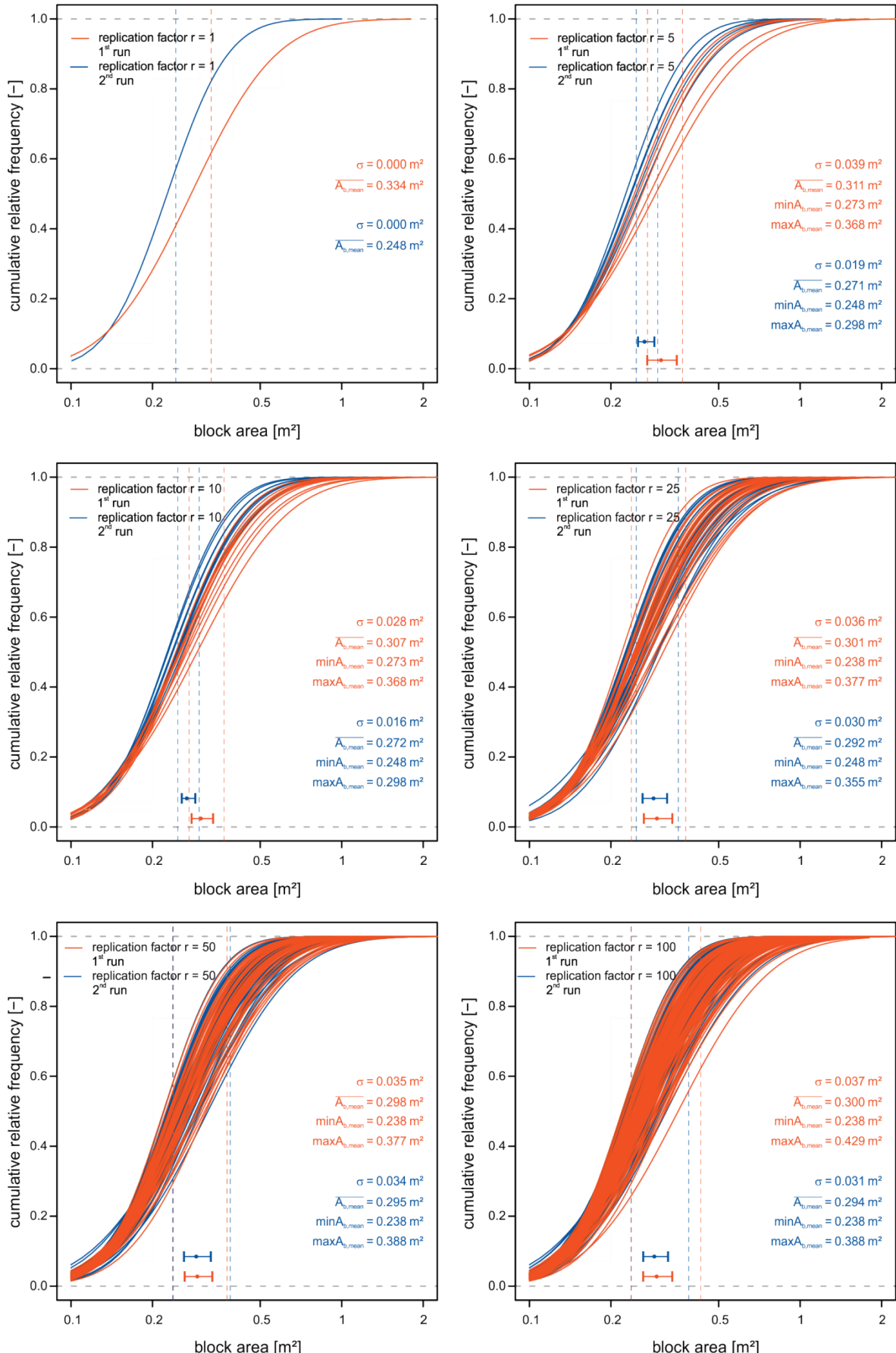


Figure 3.8: Results of replication test 4 (for model parameters see Table 3.3).

The following conclusions can be drawn from the previous analysis:

1. An increasing replication factor leads to an increasing standard deviation of the averaged mean block areas and also the bandwidths of potential mean block areas get larger (vertically dashed lines).
2. The higher the replication factor, the more approach the averaged mean block area and the size of the standard deviation of each test run (compare also Figure 3.9 to Figure 3.12).
3. Comparing the diagrams with a replication factor $r = 50$ and $r = 100$, the averaged mean block area and the standard deviations are approaching progressively.
4. A higher replication factor results in a decreasing difference between the two test runs with regard to the standard deviation and the total mean block area.

In order to emphasize the importance of the replication the gained results are assembled in Figure 3.9 to Figure 3.12 for each replication test using a compact diagram. In these diagrams the abscissa represents the replication factor whereas the ordinate shows the average of the mean areas. Also the standard deviations (colored solid lines) are arranged to the corresponding mean values.

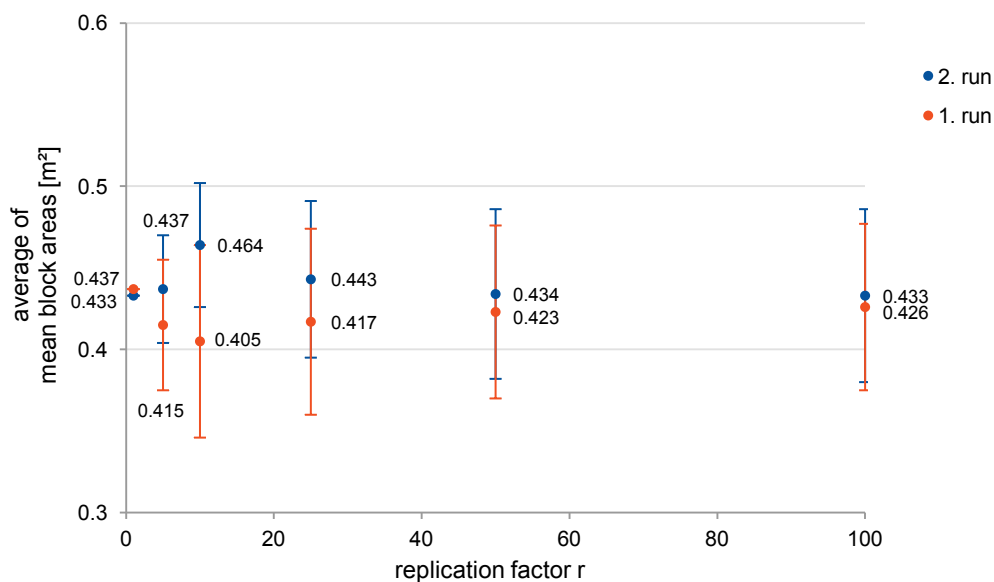


Figure 3.9: Assembly of replication test 1: the averaged mean block areas and the according standard deviations in dependence of the replication factor.

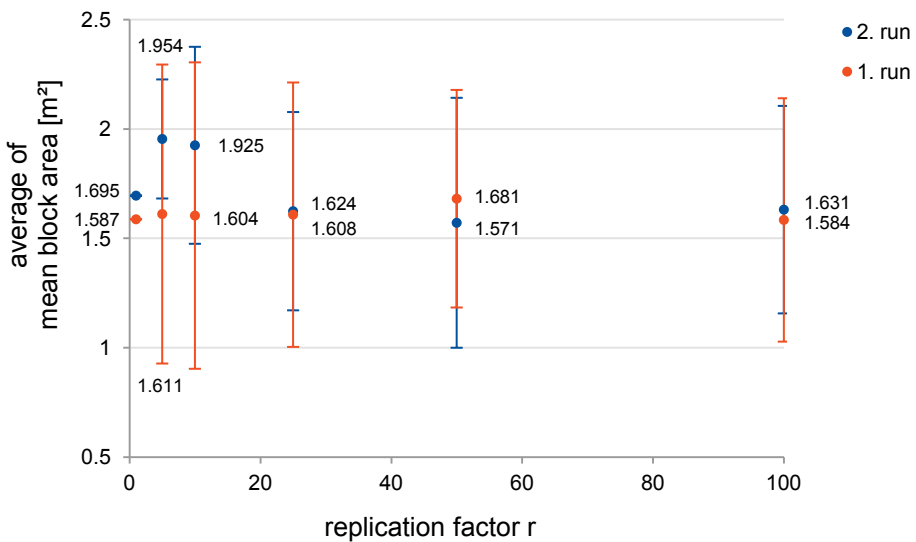


Figure 3.10: Assembly of replication test 2: the averaged mean block areas and the according standard deviations in dependence of the replication factor.

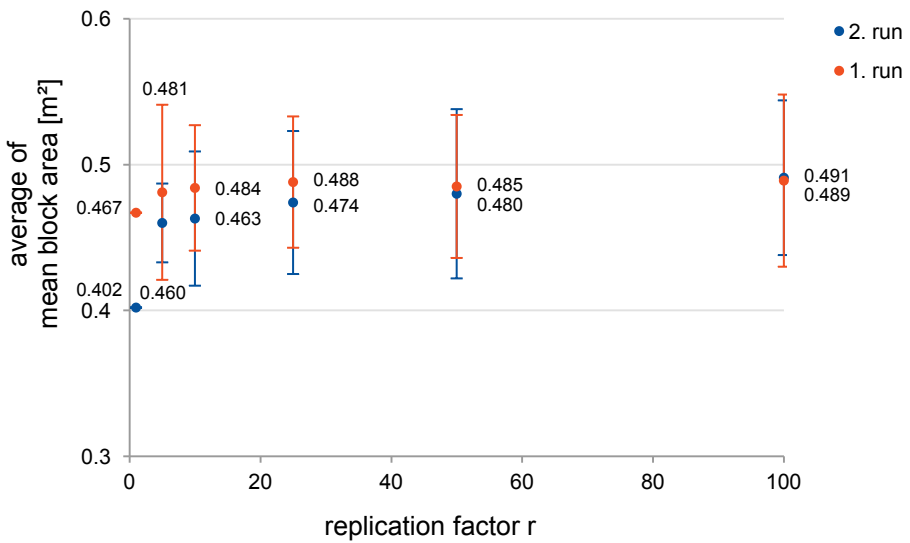


Figure 3.11: Assembly of replication test 3: the averaged mean block areas and the according standard deviations in dependence of the replication factor.

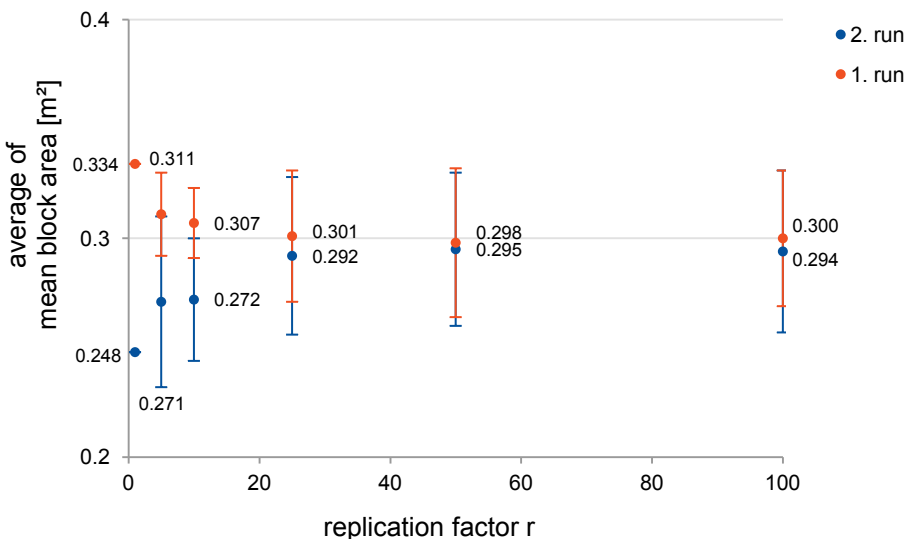


Figure 3.12: Assembly of replication test 4: the averaged mean block areas and the according standard deviations in dependence of the replication factor.

The assembled results in Figure 3.9 to Figure 3.12 prove the importance of the replication of calculations. A higher replication factor leads to progressively matching bandwidth of block size distributions and thus more reliable results can be achieved. Although, some mean block sizes of the first and second test run approaching at a relative low replication factor (compare Figure 3.9, values at $r = 1$; or Figure 3.10, values at $r = 25$), in reality this correlation arises by accident. Thus, replicating a calculation more often leads to a larger range of possible block sizes.

A replication factor of $r = 100$ has been chosen for further investigations in order to ensure the statistically representativeness. However, this fact led to a more time consuming calculation in 3DEC which have to be considered as well.

3.2 Influence of 3DEC specific input of non-persistent joint sets on block size distributions

3.2.1 Influence of the input sequence of joint sets

It is necessary to verify, if the block size distribution is independent of the input sequence of non-persistent joint sets, *i.e.* whether the internal 3DEC structure delivers the same block size distributions by changing the input order of the joint sets. Therefore, a test set-up was developed containing three mutually orthogonal joint sets with constant joint set parameters, shown in Table 3.5. For all investigations described in Chapter 3.2 the boundary blocks and the replication factor were considered.

Table 3.5: Model parameter for sequence testing.

model dimension	x[-5; 5]		y[-5; 5]		z[-5; 5]	
	dip direction [°]	dip angle [°]	spacing [m]	origin [x, y, z]	persistence [-]	
joint set ₁	0	90	0.5	0, 0, 0	0.8	
joint set ₂	0	0	0.6	0, 0, 0	0.8	
joint set ₃	90	90	0.7	0, 0, 0	0.8	

The simulations were repeated several times as claimed in Chapter 3.1 (see page 14). For reasonable results a replication factor of $r = 100$ was chosen. There are six possible options for the input order of the joint sets (Table 3.6):

Table 3.6: Sequences of joint sets.

Case 1	Case 2	Case 3
joint set ₁	joint set ₁	joint set ₂
joint set ₂	joint set ₃	joint set ₁
joint set ₃	joint set ₂	joint set ₃
Case 4	Case 5	Case 6
joint set ₂	joint set ₃	joint set ₃
joint set ₃	joint set ₁	joint set ₂
joint set ₁	joint set ₂	joint set ₁

The diagrams in Figure 3.13 and Figure 3.14 show the areal (left column) and the corresponding volumetric (right column) block size distributions of the simulated cases.

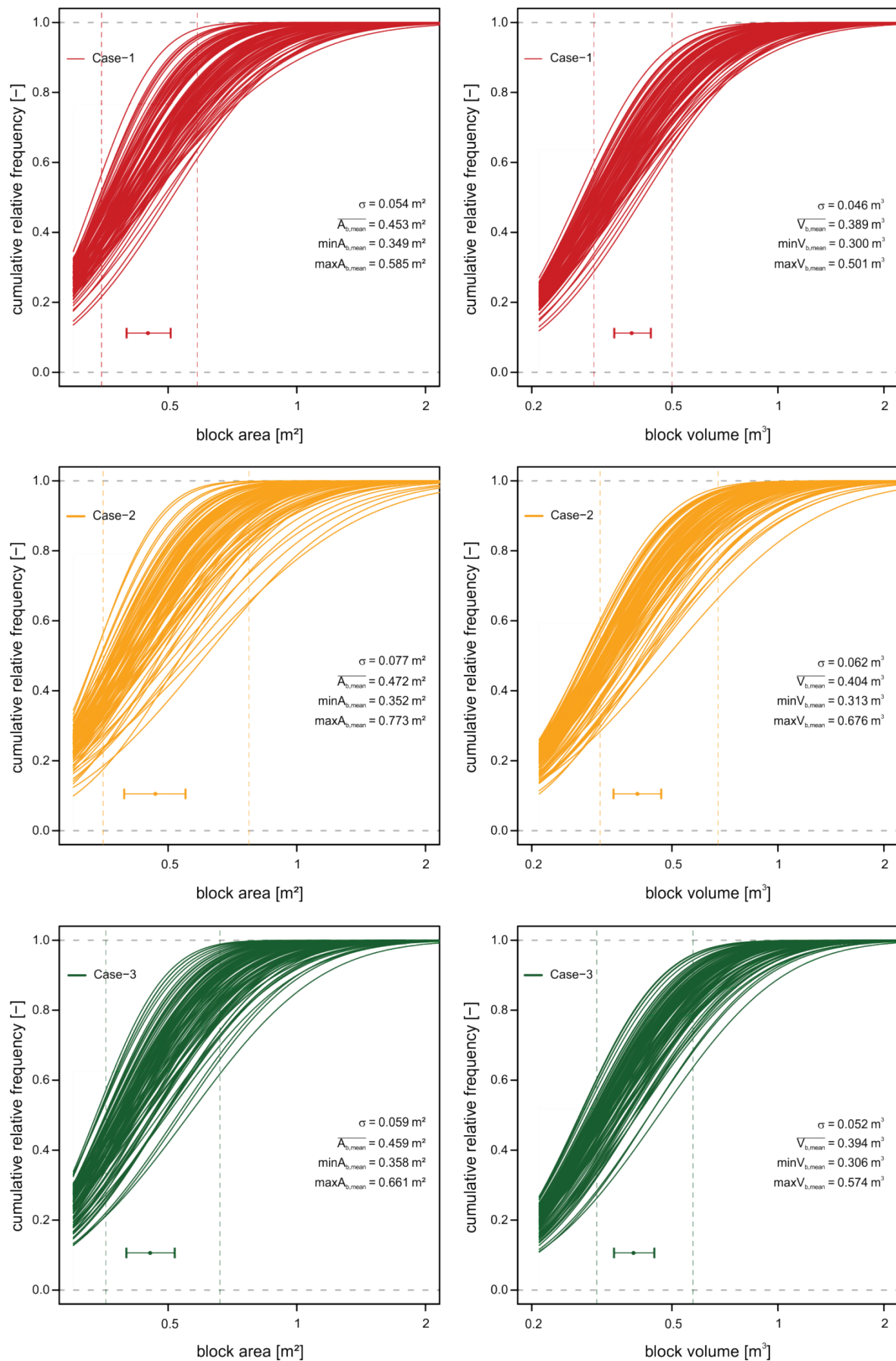


Figure 3.13: Input sequence – Results of the performed calculations, case 1 - 3.

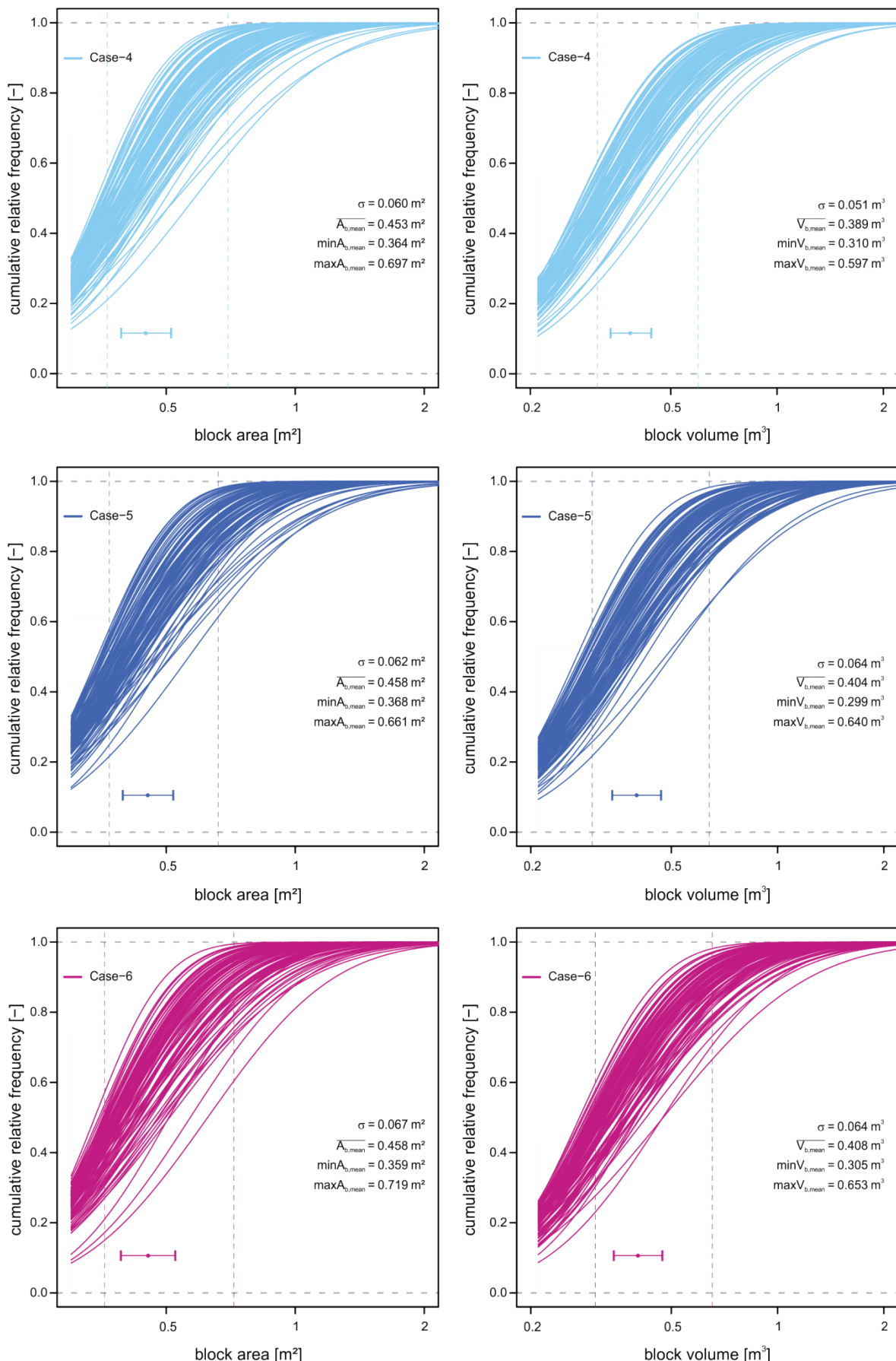


Figure 3.14: Input sequence – Results of the performed calculations, case 4 - 6.

Obviously, the distributions of the different series are in good accordance merely a few outliers occur due to the non-persistency of the joint sets. In order to emphasize the independence of the simulation results and input order of the joint sets, they are summarized in Figure 3.15 and Figure 3.16. The diagrams show similar values for mean block area and mean block volume. Although minor deviations emerge, the influence of the input sequence of the joint sets does not have a significant impact on the block size distributions given that a sufficient number of replications was applied.

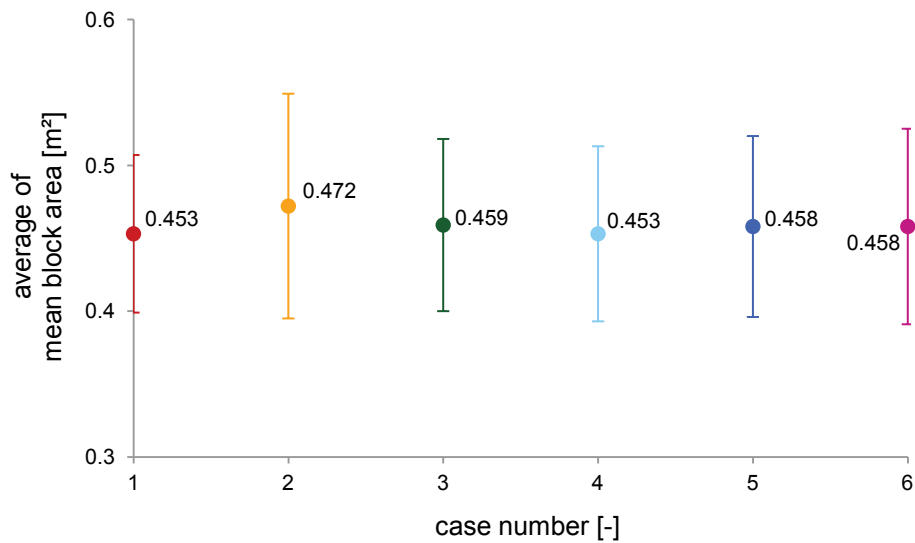


Figure 3.15: Input sequence – Assembly of the averaged mean block areas in dependence of the case number.

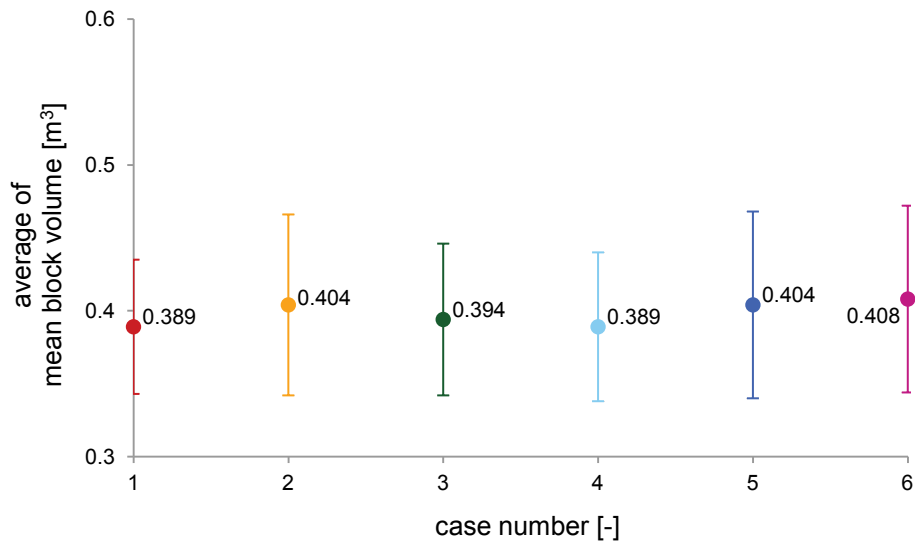


Figure 3.16: Input sequence – Assembly of the averaged mean block volumes in dependence of the case number.

3.2.2 Influence of selected origins of joint sets

In this context also the influence of the position of the joint set origins on the block size distributions was investigated. Presumably, the origin determining the initial point for joint generation may cause differences in ‘how blocks are cut’. Several simulations were performed, where the joint set origin was fixed at the center of the model, at the center of a model face, and at a model vertex, respectively. The model parameters are adopted from Table 3.5 (see page 23), however, the origins have been modified accordingly.

Table 3.7: Model parameters for simulations with origin variation.

model dimension	x[-5; 5]		y[-5; 5]	z[-5; 5]
	dip direction [°]	dip angle [°]	spacing [m]	persistence [-]
joint set ₁	0	90	0.5	0.8
joint set ₂	0	0	0.6	0.8
joint set ₃	90	90	0.7	0.8

The proposed origin coordinates, valid for all three joint sets, are headed in Table 3.8 whereas Figure 3.17 should visualize the origins in the 3DEC Model.

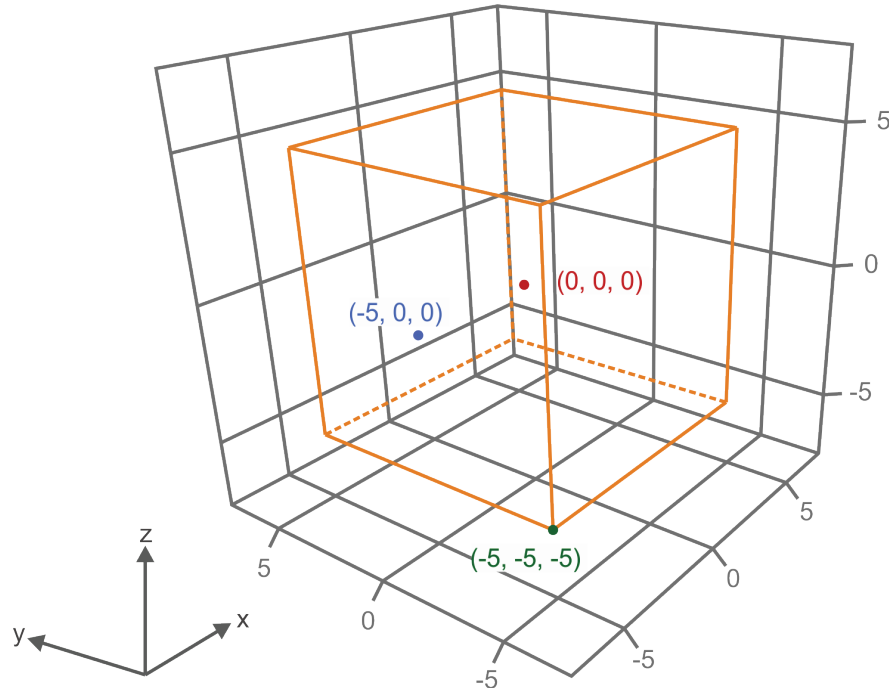


Figure 3.17: Origin coordinates for simulations with origin variation.

Table 3.8: Origin coordinates for simulations with origin variation.

	Origin [x, y, z]	Descriptive position
Case 1	0, 0, 0	Center of model
Case 2	-5, 0, 0	Center of model face
Case 3	-5, -5, -5	Vertex of model

Figure 3.19 (page 29) shows the cumulative block size distributions of performed simulations by varying the joint set origins. The left column represents the block area size distribution at the model face, the right column the corresponding block volume size distribution of the entire model. Considering the cumulative distributions, Case 1 and Case 2 differ slightly from Case 3. Although the block size distributions are similar graded, a narrower deviation of distributions of Case 3 can be noticed. Furthermore, the mean block sizes of the first two cases are rather identical, while the block sizes of the last case are smaller. The assembly of the mean block sizes in Figure 3.18 should summarize the results of the performed simulations.

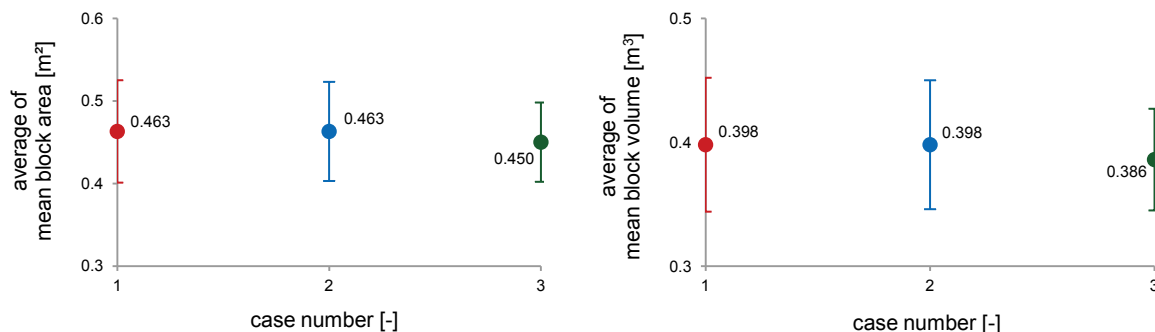


Figure 3.18: Joint set origin – Assembly of averaged mean block sizes in dependence of the case number.

The results of this test set-up indicate a certain influence of selecting different origins of joint sets. The center of the representative volume element (RVE) and the center of the model face as the origin offer almost equal block size distributions, merely the vertex case deviates marginally. This difference is caused by a combination between the boundary blocks criterion and the order of ‘block cutting’. In this case, the initially generated block volume has a maximum value but is treated as a boundary block. In Case 2 however, the same boundary block has a smaller volume due to the residual available spacing. Nevertheless, the origins for all subsequent simulations were defined to be in the center of the model face (outcrop face, observation area) in order to eliminate the additional influence of different joint set origins and to keep a uniform initial situation.

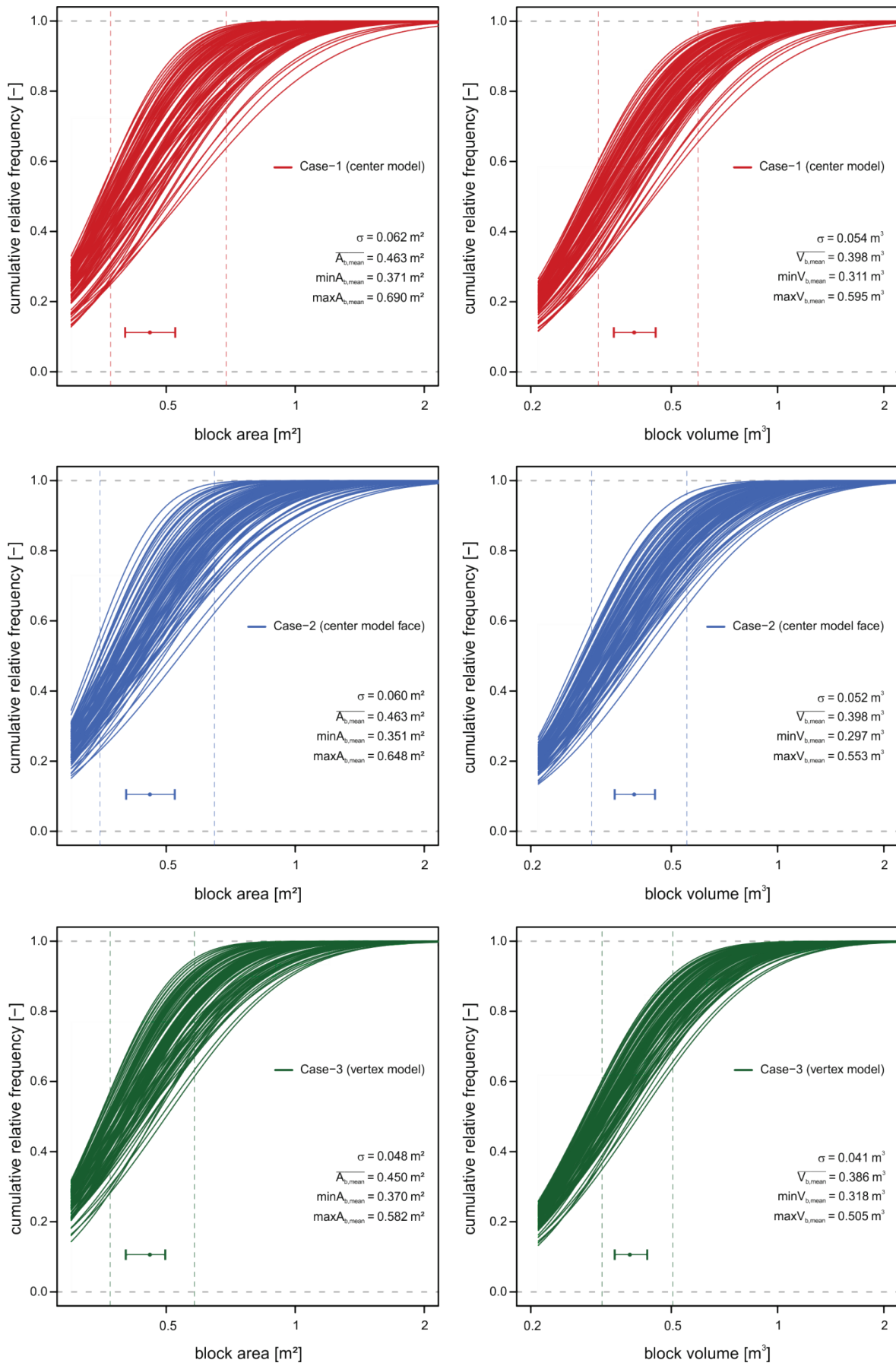


Figure 3.19: Cumulative block size distributions of origin testing.

4 Investigations

4.1 Minimally required outcrop area for determination of block sizes

A minimum outcrop area is necessary for obtaining reliable and representative block size distributions. For instance, if the outcrop area compared to the block areas at the outcrop is too small, essential information about joint set parameters (sp_i, p_i) may not be gathered. The intention of using the mean block area at the outcrop in a limitation value is that it contains the block size which is defined by the joint set parameters. Figure 4.1 illustrates a rock mass with two joint sets and two outcrops with different sizes. It is obvious that the outcrop area 1 delivers more detailed information about the joint set parameters than the outcrop area 2, where merely the orientation can be detected. Thus, the limitation ratio of the mean block area at the outcrop to the size of the outcrop area is used to provide a limit of application for determination of block sizes.

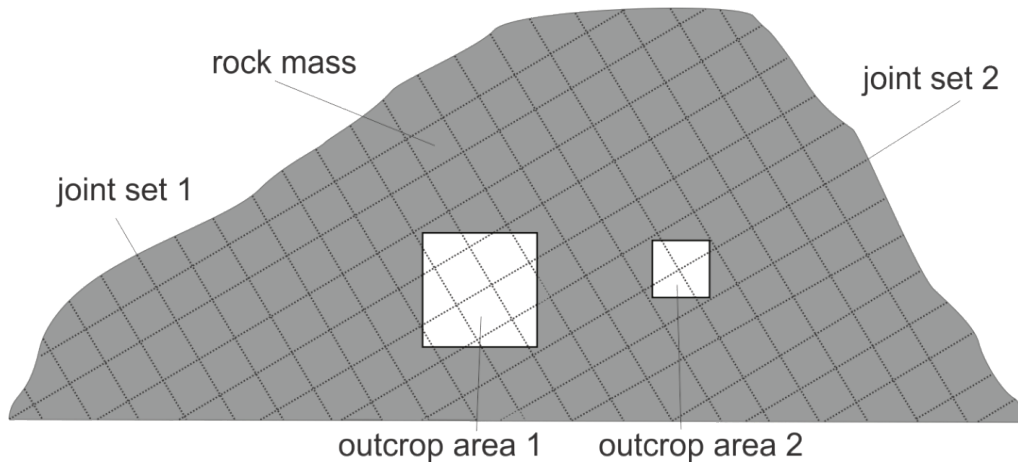


Figure 4.1: Sketch of a rock mass with two different outcrop areas.

The concept of an evaluation scheme for the block size determination is shown in Table 4.1.

Table 4.1: Concept of an evaluation scheme for block size determination.

		Limitation ratio		Determination of block size distribution	
$A_{b,mean}$	<	x		→	possible
A_{out}	>	x		→	impossible

The initial test set-up contains three mutually orthogonal joints sets, in which the orientation of the outcrop plane is parallel to the planes of joint set 3, *i.e.* the dip direction and dip angle of the outcrop area and joint set 3 are equal (test 1 – 13).

Additional, simulations were performed (test 14 – 51), where the joint sets were rotated around the z - axis. This should verify the minimally required outcrop area for cases, where the joints are not parallel to the outcrop area. The considered rotation cases are listed in Table 4.2.

Table 4.2: Considered rotation cases for the investigation of the minimally required outcrop area.

test numbers	z - rotation [°]
1 – 13	0.0
14 – 27	10.0
28 – 39	22.5
40 – 51	45.0

In the first step the entire model is created and the block areas of the outcrop face (y - z - plane; $x = -5$) and the block volumes of the entire model are extracted. In the next steps, the current model was cut by intersecting planes which define the outer block layer. The outer blocks are removed, leading to a new model size. This model has obviously a smaller outcrop area (A_{out}). The procedure is illustrated in Figure 4.2. Subsequently, the defined values are written into an output file. This described procedure was used for all simulations, respectively. For each calculation the spacing and the persistence of the joint sets were varied. Additionally, the boundary blocks and the replication factor have been considered. In Table 5.1 (see Appendix A), the test parameters are summarized.

After the calculation in 3DEC the received data were analyzed by the help of R. Firstly, the cumulative block size distributions for the block areas at the outcrop area and for the block volumes of the entire model were determined. As already mentioned above, the boundary blocks are removed from the model. Therefore, the cumulative block size distribution could not be determined for each test and each outcrop area. For instance, if the generated blocks are too big with respect to the outcrop area, they have contact to free space or contact to the outcrop frame (see Figure 3.2).

Thus, the output files rest partly empty and no distribution can be found for this explicit size of the outcrop area. All results of the simulations to obtain the minimally required outcrop area are attached to Table 5.2 (see Appendix A).

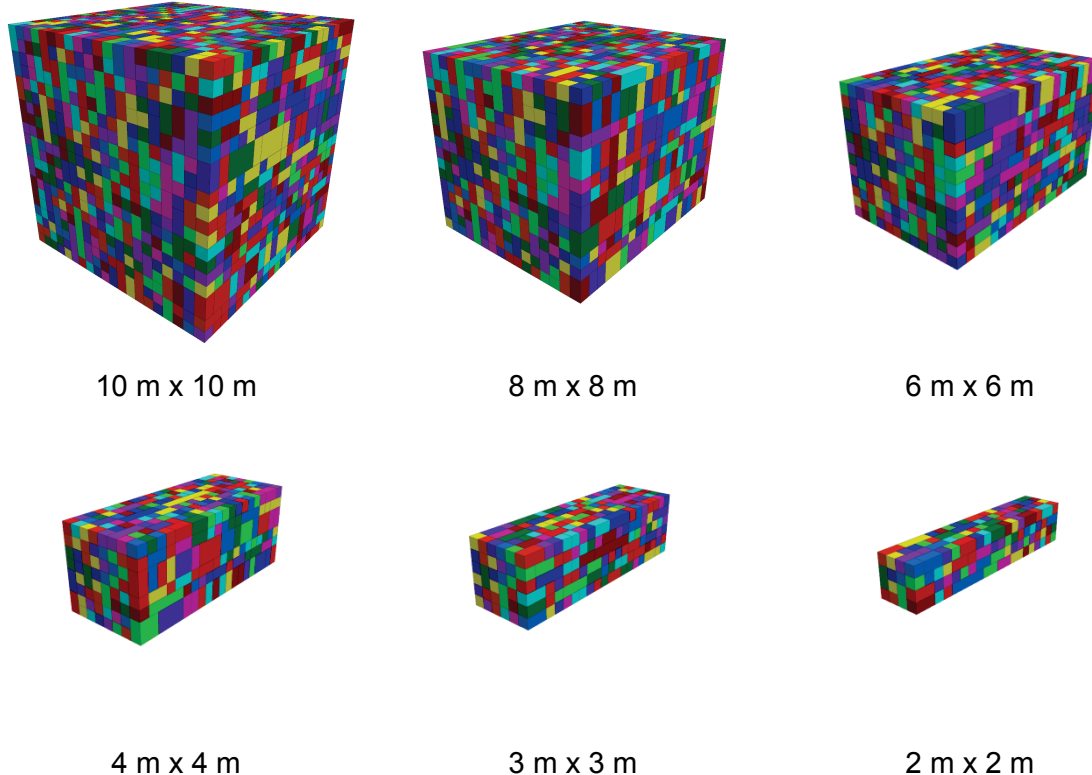


Figure 4.2: Illustration of the systematic minimization of the outcrop area.

Taking test 7 as an example, the cumulative log-normal distributions for the block area are illustrated in Figure 4.3. The six diagrams represent the areal distributions for each size of the outcrop area, beginning from the major outcrop area of 10 m x 10 m (red colored curves) up to the minor outcrop area of 2 m x 2 m (blue colored curves). A replication factor of $r = 100$ was utilized in order to achieve statistically representative results. For each outcrop area the average of all mean areas (vertically colored dashed lines), characteristic quantiles (vertically dark grey dashed lines), and their corresponding standard deviations were determined. The reasons for considering the quantiles are, on the one hand, a more detailed description of cumulative distributions, and, on the other hand, the quantiles are less sensitive to outliers in contrast to the arithmetic mean.

Looking at the cumulative distributions of test 7, two main conclusions can be drawn. A reduction of the outcrop dimensions leads to an increasing standard deviation of the averaged mean area. It was not possible to determine all block size distributions (blue colored outcrop case) due to the boundary blocks criterion. It seems likely that there is a limitation ratio between the averaged mean area and the outcrop area. In this example the outcrop area becomes too small ($A_{out} = 4 \text{ m}^2$) for these selected joint set parameters (see Table 4.3) in order to obtain an accurate distribution of the block size.

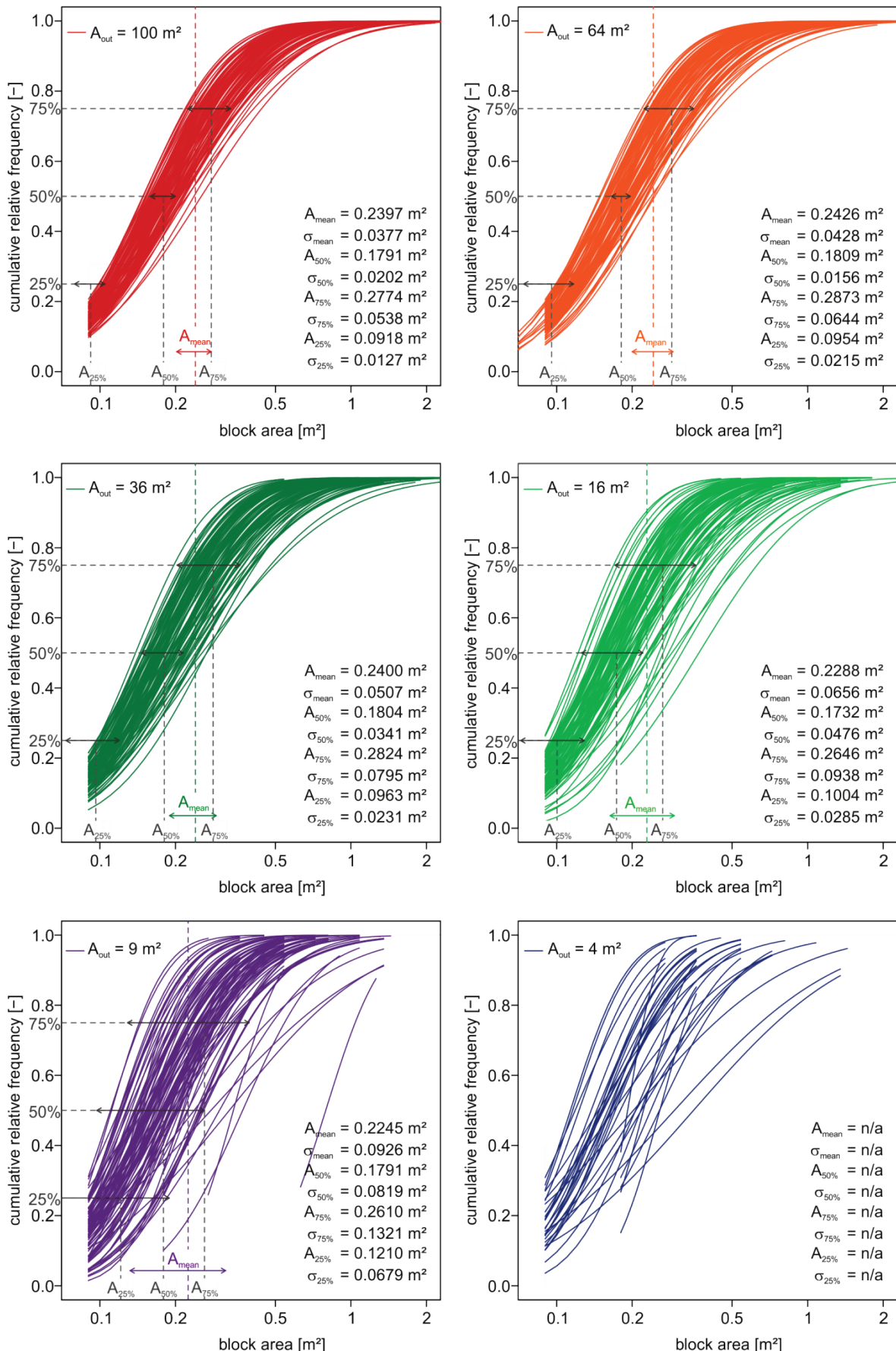


Figure 4.3: Cumulative block area distributions of test 7.

In the next step the ratio between the averaged mean block area and the outcrop area was calculated. The aim was to find the ratio at which the block size distribution cannot be determined. The ratio of $A_{\text{mean}}/A_{\text{out}}$ was increased up until only boundary blocks were generated (output file remained empty).

The results of test 7 depicted in Table 4.3 illustrate the procedure. In this case, the red colored value represents the maximum ratio.

Table 4.3: Block area results of test 7.

Test 7		z-rotation [°]			0.0		y-rotation [°]			0.0	
dd ₁ [°]	dip ₁ [°]	dd ₂ [°]	dip ₂ [°]	dd ₃ [°]	dip ₃ [°]	sp ₁ [m]	sp ₂ [m]	sp ₃ [m]	p ₁ [-]	p ₂ [-]	p ₃ [-]
0.0	90.0	0.0	0.0	90.0	90.0	0.3	0.3	0.3	0.6	0.6	0.6
A _{out} [m ²]	A _{mean} [m ²]	A _{mean} /A _{out} [-]	$\sigma_{A\text{mean}}$ [m ²]	A _{50%,mean} [m ²]	$\sigma_{A50\%,\text{mean}}$ [m ²]	A _{75%,mean} [m ²]	$\sigma_{A75\%,\text{mean}}$ [m ²]	A _{25%,mean} [m ²]	$\sigma_{A25\%,\text{mean}}$ [m ²]		
100.0	0.2397	0.0024	0.0377	0.1791	0.0202	0.2774	0.0538	0.0918	0.0127		
64.0	0.2426	0.0038	0.0428	0.1809	0.0156	0.2873	0.0644	0.0954	0.0215		
36.0	0.2400	0.0067	0.0507	0.1804	0.0341	0.2824	0.0795	0.0963	0.0231		
16.0	0.2288	0.0143	0.0656	0.1732	0.0476	0.2646	0.0938	0.1004	0.0285		
9.0	0.2245	0.0249	0.0926	0.1791	0.0819	0.2610	0.1321	0.1210	0.0679		
4.0	n.a.	n.a.	n.a.	n.a.	n.a.	n.a.	n.a.	n.a.	n.a.		

The above mentioned analysis was performed for all tests and led to the following diagram in Figure 4.4 summarizing the maximum ratios.

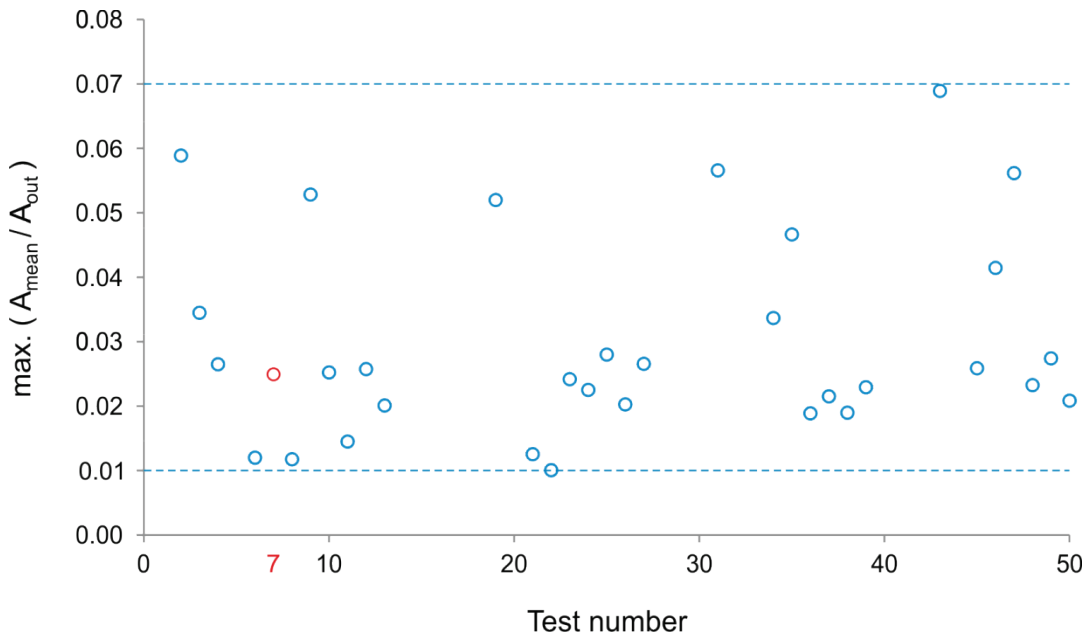


Figure 4.4: Compilation of the maximal ratio $A_{\text{mean}}/A_{\text{out}}$.

The diagram shows the maximal $A_{\text{mean}}/A_{\text{out}}$ ratio on the vertical axis against the test number on the horizontal axis. Obviously, all values are located between the ratio 0.01 and 0.07. Having in mind that a *maximum ratio value* were captured only, if for a specific size of the outcrop area the block size distribution could not be determined, this range can be interpreted as a confidence interval (*i.e.* only partly statements are feasible). For a ratio below 0.01, reliable statements about block size distributions can be made, because the outcrop area with respect to the averaged mean area is large enough. Imagining a ratio above 0.25 no reliable conclusions can be drawn concerning the block size or block size distribution, because the averaged mean area becomes too large compared to the outcrop area. Moreover, if the ratio is too high, the number of visible block faces at the outcrop area may be too low in order to gather sufficient information about the joint sets and thus, no adequate drawbacks can be made anymore. Figure 4.5 shows two examples illustrating the problem of insufficient information about the joint set parameters caused by exceeded limitation ratios of 0.25 and 1.00.

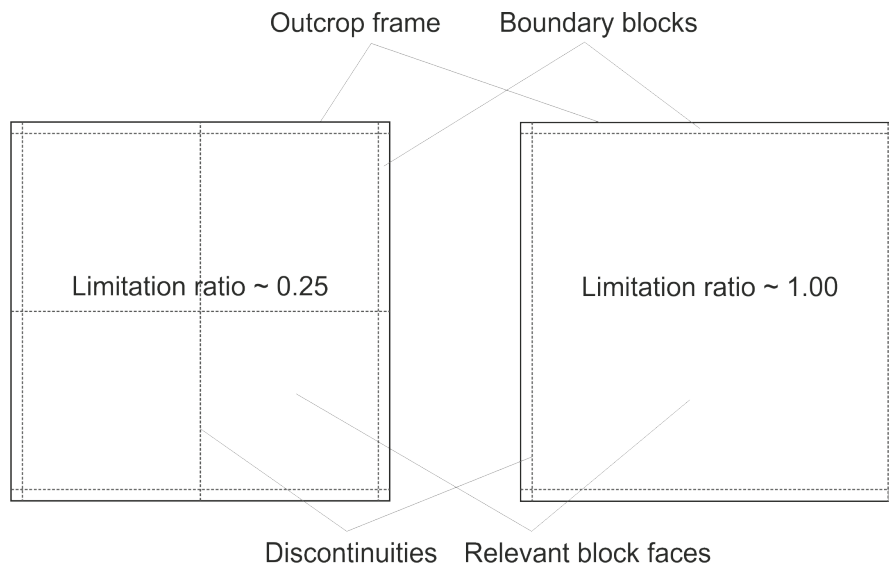


Figure 4.5: Examples of an outcrop at a limitation ratio of 0.25 (left illustration) and 1.00 (right illustration).

To strengthen the significance of the limitation ratio of 0.01, the averaged mean area and the averaged quantiles for each test (calculation was replicated 100 times) in dependence of the different outcrop areas were determined and analyzed. As a further example the results of test 14 (joint sets are rotated 10° around z - axis) are illustrated in Table 4.4.

Table 4.4: Block area results of test 14.

Test 14		z-rotation [°]			10.0		y-rotation [°]			0.0	
dd ₁ [°]	dip ₁ [°]	dd ₂ [°]	dip ₂ [°]	dd ₃ [°]	dip ₃ [°]	sp ₁ [m]	sp ₂ [m]	sp ₃ [m]	p ₁ [-]	p ₂ [-]	p ₃ [-]
10.0	90.0	0.0	0.0	100.0	90.0	0.3	0.3	0.3	0.8	0.8	0.8
A _{out} [m ²]	A _{mean} [m ²]	A _{mean} /A _{out} [-]	$\sigma_{A\text{mean}}$ [m ²]	A _{50%,mean} [m ²]	$\sigma_{A50\%,\text{mean}}$ [m ²]	A _{75%,mean} [m ²]	$\sigma_{A75\%,\text{mean}}$ [m ²]	A _{25%,mean} [m ²]	$\sigma_{A25\%,\text{mean}}$ [m ²]		
100.0	0.1248	0.0012	0.0091	0.0914	0.0000	0.1645	0.0302	0.0914	0.0000		
64.0	0.1219	0.0019	0.0093	0.0914	0.0000	0.1578	0.0352	0.0909	0.0037		
36.0	0.1258	0.0035	0.0114	0.0923	0.0052	0.1622	0.0367	0.0914	0.0000		
16.0	0.1206	0.0075	0.0138	0.0914	0.0000	0.1467	0.0403	0.0833	0.0132		
9.0	0.1370	0.0152	0.0264	0.1060	0.0324	0.1622	0.0559	0.0921	0.0069		
4.0	0.1307	0.0327	0.0278	0.1014	0.0287	0.1474	0.0556	0.0925	0.0094		

Considering the conclusions made above, the limitation ratio has to be arranged between the outcrop area of 4 m x 4 m and 3 m x 3 m (red horizontal line). In Figure 4.6 the corresponding A_{out}-A_{mean}-diagram is shown. A variation takes place where the current ratio exceeds the established limitation ratio of 0.01 (red dashed circle).

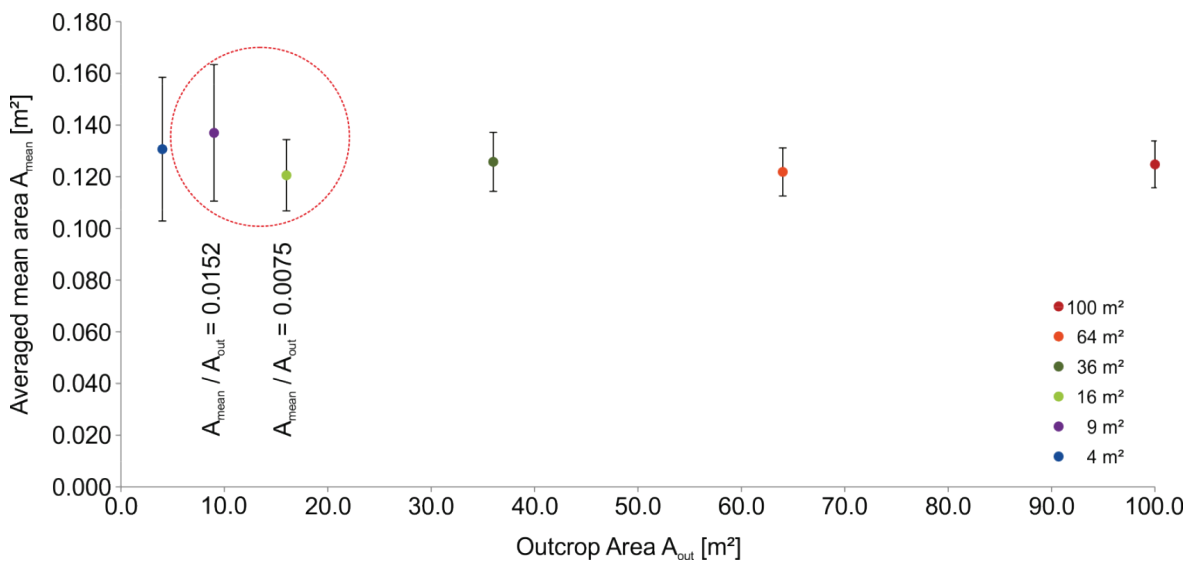


Figure 4.6: Outcrop area versus averaged mean area (test 14).

A similar irregularity can be observed on closer inspection of the quantiles (see Figure 4.7). Decreasing the outcrop area leads to a higher deviation of the quantiles (red dashed circle). An explicit deviation at a limitation ratio of 0.01 cannot be confirmed by all quantiles, in this case (test 14) merely the 50%-quantiles show the expected deviation.

These deviations at a limitation ratio of 0.01 can be detected in a majority of the tests.

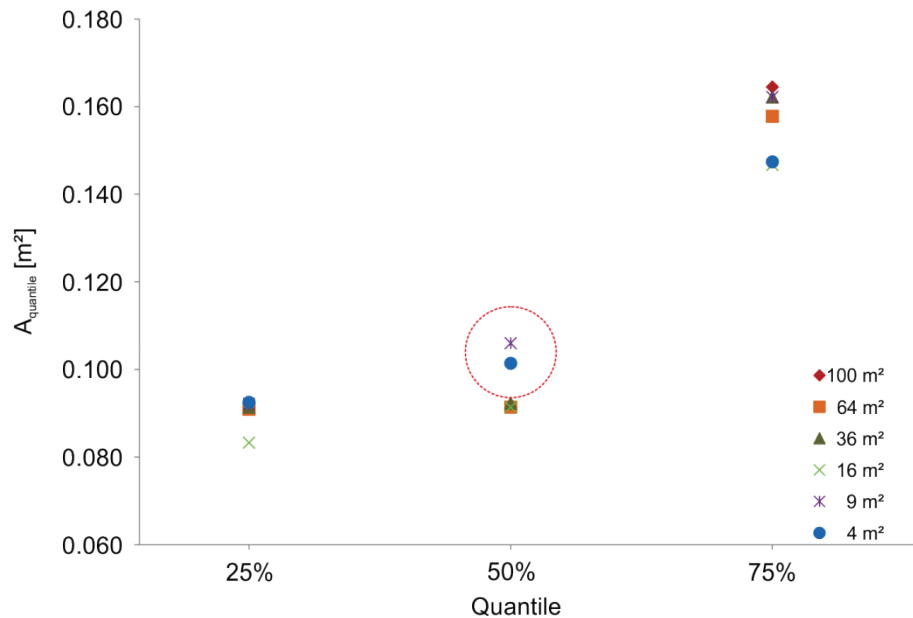


Figure 4.7: Quantiles versus $A_{quantile}$ (test 14).

The present investigations showed that an increasing ratio of averaged mean area to the outcrop area leads to an increasing variation of the representative distribution parameters (mean block area, mean quantiles). Nevertheless, if the mean block area at the outcrop is smaller than 1% of the outcrop area, reliable block size distributions can be found. A diagram (Figure 4.8) was developed to illustrate the previously described findings. It shows the outcrop area on the abscissa and the mean block area on the ordinate, both of which having a logarithmic scale. The values depend on the limitation ratio. A fast and easy model test for the reliability of block size distributions derived from simulations can be made.

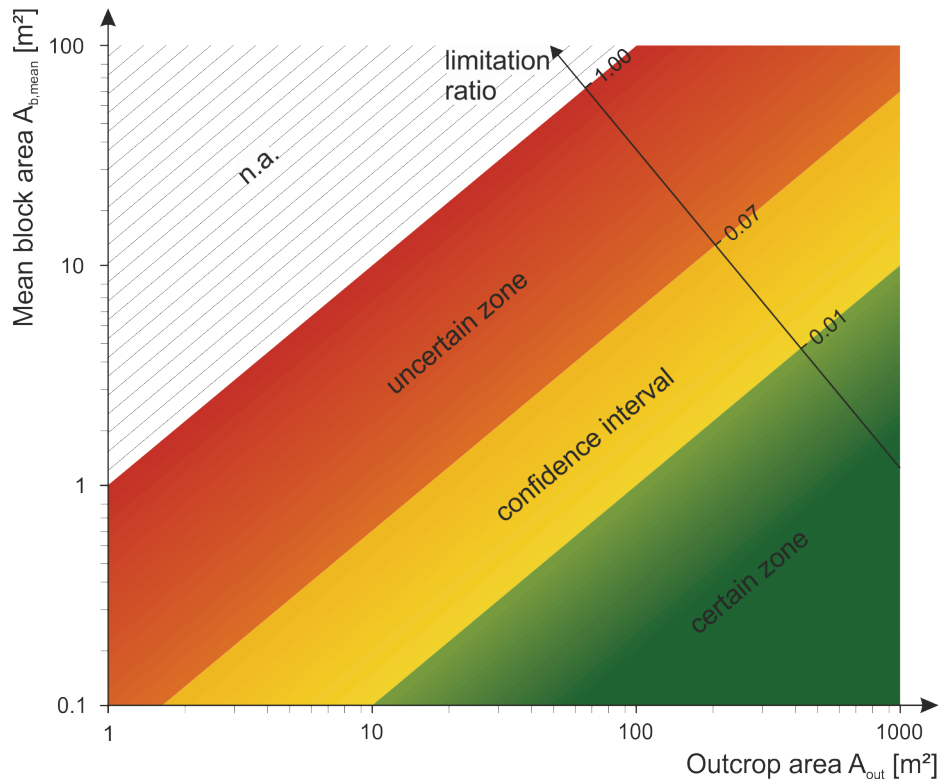


Figure 4.8: Evaluation diagram for minimally required outcrop area.

Figure 4.8 is divided into four categories:

- The *certain zone* (green) has a range of the limitation ratio between 0.00 and 0.01. Accurate block size distributions are achieved.
- The *confidence zone* (yellow) has a range of the limitation ratio between 0.01 and 0.07. Reliable distributions can be developed partially only. This zone should be treated with care.
- The *uncertain zone* (red) in the range of the limitation ratio between 0.07 up to 1.00. The determination of block size distributions is barely or not possible at all .
- The zone with a limitation ratio bigger than 1.00 is the hatched area. No distributions are found because the generated block is larger than the defined rock mass model face.

The proposed limitation ratio is valid for three mutually orthogonal joint sets. In addition, the number of visible block faces on the outcrop area and the block shapes (see also (Palmström, 2001 pp. 9-10)) are not considered in this work. Further investigations are recommended.

4.2 Development of a calculation tool for mean block size estimation

The investigations described in Chapter 4.1 provide sufficient information about the correlation between the calculated mean block volume from non-persistent joint sets and the according mean block volume from persistent joint sets. The ratio between the two mean block volumes is defined as the transformation factor (equation (3)).

$$T = \frac{V_{\text{per}}}{V_{\text{per}}} \quad (3)$$

V_{per} is the block volume determined as the product of the mean spacings of three persistent joint sets. V_{per} is the corresponding mean block volume determined from simulations with non-persistent joint sets. The spacings of the persistent and non-persistent joint sets are the same. For better understanding, the procedure is illustrated for the results of test 14 (see Appendix A).

Table 4.5: Block volume results of test 14.

Test 14		z-rotation [°]				10.0		y-rotation [°]			0.0	
dd ₁ [°]	dip ₁ [°]	dd ₂ [°]	dip ₂ [°]	dd ₃ [°]	dip ₃ [°]	sp ₁ [m]	sp ₂ [m]	sp ₃ [m]	p ₁ [-]	p ₂ [-]	p ₃ [-]	
10.0	90.0	0.0	0.0	100.0	90.0	0.3	0.3	0.3	0.8	0.8	0.8	
V _{model} [m ³]	V _{mean} [m ³]	σ _{Vmean} [m ³]	V _{50%,mean} [m ³]	σ _{V50%,mean} [m ³]	V _{75%,mean} [m ³]	σ _{V75%,mean} [m ³]	V _{25%,mean} [m ³]	σ _{V25%,mean} [m ³]				
1000.0	0.0520	0.0037	0.0362	0.0129	0.0543	0.0027	0.0270	0.0000				
640.0	0.0516	0.0041	0.0378	0.0133	0.0545	0.0038	0.0270	0.0000				
360.0	0.0514	0.0050	0.0367	0.0130	0.0548	0.0046	0.0270	0.0000				
160.0	0.0506	0.0065	0.0364	0.0129	0.0556	0.0073	0.0270	0.0000				
90.0	0.0502	0.0082	0.0373	0.0132	0.0575	0.0119	0.0275	0.0038				
40.0	0.0487	0.0092	0.0362	0.0129	0.0586	0.0139	0.0281	0.0053				
V _{per}	T _{mean}		T _{50%}		T _{75%}		T _{25%}					
0.027	1.92		1.34		2.01		1.00					

In this case V_{per} is calculated as

$$V_{\text{per}} = 0.3 \text{ m} \cdot 0.3 \text{ m} \cdot 0.3 \text{ m} = 0.027 \text{ m}^3 \quad (4)$$

The according V_{per} for all cases is selected at a model volume of 1000 m^3 (in this case: $V_{\text{per}} = 0.052 \text{ m}^3$). The limitation ratio (according to the mean block area) of smaller than 1% has to be fulfilled (in this case: $A_{\text{mean}}/A_{\text{out}} = 0.0012 < 0.01$). The red horizontal line in Table 4.5 show where the limitation ratio of 0.01 is arranged. The transformation factor T for mean block volume estimation is calculated as

$$T_{\text{mean}} = \frac{V_{\text{mean}}}{V_{\text{per}}} = \frac{0.052 \text{ m}^3}{0.027 \text{ m}^3} = 1.92 \quad (5)$$

The investigations of the all results in Appendix A show that the transformation factor is independent of spacing variation. It delivers constant values for a defined persistence. The transformation factor merely depends on the persistence. With the help of the proposed equation (3), it is easily possible to approximate the mean block volume of an arbitrary example with three mutually orthogonal joint sets by estimating the spacing and persistence:

$$V_{b,\text{mean}} = sp_1 \cdot sp_2 \cdot sp_3 \cdot T_{\text{mean}} \quad (6)$$

A similar relationship could be observed for the quantiles of the block size distribution. Therefore, the procedure was applied for the 25%--, 50%- and 75%-quantiles, as well. Figure 4.9 illustrates the fitted distributions of the transformation factor T in dependence on the average persistence of the joints, for each statistical dimension (mean value; 25%--, 50%- and 75%-quantiles). The plotted values were obtained from the results of the simulations described in Chapter 4.1.

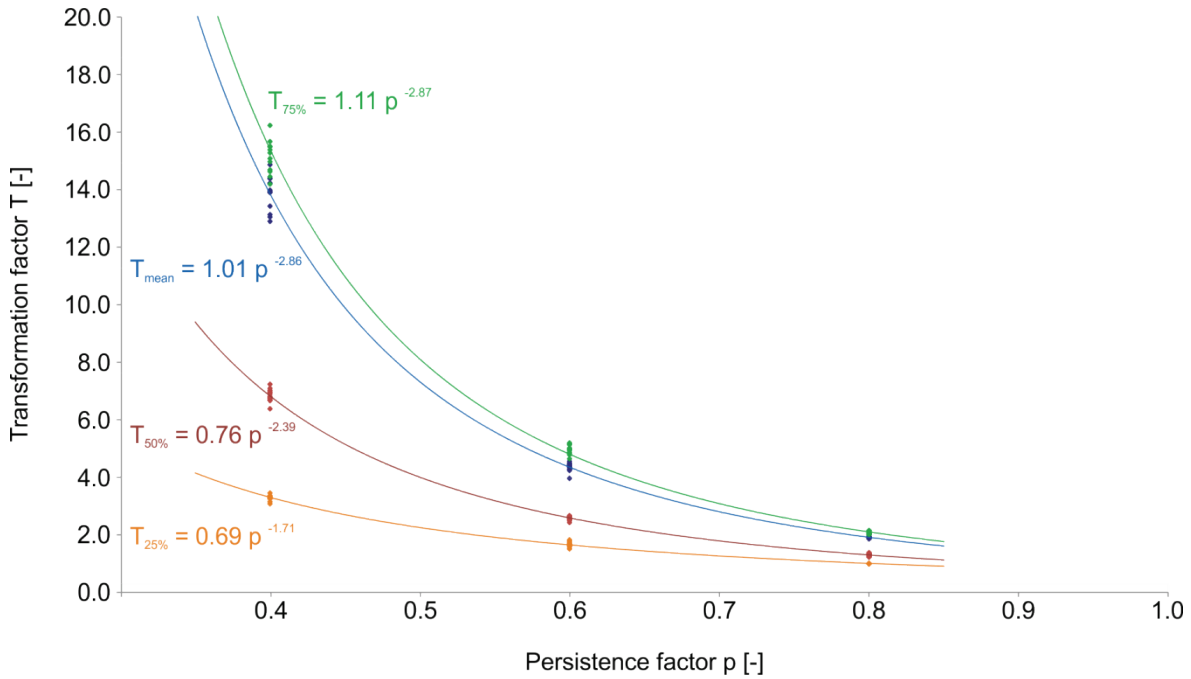


Figure 4.9: Correlation between persistence factor and transformation factor – Fitted curves for mean values (blue), 25%- (orange), 50%- (red) and 75%-quantiles (green).

The investigation showed that the transformation factor obeys a trend being best described by a power function. The transformation factor for mean value of the block volume is:

$$T_{\text{mean}} = 1.01 \cdot \left(\frac{p_1 + p_2 + p_3}{3} \right)^{-2.86} \quad (7),$$

and for the quantiles:

$$T_{75\%} = 1.11 \cdot \left(\frac{p_1 + p_2 + p_3}{3} \right)^{-2.87} \quad (8),$$

$$T_{50\%} = 0.76 \cdot \left(\frac{p_1 + p_2 + p_3}{3} \right)^{-2.39} \quad (9),$$

$$T_{25\%} = 0.69 \cdot \left(\frac{p_1 + p_2 + p_3}{3} \right)^{-1.71} \quad (10).$$

The required transformation factor for an estimation of the distribution of the block volumes can be read off the diagram or by applying the respective formula.

It has to be pointed out that decreasing the persistence leads to a slightly increasing deviation of the transformation factor. If each joint set features a different persistence, the arithmetic mean has to be determined (see equation (7) to (10)). Investigations to prove the validity of using the arithmetic mean of the persistence are outlined in the next chapter.

Based on equation (2) by Cai *et al.* their term of persistence was replaced by the transformation factor. With this modification it is possible to calculate the mean block volumes as well as the block volume quantiles. Moreover, the following expressions (11) to (14) should be valid for three joint sets with arbitrary joint set parameters, e.g. different joint set spacing, different joint persistence and also for non-orthogonally orientated joint sets. The approach by Cai *et al.* merely delivers a block volume without any quantitative information. The new approach however, is able to give qualitative and quantitative information about the block size distribution. For calculating specific block volumes of a rock mass model following formulas are proposed:

$$V_{b,\text{mean}} = \frac{sp_1 \cdot sp_2 \cdot sp_3}{\sin\gamma_1 \cdot \sin\gamma_2 \cdot \sin\gamma_3} \cdot T_{\text{mean}} = \frac{sp_1 \cdot sp_2 \cdot sp_3}{\sin\gamma_1 \cdot \sin\gamma_2 \cdot \sin\gamma_3} \cdot 1.01 \cdot \left(\frac{p_1 + p_2 + p_3}{3}\right)^{-2.86} \quad (11),$$

$$V_{b,75\%} = \frac{sp_1 \cdot sp_2 \cdot sp_3}{\sin\gamma_1 \cdot \sin\gamma_2 \cdot \sin\gamma_3} \cdot T_{75\%} = \frac{sp_1 \cdot sp_2 \cdot sp_3}{\sin\gamma_1 \cdot \sin\gamma_2 \cdot \sin\gamma_3} \cdot 1.11 \cdot \left(\frac{p_1 + p_2 + p_3}{3}\right)^{-2.87} \quad (12),$$

$$V_{b,50\%} = \frac{sp_1 \cdot sp_2 \cdot sp_3}{\sin\gamma_1 \cdot \sin\gamma_2 \cdot \sin\gamma_3} \cdot T_{50\%} = \frac{sp_1 \cdot sp_2 \cdot sp_3}{\sin\gamma_1 \cdot \sin\gamma_2 \cdot \sin\gamma_3} \cdot 0.76 \cdot \left(\frac{p_1 + p_2 + p_3}{3}\right)^{-2.39} \quad (13),$$

$$V_{b,25\%} = \frac{sp_1 \cdot sp_2 \cdot sp_3}{\sin\gamma_1 \cdot \sin\gamma_2 \cdot \sin\gamma_3} \cdot T_{25\%} = \frac{sp_1 \cdot sp_2 \cdot sp_3}{\sin\gamma_1 \cdot \sin\gamma_2 \cdot \sin\gamma_3} \cdot 0.69 \cdot \left(\frac{p_1 + p_2 + p_3}{3}\right)^{-1.71} \quad (14).$$

In order to prove the validity of the equations, further simulations have been performed. The detailed evaluation can be found in the following Chapter 4.3

4.3 Evaluation of analytic block size calculation

This chapter is dedicated to the evaluation and validation of the above proposed formulas (equation (11) to (14)) for calculating the specific block volumes. Furthermore, the obtained results are compared with those of 3DEC and with the results calculated with the formula by Cai *et al.* (2004) (equation (2)). These investigations will prove that the developed formulas are able to calculate the block sizes on a comprehensive level. Additionally, it is possible to estimate a range of potential block volumes with respect to a statistical probability.

4.3.1 Evaluation of joint sets with different spacings

The proposed transformation factors (equation (7) to (10)) have been developed by varying the spacing of all three joint sets simultaneously. The following investigations will demonstrate that the specific block volume formulas (equation (11) to (12)) and the introduced transformation factors are valid for a jointed rock mass with different spacing for each joint set. The joint sets are perpendicular to each other and the rotation around the z - axis has been varied. Thus, three tests have been performed. The model dimension, the joint set origins and the replication factor are the same as for previous simulations.

The selected average joint spacing ranges between 0.2 m and 0.8 m. On the one hand, the computation of a model with a smaller spacing is more time consuming. On the other hand, a larger spacing leads to misleading results regarding the block size distribution because of the size of the model (exceeding the limitation factor). Test 1 features different spacing but equal persistence for each joint set. The joint sets are not rotated, *i.e.* the outcrop face and the joint set 3 have the same orientation.

Table 4.6: Joint set parameters for evaluation test 1.

Test 1

$dd_1 [^\circ]$	$dip_1 [^\circ]$	$dd_2 [^\circ]$	$dip_2 [^\circ]$	$dd_3 [^\circ]$	$dip_3 [^\circ]$	$sp_1 [m]$	$sp_2 [m]$	$sp_3 [m]$	$p_1 [-]$	$p_2 [-]$	$p_3 [-]$
0.0	90.0	0.0	0.0	90.0	90.0	0.8	0.4	0.2	0.9	0.9	0.9

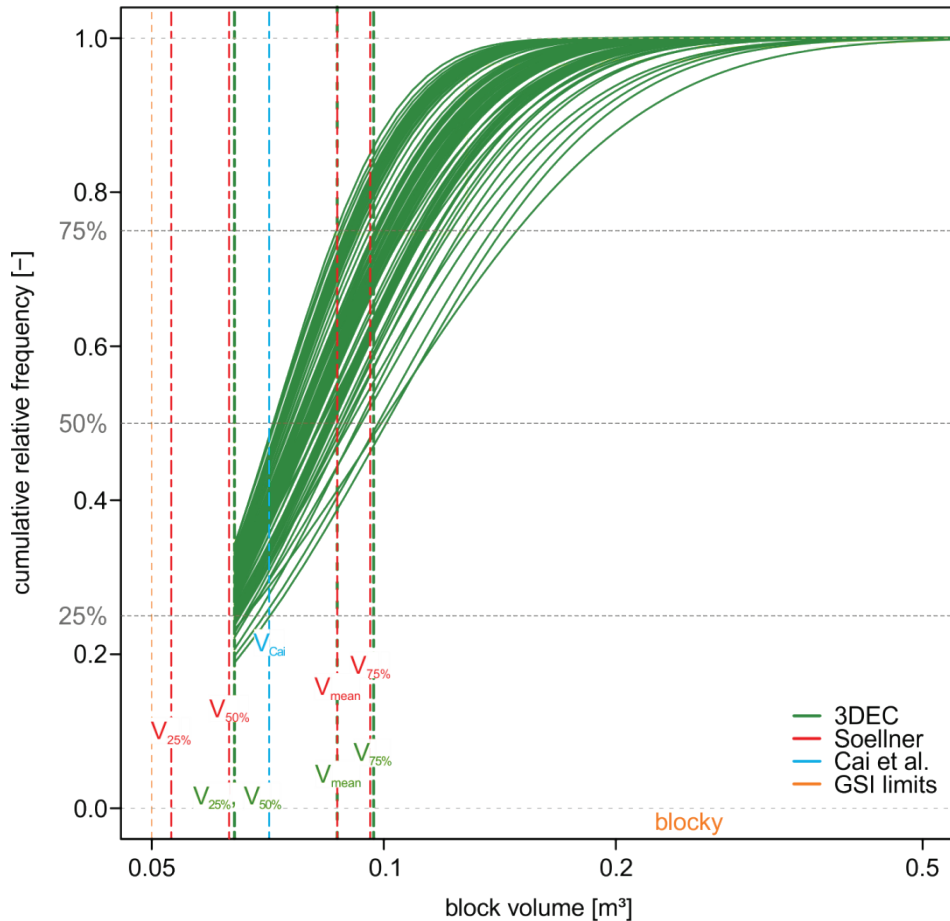


Figure 4.10: Cumulative block size distributions of evaluation test 1.

Table 4.7: Comparison of simulated and calculated results of evaluation test 1.

	$V_{\text{mean}} [\text{m}^3]$	$V_{75\%} [\text{m}^3]$	$V_{50\%} [\text{m}^3]$	$V_{25\%} [\text{m}^3]$	$V_{\text{Cai}} [\text{m}^3]$
3DEC	0.087	0.097	0.064	0.064	
Soellner	0.087	0.096	0.063	0.053	
Cai <i>et al.</i>					0.071
Deviation [%]	0.0	-0.9	-2.2	-17.4	

The values determined with 3DEC and with the proposed formulas correlate quite well, merely the 25%-quantiles deviate slightly. The block volume according Cai *et al.* is arranged above the 50%-quantiles. The reason why the 50%- and 25%-quantiles of 3DEC have the same block volumes is caused by relatively continuous joint sets where predominantly blocks with same sizes are generated.

Test 2 represents three mutually orthogonal joint sets, rotated around the z - axis for 15°. The joint persistence has been decreased compared to test 1 and different spacing has been chosen.

Table 4.8: Joint set parameters for evaluation test 2.

Test 2												
dd ₁ [°]	dip ₁ [°]	dd ₂ [°]	dip ₂ [°]	dd ₃ [°]	dip ₃ [°]	sp ₁ [m]	sp ₂ [m]	sp ₃ [m]	p ₁ [-]	p ₂ [-]	p ₃ [-]	
15.0	90.0	0.0	0.0	105.0	90.0	0.6	0.4	0.3	0.7	0.7	0.7	

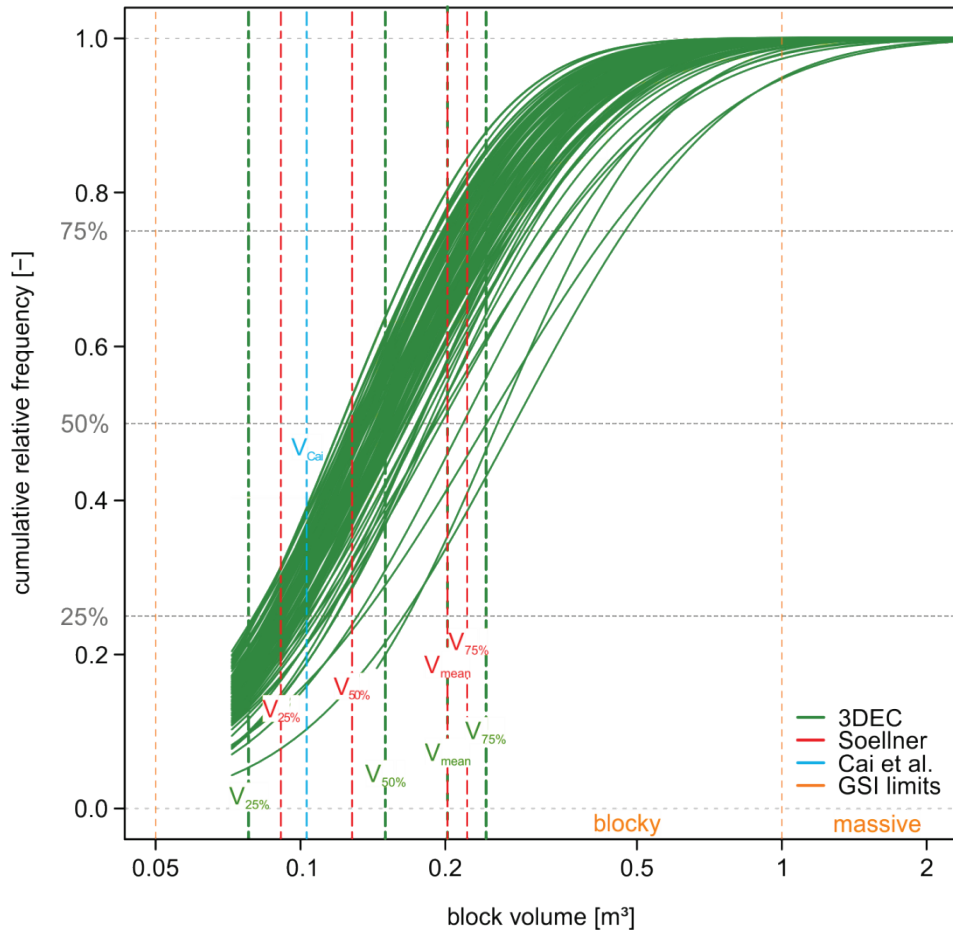


Figure 4.11: Cumulative block size distributions of evaluation test 2.

Table 4.9: Comparison of simulated and calculated results of evaluation test 2.

	V _{mean} [m ³]	V _{75%} [m ³]	V _{50%} [m ³]	V _{25%} [m ³]	V _{Cai} [m ³]
3DEC	0.202	0.243	0.150	0.078	
Soellner	0.202	0.222	0.128	0.091	
Cai et al.					0.103
Deviation [%]	0.0	-8.5	-14.4	17.2	

Although the joint persistence is lower, the results obtained with 3DEC and the calculated block volumes match quite well. However, the block volume according to Cai *et al.* is now located between the 25%- and 50%-quantiles meaning that the equation (2) according to Cai *et al.* for this model set-up would underestimate the block size.

4.3.2 Evaluation of joint sets with different persistences

The current investigation should confirm that the arithmetic mean of arbitrary persistence factors can be applied in equation (9) to (12). The test set-up is similar constructed as in Chapter 4.3.1 , merely different persistence factors were selected.

Table 4.10: Joint set parameters for evaluation test 3.

Test 3											
dd ₁ [°]	dip ₁ [°]	dd ₂ [°]	dip ₂ [°]	dd ₃ [°]	dip ₃ [°]	sp ₁ [m]	sp ₂ [m]	sp ₃ [m]	p ₁ [-]	p ₂ [-]	p ₃ [-]
0.0	90.0	0.0	0.0	90.0	90.0	0.4	0.4	0.4	0.5	0.6	0.9

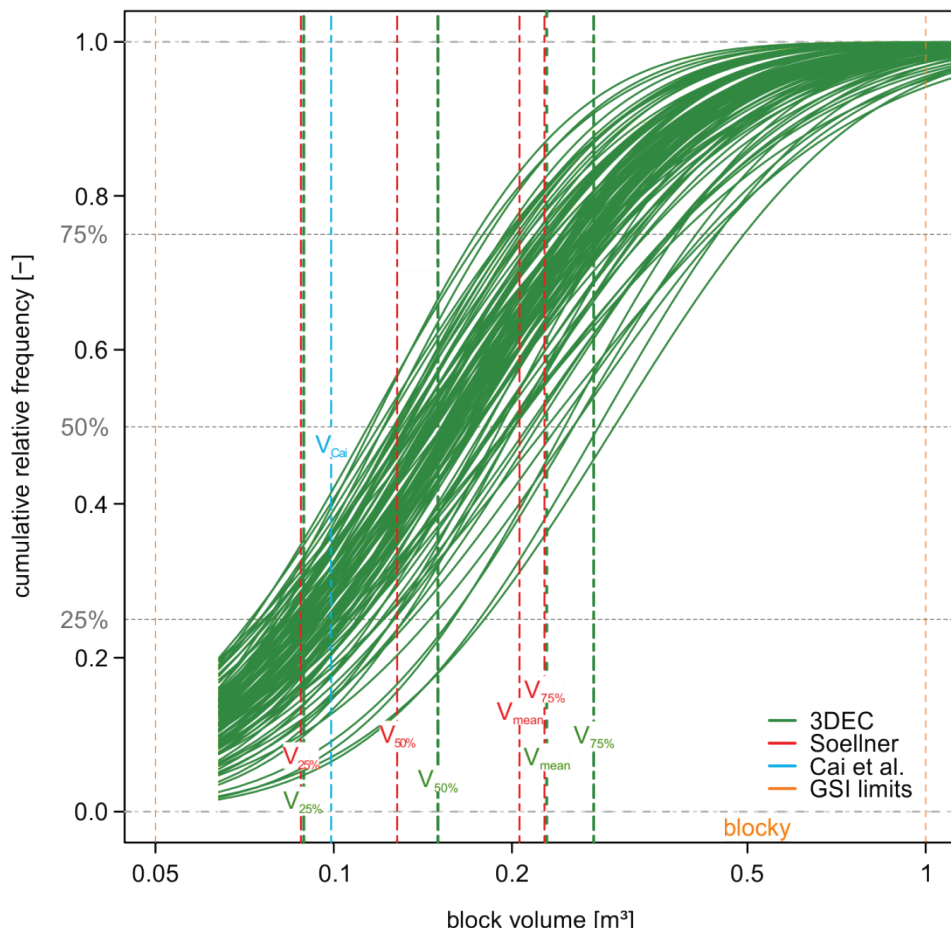


Figure 4.12: Cumulative block size distributions of evaluation test 3.

Table 4.11: Comparison of simulated and calculated results of evaluation test 3.

	$V_{\text{mean}} [\text{m}^3]$	$V_{75\%} [\text{m}^3]$	$V_{50\%} [\text{m}^3]$	$V_{25\%} [\text{m}^3]$	$V_{\text{Cai}} [\text{m}^3]$
3DEC	0.229	0.275	0.150	0.089	
Soellner	0.206	0.227	0.128	0.088	
Cai et al.					0.099
Deviation [%]	-10.0	-17.3	-14.5	-0.7	

At first sight, the deviations between the simulated and calculated block volumes seem to have increased, however this is based on the larger span of block size distributions. The block volume as per Cai *et al.* can be found in the lower quarter of the distributions.

Table 4.12: Joint set parameters for evaluation test 4.

Test 4												
$dd_1 [\circ]$	$dip_1 [\circ]$	$dd_2 [\circ]$	$dip_2 [\circ]$	$dd_3 [\circ]$	$dip_3 [\circ]$	$sp_1 [\text{m}]$	$sp_2 [\text{m}]$	$sp_3 [\text{m}]$	$p_1 [-]$	$p_2 [-]$	$p_3 [-]$	
40.0	90.0	40.0	0.0	130.0	90.0	0.5	0.5	0.5	0.4	0.5	0.9	

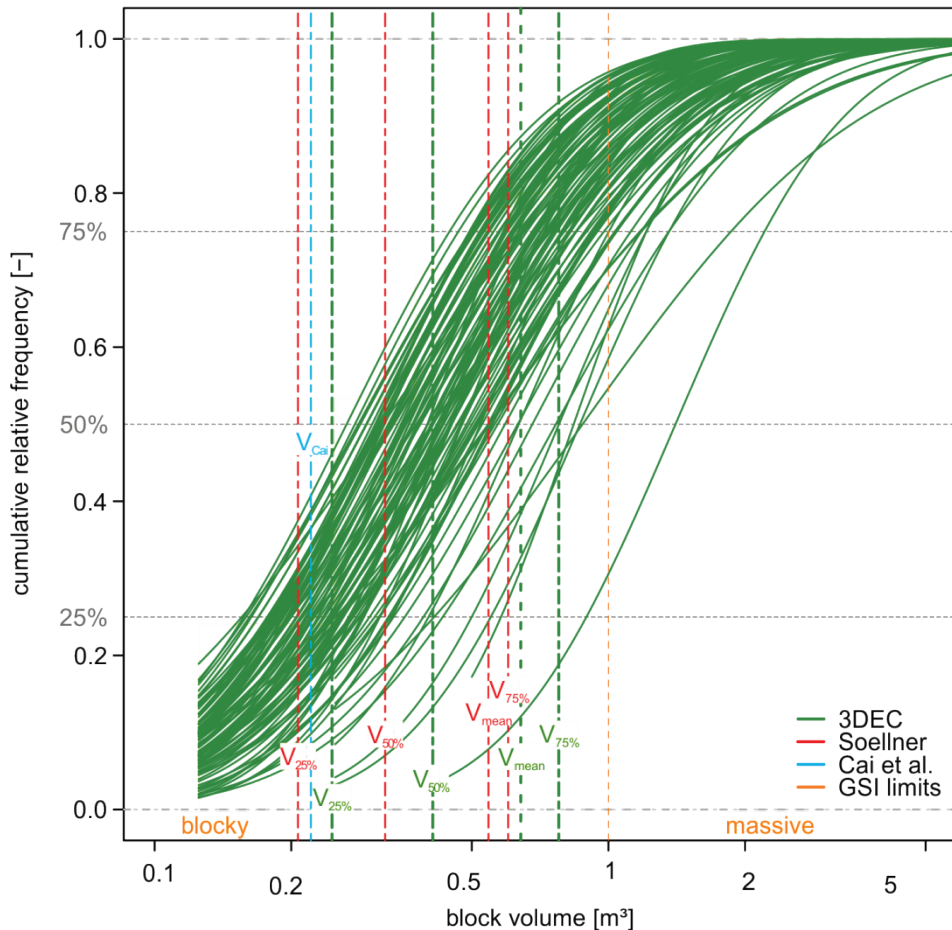


Figure 4.13: Cumulative block size distributions of evaluation test 4.

Table 4.13: Comparison of simulated and calculated results of evaluation test 4.

	$V_{\text{mean}} [\text{m}^3]$	$V_{75\%} [\text{m}^3]$	$V_{50\%} [\text{m}^3]$	$V_{25\%} [\text{m}^3]$	$V_{\text{Cai}} [\text{m}^3]$
3DEC	0.641	0.777	0.410	0.246	
Soellner	0.544	0.601	0.322	0.207	
Cai et al.					0.221
Deviation [%]	-15.1	-22.6	-21.6	-16.0	

Test 4 represents similar results compared to test 3.

4.3.3 Evaluation of non-orthogonal joint sets

In rock masses joint sets are typically not mutually orthogonally orientated. This investigation will prove the validity of the proposed formulas (equation (11) to (14)) by varying the relative angle γ_i between each joint set. In test 5 the angle γ_1 between joint set 1 and joint set 2 is set to 50°.

Table 4.14: Joint set parameters for evaluation test 5.

Test 5												
$dd_1 [\text{°}]$	$dip_1 [\text{°}]$	$dd_2 [\text{°}]$	$dip_2 [\text{°}]$	$dd_3 [\text{°}]$	$dip_3 [\text{°}]$	$sp_1 [\text{m}]$	$sp_2 [\text{m}]$	$sp_3 [\text{m}]$	$p_1 [-]$	$p_2 [-]$	$p_3 [-]$	
0.0	130.0	0.0	0.0	90.0	90.0	0.5	0.6	0.7	0.5	0.6	0.7	

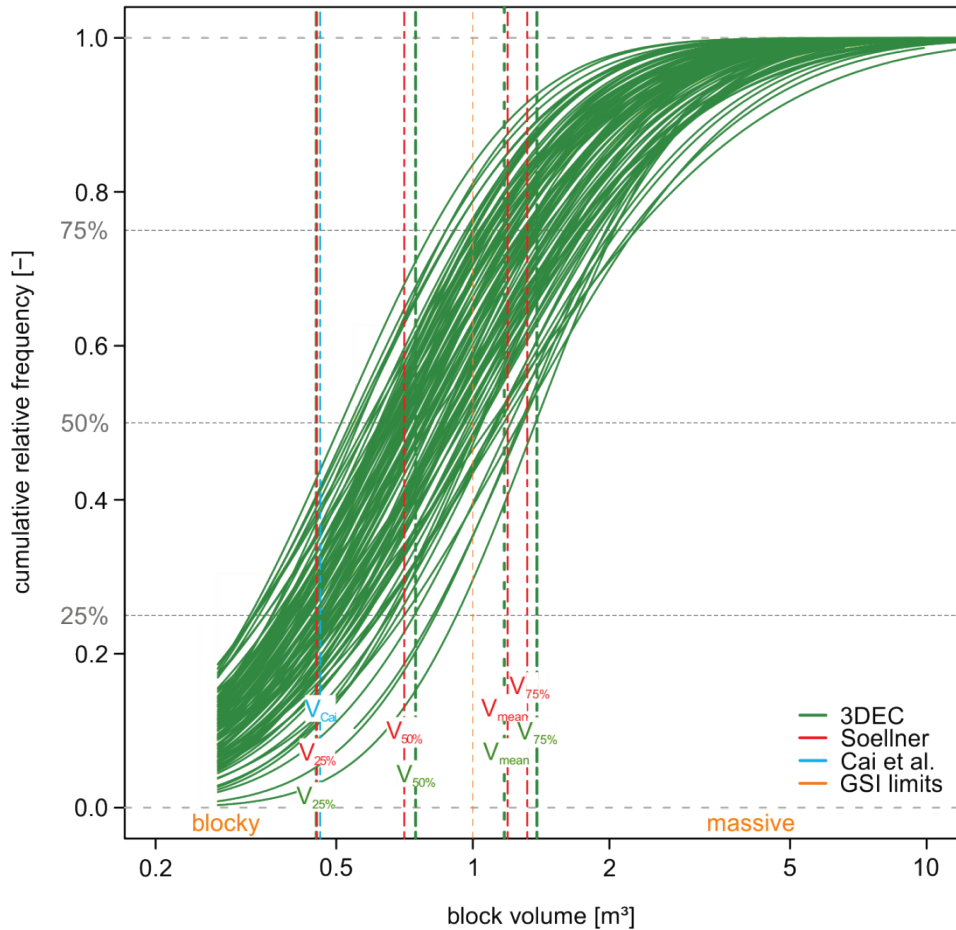


Figure 4.14: Cumulative block size distributions of evaluation test 5.

Table 4.15: Comparison of simulated and calculated results of evaluation test 5.

	$V_{\text{mean}} [\text{m}^3]$	$V_{75\%} [\text{m}^3]$	$V_{50\%} [\text{m}^3]$	$V_{25\%} [\text{m}^3]$	$V_{\text{Cai}} [\text{m}^3]$
3DEC	1.173	1.384	0.748	0.452	
Soellner	1.193	1.318	0.706	0.453	
Cai et al.					0.461
Deviation [%]	1.7	-4.8	-5.6	0.2	

Although different joint set parameters are used, the achieved results are in an excellent accordance. However, V_{Cai} can merely represent the 25%-quantiles of block volumes.

In test 6 all three joint sets are non-orthogonal, the relative angle between each joint set counts 64.3° , respectively.

Table 4.16: Joint set parameters for evaluation test 6.

Test 6												
dd ₁ [°]	dip ₁ [°]	dd ₂ [°]	dip ₂ [°]	dd ₃ [°]	dip ₃ [°]	sp ₁ [m]	sp ₂ [m]	sp ₃ [m]	p ₁ [-]	p ₂ [-]	p ₃ [-]	
0.0	120.0	90.0	30.0	120.0	90.0	0.7	0.8	0.4	0.8	0.9	0.6	

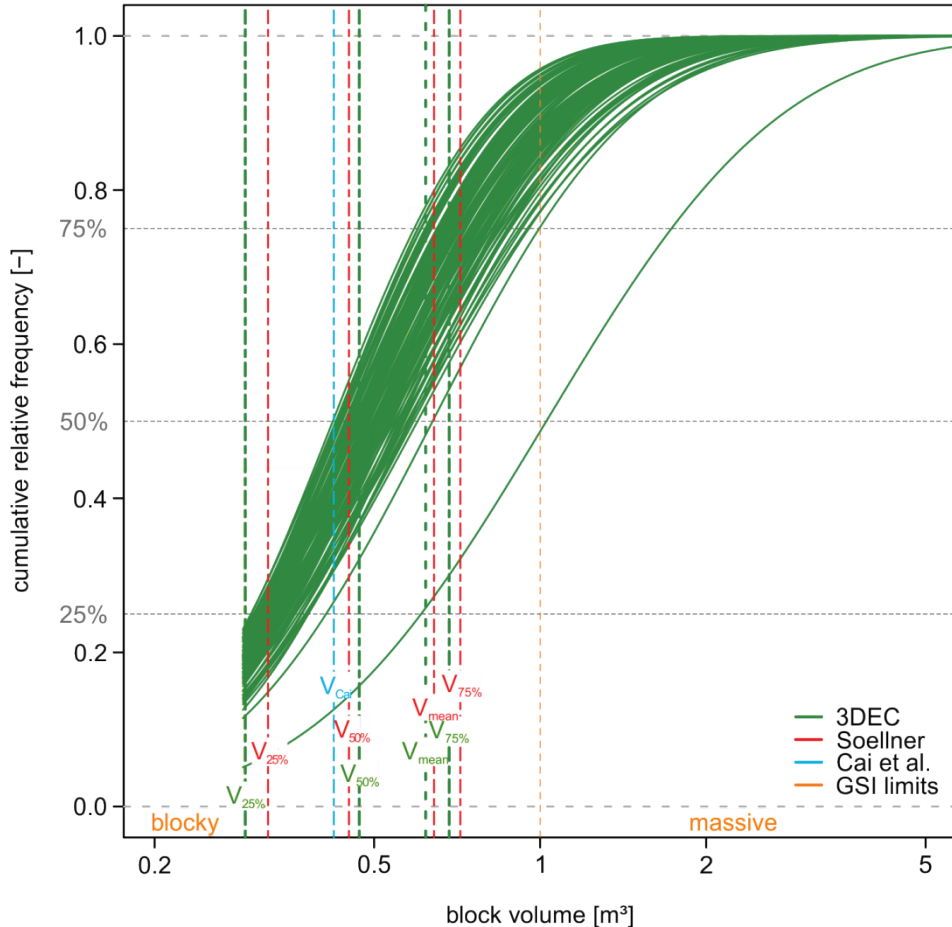


Figure 4.15: Cumulative block size distributions of evaluation test 6.

Table 4.17: Comparison of simulated and calculated results of evaluation test 6.

	V _{mean} [m ³]	V _{75%} [m ³]	V _{50%} [m ³]	V _{25%} [m ³]	V _{Cai} [m ³]
3DEC	0.620	0.684	0.470	0.292	
Soellner	0.658	0.727	0.445	0.331	
Cai et al.					0.405
Deviation [%]	6.6	6.5	-6.6	14.0	

The calculated values are arranged in an acceptable scope in order to approximately state a quantitative description of the block size distribution.

In the final test 7 the investigation should analyze whether the method is valid when standard deviations are added to orientation and spacing (calculated angles between each joint set: $\gamma_1 = 70^\circ$; $\gamma_2 = 55^\circ$; $\gamma_3 = 60^\circ$).

Table 4.18: Joint set parameters for evaluation test 7.

Test 7											
dd ₁ [°]	dip ₁ [°]	dd ₂ [°]	dip ₂ [°]	dd ₃ [°]	dip ₃ [°]	sp ₁ [m]	sp ₂ [m]	sp ₃ [m]	p ₁ [-]	p ₂ [-]	p ₃ [-]
0.0 ± 5	70.0 ± 5	0.0 ± 5	0.0 ± 5	60.0 ± 5	60.0 ± 5	0.7 ± 0.1	0.8 ± 0.1	0.4 ± 0.1	0.7	0.7	0.7

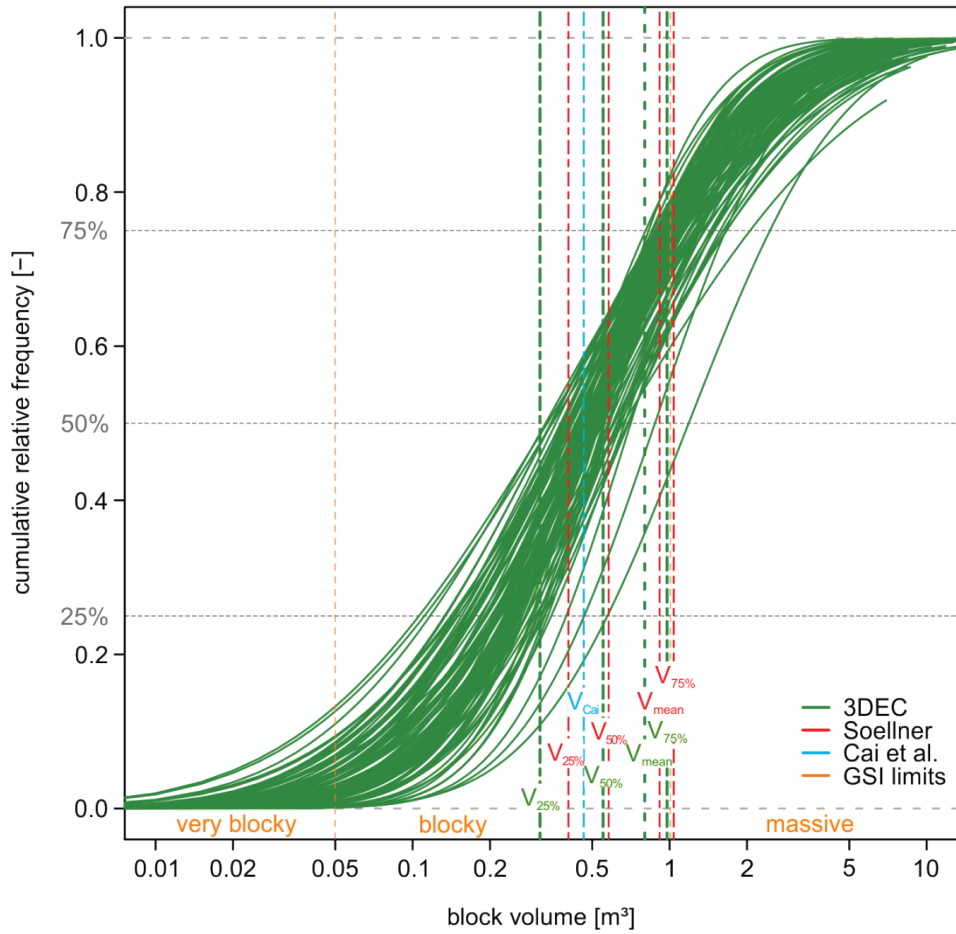


Figure 4.16: Cumulative block size distributions of evaluation test 7.

Table 4.19: Comparison of simulated and calculated results of evaluation test 7.

	V _{mean} [m ³]	V _{75%} [m ³]	V _{50%} [m ³]	V _{25%} [m ³]	V _{Cai} [m ³]
3DEC	0.800	0.977	0.551	0.313	
Soellner	0.945	1.042	0.601	0.428	
Cai <i>et al.</i>					0.482
Deviation [%]	18.1	6.7	9.1	36.8	

Although deviations are added, the results show quite well accordance. So the proposed formulas can also be applied to rock mass models with deviating joint set parameters.

In order to emphasize the validation, the simulated block volumes (means, quantiles) are compared to the calculated block volumes (means, quantiles) in Figure 4.19. The performed linear regression offers an acceptable correlation between analytical and numerical results (test 1 to 7).

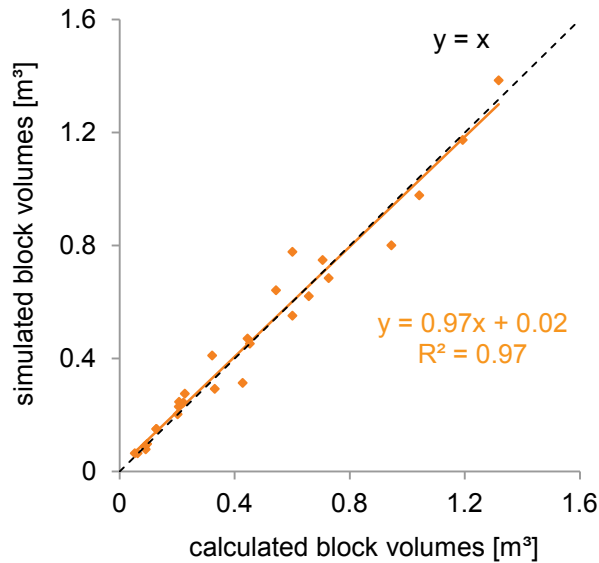


Figure 4.17: Comparison of simulated and calculated block volumes of evaluation tests.

The findings in Chapter 4.3 show quite well that the application of the proposed formulas is valid for three joint sets with arbitrary persistence, spacing, orientations and parameter variation. The calculated results are throughout in accordance to the simulated results.

The results of V_{Cai} vary from the 25%-quantiles up to values exceeding the 50%-quantiles. This fact indicates that this method is not sufficiently representative for calculating the block volume. Considering all analyzed cases, the approach of Cai *et al.* can be evaluated to be more conservative, *i.e.* the equivalent block volumes are arranged mostly in the lower distribution section leading to smaller GSI values. While the equivalent block volume according to Cai *et al.* only offers a single value without any quantitative statement about the probability of the according number of blocks, the introduced equations (11) to (14) enable the engineer to obtain a qualitative estimation of specific block volumes as well as a quantitative description of the block size distribution.

4.4 Determination of block size distribution from ShapeMetriX3D measurements

This chapter illustrates the application of the proposed method on an example of a tunnel face surveyed with the measurement system ShapeMetriX3D. The 3D image of a tunnel face is assessed for the joint set parameters in the software JMX Analyst, developed by 3GSM GmbH (2014). In the first step the structure sets are mapped. This map provides information about the orientation of joints. Figure 4.20 visualizes the tunnel face with three joint sets.

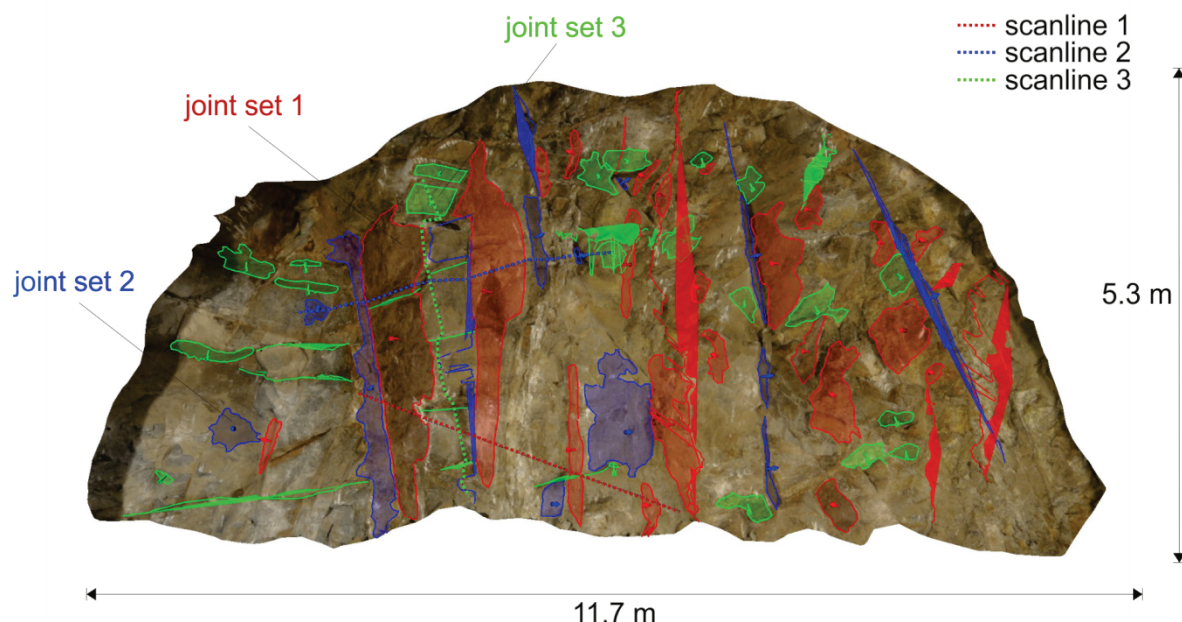


Figure 4.18: Illustration of analyzed joint sets of the investigated tunnel face (3D image provided by 3GSM GmbH (2014)).

The corresponding mean dip directions and mean dip angles are shown in Table 4.24.

Table 4.20: Investigated mean orientations of the joint sets.

	dd [°]	dip [°]	number of measurements [-]
joint set 1	227	88	28
joint set 2	124	79	16
joint set 3	348	40	30

Figure 4.21 shows the *Lambert projection* of the investigated joint sets as well as the great circle of the tunnel face. The poles of joint set 1 lie close together whereas the poles of joint set 2 and joint set 3 deviate more.

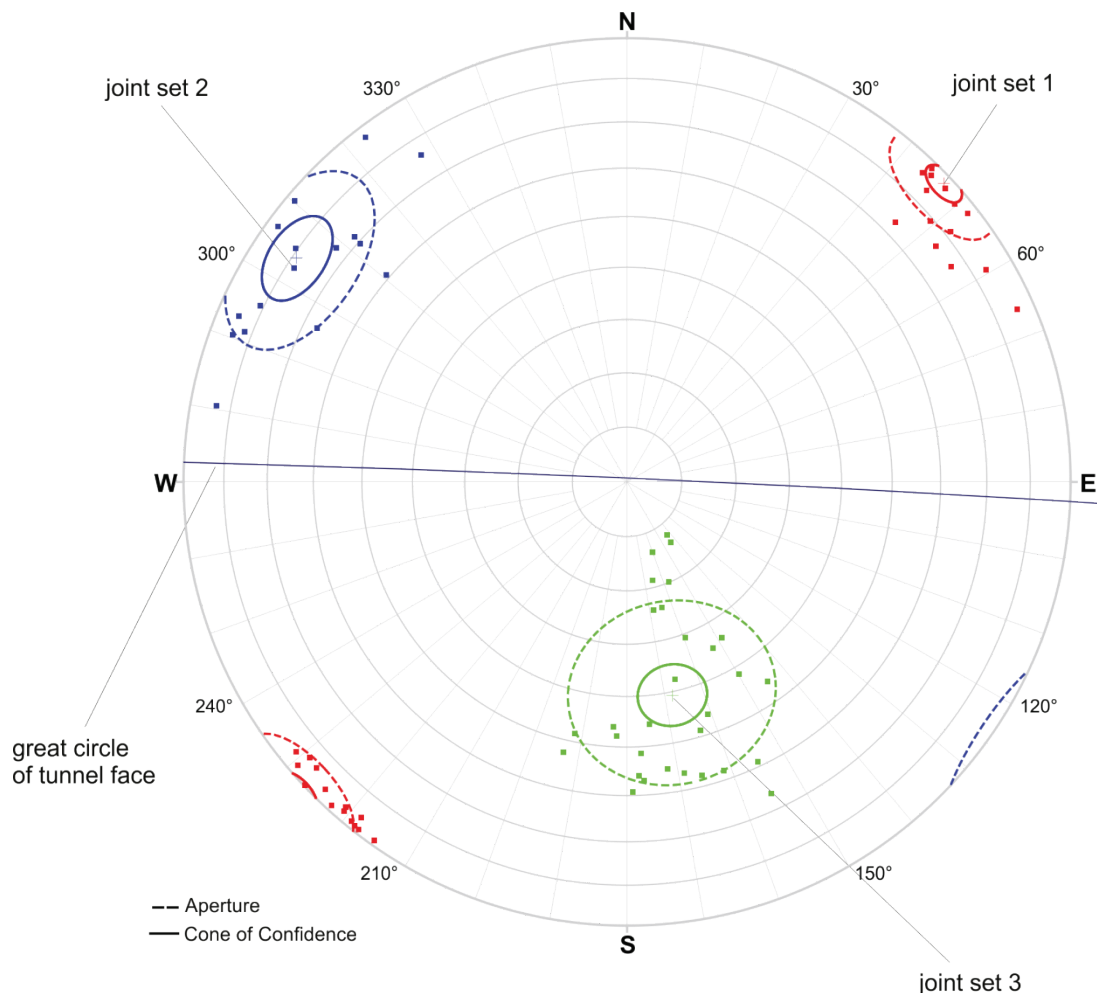


Figure 4.19: Lambert projection of investigated joint sets.

At next, the normal spacing of the joint sets was determined using the implemented scanline tool. The traces of the scanlines are shown in Figure 4.20 (colored dashed lines). The results can be found in Table 4.25.

Table 4.21: Normal joint set spacing of the investigated joints sets.

	mean spacing [m]	minimal spacing [m]	maximal spacing [m]
joint set 1	0.7	0.7	0.7
joint set 2	0.9	0.2	1.5
joint set 3	0.8	0.5	1.2

The most challenging part of estimating the block size is the determination of the persistence of each joint set. This procedure requires a long-term experience in this field. Nevertheless, in this example the persistence is roughly estimated for demonstration purposes. The proposed persistence for each joint set is listed in Table 4.26.

Table 4.22: Proposed persistence factors of investigated joint sets.

	joint set 1	joint set 2	joint set 3
p [-]	0.9	0.7	0.4

In the last step, the angles between the joint sets are required in order to apply the new method. The convention for the respective angles can be found in Figure 2.3 p.9. Table 4.27 shows the proposed angles γ_i .

Table 4.23: Angles between investigated joint sets.

γ_1 [°]	γ_2 [°]	γ_3 [°]
77	70	72

After investigating the joint set parameters, the values can be inserted into the above introduced equations (11) to (14). The calculated feasible mean block volumes are shown in Table 4.28.

Table 4.24: Calculated block volumes.

$V_{b,\text{mean}}$ [m^3]	1.9
$V_{b,75\%}$ [m^3]	2.1
$V_{b,50\%}$ [m^3]	1.2
$V_{b,25\%}$ [m^3]	0.8

The results of the block size estimation state that 50% of all blocks in the investigated section should have a block volume between 0.8 m^3 and 2.1 m^3 . Thus, less than 25% of all blocks have a block volume smaller than 0.8 m^3 and greater than 2.1 m^3 , respectively. Due to these findings a potential range of GSI can be proposed. The joint or block wall condition is assumed to be in a *good* range. The estimation of the GSI is illustrated in Figure 4.22.

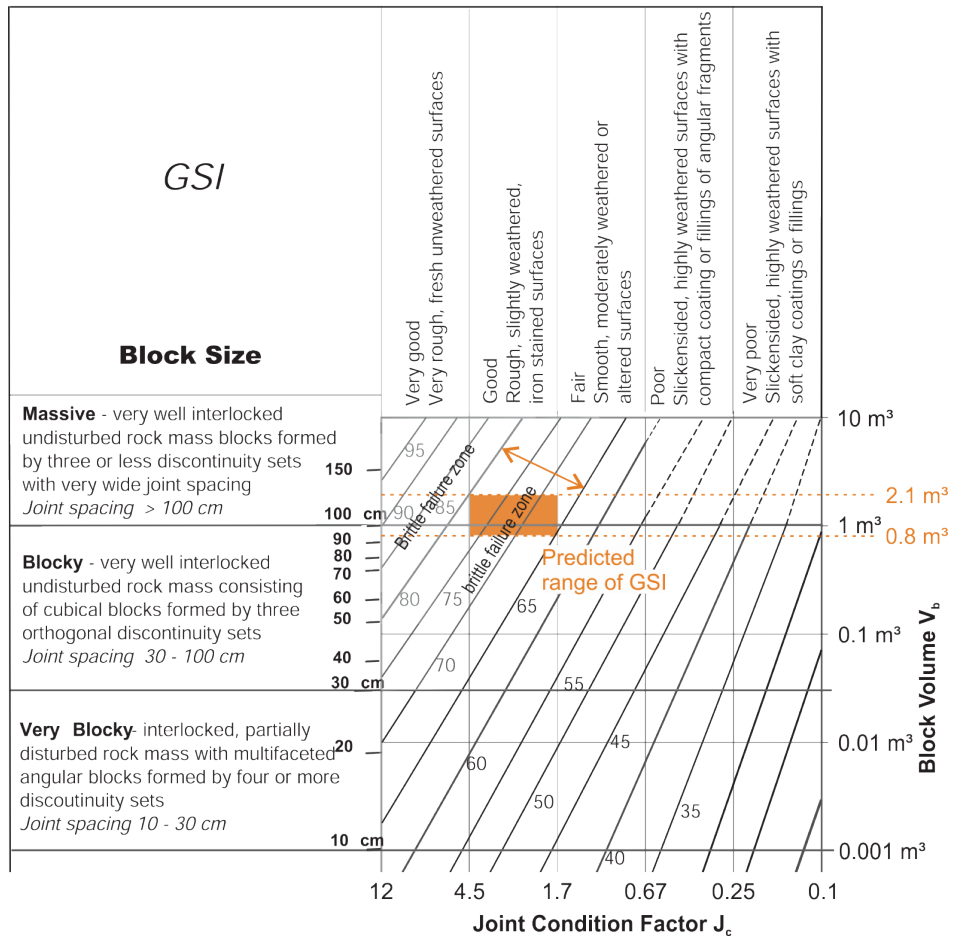


Figure 4.20: Estimation of a potential GSI range (chart modified from Cai et al. (2004)).

Although the investigated mean spacings are arranged in the upper section of the *blocky* range ($s_i < 1.0 \text{ m}$), the majority of the calculated block volumes are located in the lower section of the *massive* range. This difference is caused by the persistence which is included in the block volume, however, the spacing cannot respect the influence of the persistence. For instance, having an average joint set spacing of 100 cm for each of three joint sets, is according to the above illustrated GSI Chart (Figure 4.22) equivalent to a block volume of 1 m³. This statement is only valid if each persistence has value of $p_i = 1$, respectively. Otherwise, a decreasing persistence leads to an increasing block volume having already been shown in the present thesis.

The investigation of the tunnel face delivers a GSI range between 65 and 80 which represents 50% of all blocks in the considered tunnel section. With this introduced method it is possible to obtain a quantitative estimation of the GSI.

5 Conclusions

For investigating the block size distribution in a rock mass a numerical code was developed in 3DEC in order to analyze correlations between joint set parameters and the resulting block sizes. With this code it is feasible to insert arbitrary model dimensions and arbitrary discontinuity systems. The block volumes as well as the block areas of a defined outcrop face can be extracted automatically. Subsequently, the desired values are processed in a statistical analysis in which cumulative block size distributions are established. Moreover, a replication factor was proposed to ensure the statistically representativeness of simulations. A criterion for boundary blocks was introduced eliminating blocks generated by artificial model boundaries. An evaluation scheme for the minimally required outcrop area in dependence on mean block area was presented. Thus, the engineer can figure out if a considered exposed rock face can deliver reliable and sufficient information about block sizes. A transformation factor was found describing the correlation between block volumes generated by persistent and non-persistent joint sets. By implementing this factor in the formula of Cai *et al.*, advanced block size estimations can be performed. A volumetric block size distribution of a considered rock mass volume can be constructed. The proposed method was compared with simulation results and with the original method by Cai *et al.* The evaluation shows excellent agreement between simulated and calculated results and could therefore be validated. Finally, the new approach was applied on a practical example based on 3D imaging technology.

Although a direct correlation between the areal and volumetric block size distribution has not been found yet, a quantitative approach for block size estimation based on joint set spacing, persistence and orientation was developed. In this approach the quantiles of simulated block size distributions can be considered to obtain more detailed information about the calculated block volumes. The numerical code can be used for further research in the field of rock mass characterization, especially for determination of block size. Further investigation shall focus on finding a direct relation between areal and volumetric block size distribution. Additionally, *in situ* data should be collected in order to obtain a statistical correlation between *in situ* discontinuity distributions. Also the proposed method, which is valid for three joint sets, may be enhanced for four and more sets. The transformation factor should be tested in a wider range to ensure its correctness.

References

- (OEGG), Austrian Society for Geomechanics. 2010. *Guideline for the geotechnical design of underground structures with conventional excavation*. Salzburg, 2010.
- 3GSM GmbH. 2014. http://www.3gsm.at/dt/home_dt.asp?ID=2. [Online] 2014. [Cited: 07 15, 2014.]
- Barton, N.R., Lien, R. and Lunde, J. 1974. Engineering classification of rock masses for the design. *Rock Mechanics*. 1974, 6(4), pp. 189-239.
- Bieniawski, Z.T. 1973. Engineering classification of jointed rock masses. *Transactions of the South African Institution of Civil Engineers*. 1973, pp. 335-344.
- Cai, M., Kaiser, P.K., Uno, H., Tasaka, Y. and Minami, M. 2004. Estimation of rock mass strength and deformation modulus of jointed hard rock masses using the GSI system. *International Journal of Rock Mechanics and Mining Sciences*. 2004, 41(1), pp. 3-19.
- Elmouttie, M.K. and Poropat, G.V. 2012. A method to estimate in situ block size distribution. *Rock Mechanics and Rock Engineering*. 2012, 45, pp. 401-407.
- Giafferi, J.L., Amelot, A., Andre, D. and Berbet, F. 2003. AFTES guidelines for Characterisation of rock masses useful for the design and the construction of underground structures. *Tunnels et ouvrages souterrains*. 2003, 177.
- GNU R. 2014. <http://www.r-project.org/>. [Online] 2014. [Cited: 06 06, 2014.]
- Hoek, E., Kaiser, P.K. and Bawden, W.F. 1995. *Support of underground excavations in hard rock*. Rotterdam : A.A. Balkema, 1995.
- Itasca Consulting Group. 2014. <http://www.itascacg.com/software/3dec>. [Online] 2014. [Cited: 01 27, 2014.]
- Kim, B.H., Cai, M., Kaiser, P.K. and Yang, H.S. 2007. Estimation of block sizes for rock masses with non-persistent joints. *Rock Mechanics and Rock Engineering*. 2007, 40 (2), pp. 169-192.
- Moser, P., Grasedieck, A., Arsic, V. and Reichholz, G. 2003. Charakteristik der Korngrößenverteilung von Sprengbauwerk im Feinbereich. *Berg- und Hüttenmännische Monatshefte*. 2003, Vol. 148, 6, pp. 205-216.
- Palmström, A. 2001. Measurement and characterization of rock mass jointing. *In-Situ Characterization of rocks*. Oslo : A.A. Balkema Publishers, 2001.
- . 2005. Measurements of and correlations between block size and Rock Quality Designation (RQD). *Tunnelling and Underground Space Technology*. 2005, 20, pp. 362-377.

- Song, J.J. and Lee, C.I. 2001.** Estimation of joint length distribution using window sampling. *International Journal of Rock Mechanics & Mining Sciences*. 2001, 38, pp. 519-528.
- Song, J.J., Lee, C.I. and Seto, M. 2001.** Stability analysis of rock blocks around a tunnel using a statistical joint modeling technique. *Tunnelling and Underground Space Technology*. 2001, 16, pp. 341-351.
- Wang, L.G., Yamashita, S., Sugimoto, F., Pan, C. and Tan, G. 2003.** A methodology for predicting the in situ size and shape distributions of rock blocks. *Rock Mechanics and Rock Engineering*. 2003, 36 (2), pp. 121-142.

Appendix A

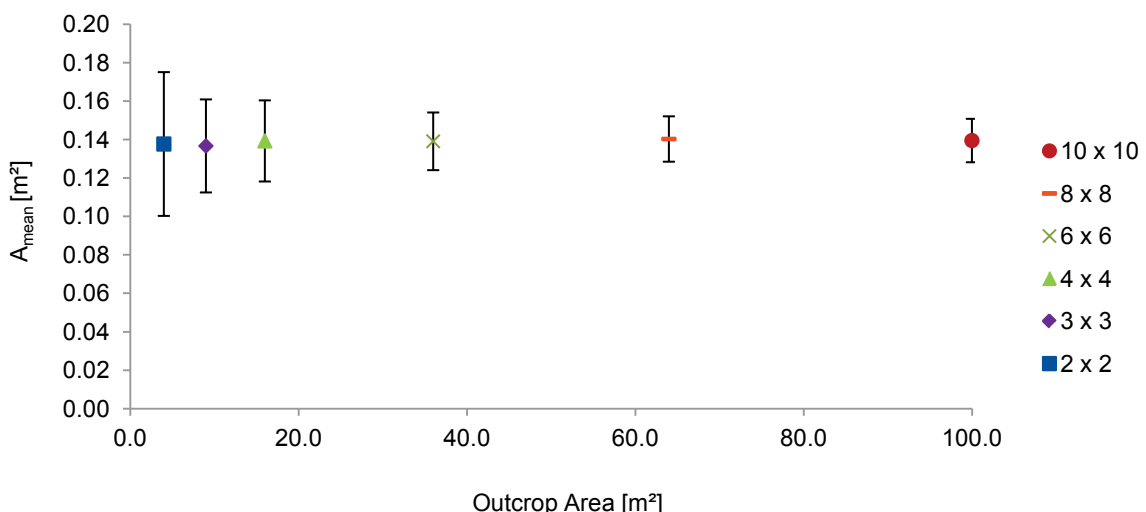
Table 5.1: Test parameters for minimally required outcrop area.

model dimension	x[-5; 5]			y[-5; 5]			z[-5; 5]			
$A_{out,1}$	x[-5; -5]			y[-5; 5]			z[-5; 5]			
$A_{out,2}$	x[-5; -5]			y[-4; 4]			z[-4; 4]			
$A_{out,3}$	x[-5; -5]			y[-3; 3]			z[-3; 3]			
$A_{out,4}$	x[-5; -5]			y[-2; 2]			z[-2; 2]			
$A_{out,5}$	x[-5; -5]			y[-1.5; 1.5]			z[-1.5; 1.5]			
$A_{out,6}$	x[-5; -5]			y[-1; 1]			z[-1; 1]			
replication factor r	100									
origin jset _i	x[-5]			y[0]			z[0]			
test number	dd ₁ [°]	dip ₁ [°]	dd ₂ [°]	dip ₂ [°]	dd ₃ [°]	dip ₃ [°]	sp ₁ [m]	sp ₂ [m]	sp ₃ [m]	p _i [-]
1	0	90	0	0	90	90	0.3	0.3	0.3	0.8
2	0	90	0	0	90	90	0.6	0.6	0.6	0.8
3	0	90	0	0	90	90	0.9	0.9	0.9	0.8
4	0	90	0	0	90	90	0.4	0.4	0.4	0.8
5	0	90	0	0	90	90	0.2	0.2	0.2	0.8
6	0	90	0	0	90	90	0.2	0.2	0.2	0.6
7	0	90	0	0	90	90	0.3	0.3	0.3	0.6
8	0	90	0	0	90	90	0.4	0.4	0.4	0.6
9	0	90	0	0	90	90	0.6	0.6	0.6	0.6
10	0	90	0	0	90	90	0.2	0.2	0.2	0.4
11	0	90	0	0	90	90	0.3	0.3	0.3	0.4
12	0	90	0	0	90	90	0.4	0.4	0.4	0.4
13	0	90	0	0	90	90	0.6	0.6	0.6	0.4
14	10	90	0	0	100	90	0.3	0.3	0.3	0.8
15	20	90	0	0	110	90	0.3	0.3	0.3	0.8
16	45	90	0	0	135	90	0.3	0.3	0.3	0.8
17	10	90	0	0	100	90	0.2	0.2	0.2	0.8
18	10	90	0	0	100	90	0.4	0.4	0.4	0.8

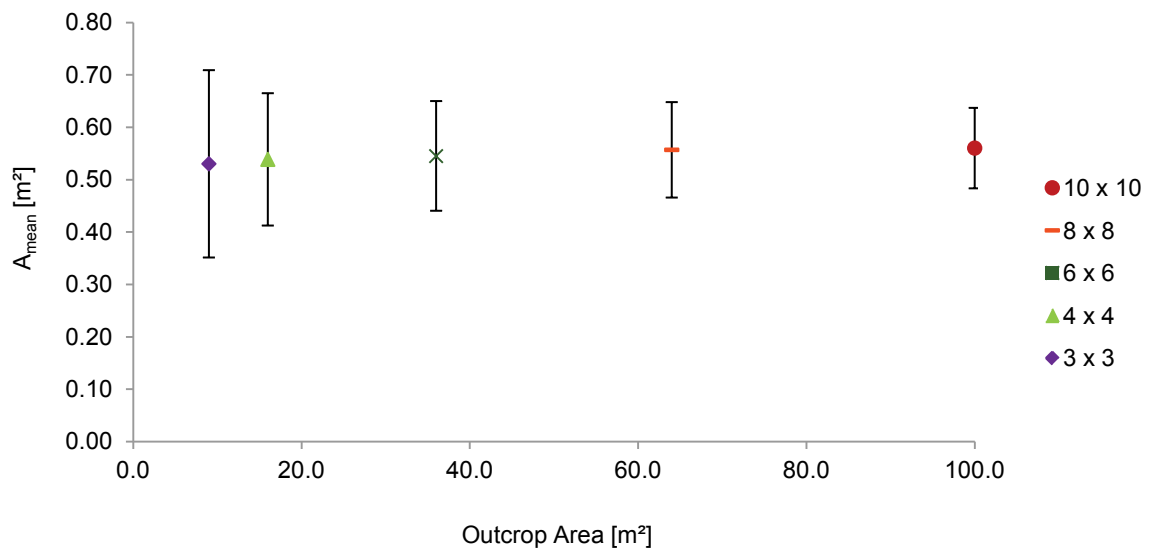
19	10	90	0	0	100	90	0.6	0.6	0.6	0.8
20	10	90	0	0	100	90	0.2	0.2	0.2	0.6
21	10	90	0	0	100	90	0.3	0.3	0.3	0.6
22	10	90	0	0	100	90	0.4	0.4	0.4	0.6
23	10	90	0	0	100	90	0.6	0.6	0.6	0.6
24	10	90	0	0	100	90	0.2	0.2	0.2	0.4
25	10	90	0	0	100	90	0.3	0.3	0.3	0.4
26	10	90	0	0	100	90	0.4	0.4	0.4	0.4
27	10	90	0	0	100	90	0.6	0.6	0.6	0.4
28	22.5	90	0	0	112.5	90	0.2	0.2	0.2	0.8
29	22.5	90	0	0	112.5	90	0.3	0.3	0.3	0.8
30	22.5	90	0	0	112.5	90	0.4	0.4	0.4	0.8
31	22.5	90	0	0	112.5	90	0.6	0.6	0.6	0.8
32	22.5	90	0	0	112.5	90	0.2	0.2	0.2	0.6
33	22.5	90	0	0	112.5	90	0.3	0.3	0.3	0.6
34	22.5	90	0	0	112.5	90	0.4	0.4	0.4	0.6
35	22.5	90	0	0	112.5	90	0.6	0.6	0.6	0.6
36	22.5	90	0	0	112.5	90	0.2	0.2	0.2	0.4
37	22.5	90	0	0	112.5	90	0.3	0.3	0.3	0.4
38	22.5	90	0	0	112.5	90	0.4	0.4	0.4	0.4
39	22.5	90	0	0	112.5	90	0.6	0.6	0.6	0.4
40	45	90	0	0	135.0	90	0.2	0.2	0.2	0.8
41	45	90	0	0	135.0	90	0.3	0.3	0.3	0.8
42	45	90	0	0	135.0	90	0.4	0.4	0.4	0.8
43	45	90	0	0	135.0	90	0.6	0.6	0.6	0.8
44	45	90	0	0	135.0	90	0.2	0.2	0.2	0.6
45	45	90	0	0	135.0	90	0.3	0.3	0.3	0.6
46	45	90	0	0	135.0	90	0.4	0.4	0.4	0.6
47	45	90	0	0	135.0	90	0.6	0.6	0.6	0.6
48	45	90	0	0	135.0	90	0.2	0.2	0.2	0.4
49	45	90	0	0	135.0	90	0.3	0.3	0.3	0.4
50	45	90	0	0	135.0	90	0.4	0.4	0.4	0.4
51	45	90	0	0	135.0	90	0.6	0.6	0.6	0.4

Table 5.2: Results of minimally required outcrop testing.

Test 1		z-rotation [°]			0.0		y-rotation [°]			0.0	
dd ₁ [°]	dip ₁ [°]	dd ₂ [°]	dip ₂ [°]	dd ₃ [°]	dip ₃ [°]	sp ₁ [m]	sp ₂ [m]	sp ₃ [m]	p ₁ [-]	p ₂ [-]	p ₃ [-]
0.0	90.0	0.0	0.0	90.0	90.0	0.3	0.3	0.3	0.8	0.8	0.8
A _{out} [m ²]	A _{mean} [m ²]	A _{mean} /A _{out} [-]	$\sigma_{A\text{mean}}$ [m ²]	A _{50%,mean} [m ²]	$\sigma_{A\text{50%,mean}}$ [m ²]	A _{75%,mean} [m ²]	$\sigma_{A\text{75%,mean}}$ [m ²]	A _{25%,mean} [m ²]	$\sigma_{A\text{25%,mean}}$ [m ²]		
100.0	0.1395	0.0014	0.0113	0.0918	0.0127	0.1739	0.0258	0.0900	0.0000		
64.0	0.1403	0.0022	0.0118	0.0918	0.0127	0.1721	0.0253	0.0900	0.0000		
36.0	0.1391	0.0039	0.0150	0.0972	0.0245	0.0169	0.0350	0.0900	0.0000		
16.0	0.1393	0.0087	0.0211	0.0972	0.0237	0.1613	0.0405	0.0900	0.0000		
9.0	0.1367	0.0152	0.0242	0.1017	0.0297	0.1593	0.0515	0.0902	0.0023		
4.0	0.1377	0.0344	0.0374	0.1107	0.0440	0.1638	0.0736	0.0922	0.0130		
V _{model} [m ³]	V _{mean} [m ³]	$\sigma_{V\text{mean}}$ [m ³]	V _{50%,mean} [m ³]	$\sigma_{V\text{50%,mean}}$ [m ³]	V _{75%,mean} [m ³]	$\sigma_{V\text{75%,mean}}$ [m ³]	V _{25%,mean} [m ³]	$\sigma_{V\text{25%,mean}}$ [m ³]			
1000.0	0.0519	0.0042	0.0348	0.0123	0.0548	0.0046	0.0270	0.0000			
640.0	0.0522	0.0044	0.0370	0.0131	0.0548	0.0046	0.0270	0.0000			
360.0	0.0518	0.0056	0.0364	0.0129	0.0554	0.0059	0.0270	0.0000			
160.0	0.0518	0.0079	0.0362	0.0129	0.0575	0.0099	0.0270	0.0000			
90.0	0.0509	0.0093	0.0373	0.0132	0.0509	0.0137	0.0273	0.0027			
40.0	0.0512	0.0141	0.0385	0.0172	0.0602	0.0175	0.0286	0.0064			
V _{per}	T_{mean}		T_{50%}		T_{75%}		T_{25%}				
0.0270	1.9222		1.2889		2.0296		1.0000				



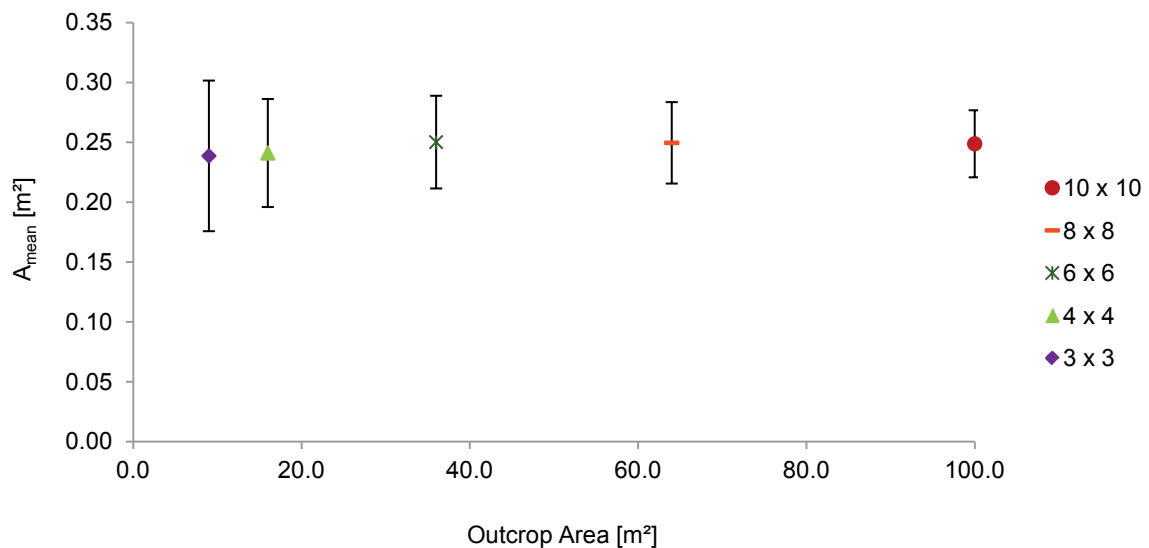
Test 2			z-rotation [°]			0.0			y-rotation [°]			0.0		
dd ₁ [°]	dip ₁ [°]	dd ₂ [°]	dip ₂ [°]	dd ₃ [°]	dip ₃ [°]	sp ₁ [m]	sp ₂ [m]	sp ₃ [m]	p ₁ [-]	p ₂ [-]	p ₃ [-]			
0.0	90.0	0.0	0.0	90.0	90.0	0.6	0.6	0.6	0.8	0.8	0.8			
A _{out} [m ²]	A _{mean} [m ²]	A _{mean} /A _{out} [-]		σ _{Amean} [m ²]	A _{50%,mean} [m ²]	σ _{A50%,mean} [m ²]	A _{75%,mean} [m ²]	σ _{A75%,mean} [m ²]	A _{25%,mean} [m ²]	σ _{A25%,mean} [m ²]				
100.0	0.5600	0.0056		0.0768	0.4068	0.1217	0.6822	0.1408	0.3600	0.0000				
64.0	0.5567	0.0087		0.0911	0.4140	0.1292	0.6624	0.1595	0.3600	0.0000				
36.0	0.5451	0.0151		0.1047	0.4158	0.1394	0.6588	0.2098	0.3600	0.0000				
16.0	0.5385	0.0337		0.1263	0.4428	0.1544	0.6174	0.2451	0.3699	0.0541				
9.0	0.5300	0.0589		0.1788	0.4572	0.1870	0.5706	0.2488	0.3978	0.1221				
4.0	n/a	n/a		n/a	n/a	n/a	n/a	n/a	n/a	n/a				
V _{model} [m ³]	V _{mean} [m ³]	σ _{Vmean} [m ³]		V _{50%,mean} [m ³]	σ _{V50%,mean} [m ³]	V _{75%,mean} [m ³]	σ _{V75%,mean} [m ³]	V _{25%,mean} [m ³]	σ _{V25%,mean} [m ³]					
1000.0	0.4136	0.0581		0.2959	0.1048	0.4622	0.0813	0.2160	0.0000					
640.0	0.4113	0.0692		0.3067	0.1071	0.4709	0.0889	0.2182	0.0216					
360.0	0.4017	0.0769		0.2981	0.1098	0.4644	0.0989	0.2225	0.0370					
160.0	0.3975	0.0922		0.3046	0.1100	0.4622	0.1108	0.2225	0.0370					
90.0	0.3932	0.1323		0.3100	0.1308	0.4639	0.2231	0.2376	0.0783					
40.0	n/a	n/a		n/a	n/a	n/a	n/a	n/a	n/a					
V _{per}	T _{mean}			T _{50%}			T _{75%}			T _{25%}				
0.2160	1.9148			1.3699			2.1398			1.0000				



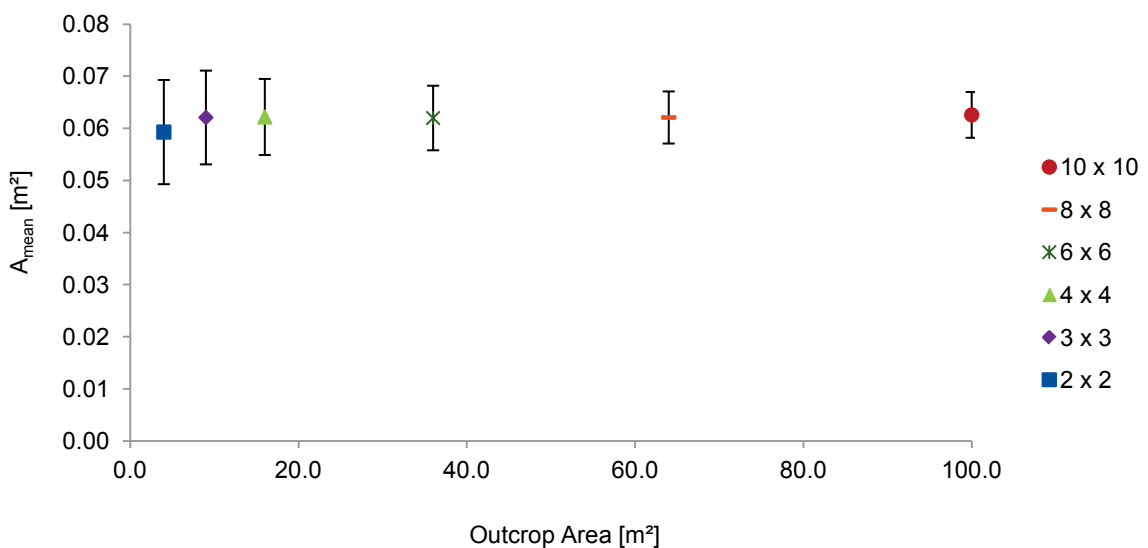
Test 3			z-rotation [°]			0.0			y-rotation [°]			0.0		
dd ₁ [°]	dip ₁ [°]	dd ₂ [°]	dip ₂ [°]	dd ₃ [°]	dip ₃ [°]	sp ₁ [m]	sp ₂ [m]	sp ₃ [m]	p ₁ [-]	p ₂ [-]	p ₃ [-]			
0.0	90.0	0.0	0.0	90.0	90.0	0.9	0.9	0.9	0.8	0.8	0.8			
A _{out} [m ²]	A _{mean} [m ²]	A _{mean} /A _{out} [-]		σ _{Amean} [m ²]	A _{50%,mean} [m ²]	σ _{A50%,mean} [m ²]	A _{75%,mean} [m ²]	σ _{A75%,mean} [m ²]	A _{25%,mean} [m ²]	σ _{A25%,mean} [m ²]				
100.0	1.2328	0.0123		0.2084	0.8748	0.2209	1.4985	0.4298	0.8100	0.0000				
64.0	1.2341	0.0193		0.2616	0.9234	0.2825	1.4560	0.5579	0.8161	0.0607				
36.0	1.2417	0.0345		0.3271	0.9882	0.3875	1.3730	0.5644	0.8546	0.1811				
16.0	n/a	n/a		n/a	n/a	n/a	n/a	n/a	n/a	n/a				
9.0	n/a	n/a		n/a	n/a	n/a	n/a	n/a	n/a	n/a				
4.0	n/a	n/a		n/a	n/a	n/a	n/a	n/a	n/a	n/a				
V _{model} [m ³]	V _{mean} [m ³]	σ _{Vmean} [m ³]		V _{50%,mean} [m ³]	σ _{V50%,mean} [m ³]	V _{75%,mean} [m ³]	σ _{V75%,mean} [m ³]	V _{25%,mean} [m ³]	σ _{V25%,mean} [m ³]					
1000.0	1.3460	0.2294		0.9659	0.3412	1.5601	0.3280	0.7290	0.0000					
640.0	1.3509	0.2907		0.9513	0.3803	1.5929	0.4010	0.7436	0.1026					
360.0	1.3631	0.3650		1.0024	0.4092	1.6494	0.6899	0.7800	0.1869					
160.0	n/a	n/a		n/a	n/a	n/a	n/a	n/a	n/a					
90.0	n/a	n/a		n/a	n/a	n/a	n/a	n/a	n/a					
40.0	n/a	n/a		n/a	n/a	n/a	n/a	n/a	n/a					
V _{per}	T_{mean}			T_{50%}			T_{75%}			T_{25%}				
0.7290	1.8464			1.3250			2.1401			1.0000				

Transformation factors invalid because limitation ratio has already been exceeded in the major outcrop area!

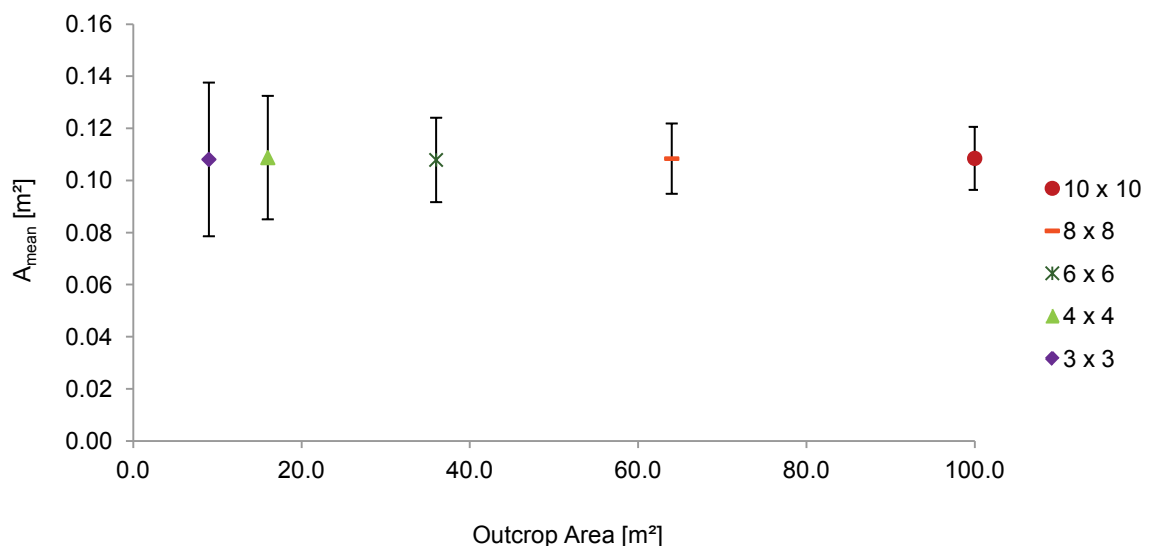
Test 4			z-rotation [°]			0.0			y-rotation [°]			0.0		
dd ₁ [°]	dip ₁ [°]	dd ₂ [°]	dip ₂ [°]	dd ₃ [°]	dip ₃ [°]	sp ₁ [m]	sp ₂ [m]	sp ₃ [m]	p ₁ [-]	p ₂ [-]	p ₃ [-]			
0.0	90.0	0.0	0.0	90.0	90.0	0.4	0.4	0.4	0.8	0.8	0.8			
A _{out} [m ²]	A _{mean} [m ²]	A _{mean/A_{out}} [-]	σ _{A_{mean}} [m ²]	A _{50%,mean} [m ²]	σ _{A_{50%,mean}} [m ²]	A _{75%,mean} [m ²]	σ _{A_{75%,mean}} [m ²]	A _{25%,mean} [m ²]	σ _{A_{25%,mean}} [m ²]					
100.0	0.2486	0.0025	0.0280	0.1640	0.0238	0.3104	0.0444	0.1600	0.0000					
64.0	0.2494	0.0039	0.0340	0.1632	0.0225	0.3084	0.0509	0.1600	0.0000					
36.0	0.2500	0.0069	0.0387	0.1768	0.0473	0.3028	0.0722	0.1600	0.0000					
16.0	0.2409	0.0151	0.0451	0.1864	0.0623	0.2844	0.0901	0.1600	0.0000					
9.0	0.2385	0.0265	0.0629	0.1928	0.0746	0.2720	0.1036	0.1660	0.0297					
4.0	n/a	n/a	n/a	n/a	n/a	n/a	n/a	n/a	n/a					
V _{model} [m ³]	V _{mean} [m ³]	σ _{V_{mean}} [m ³]	V _{50%,mean} [m ³]	σ _{V_{50%,mean}} [m ³]	V _{75%,mean} [m ³]	σ _{V_{75%,mean}} [m ³]	V _{25%,mean} [m ³]	σ _{V_{25%,mean}} [m ³]						
1000.0	0.1229	0.0138	0.0864	0.0307	0.1325	0.0164	0.0640	0.0000						
640.0	0.1233	0.0169	0.0877	0.0311	0.1331	0.0175	0.0640	0.0000						
360.0	0.1235	0.0195	0.0912	0.0329	0.1363	0.0235	0.0640	0.0000						
160.0	0.1192	0.0227	0.0912	0.0329	0.1402	0.0311	0.0640	0.0000						
90.0	0.1177	0.0301	0.0909	0.0366	0.1366	0.0399	0.0666	0.0126						
40.0	n/a	n/a	n/a	n/a	n/a	n/a	n/a	n/a						
V _{per}	T_{mean}		T_{50%}			T_{75%}			T_{25%}					
0.0640	1.9203		1.3500			2.0703			1.0000					



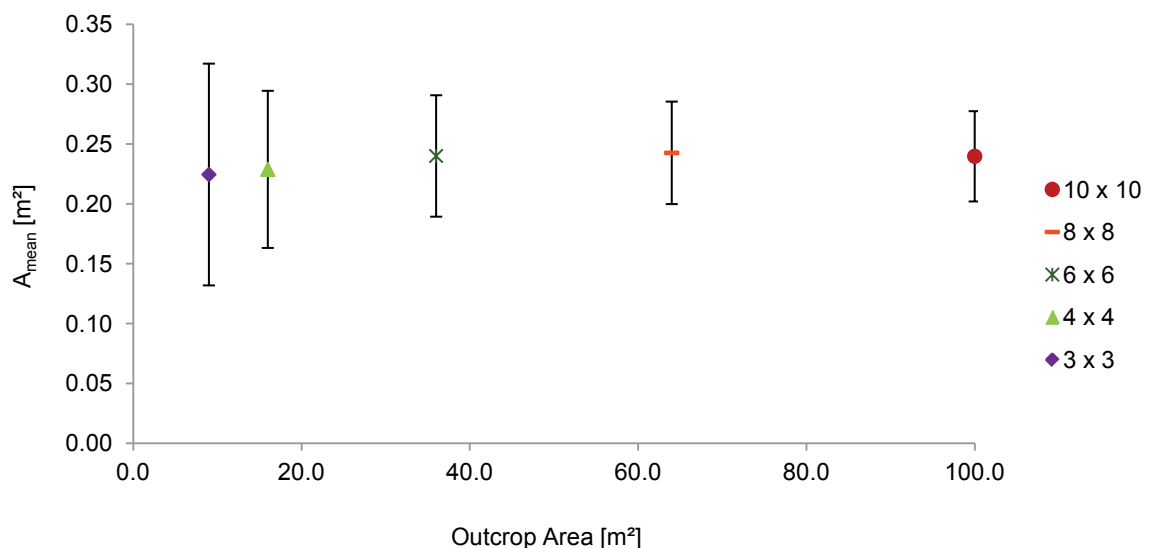
Test 5			z-rotation [°]			0.0			y-rotation [°]			0.0		
dd ₁ [°]	dip ₁ [°]	dd ₂ [°]	dip ₂ [°]	dd ₃ [°]	dip ₃ [°]	sp ₁ [m]	sp ₂ [m]	sp ₃ [m]	p ₁ [-]	p ₂ [-]	p ₃ [-]			
0.0	90.0	0.0	0.0	90.0	90.0	0.2	0.2	0.2	0.8	0.8	0.8			
A _{out} [m ²]	A _{mean} [m ²]	A _{mean/A_{out}} [-]	σ _{A_{mean}} [m ²]	A _{50%,mean} [m ²]	σ _{A_{50%,mean}} [m ²]	A _{75%,mean} [m ²]	σ _{A_{75%,mean}} [m ²]	A _{25%,mean} [m ²]	σ _{A_{25%,mean}} [m ²]					
100.0	0.0626	0.0006	0.0044	0.0400	0.0000	0.0800	0.0000	0.0400	0.0400					
64.0	0.0621	0.0010	0.0050	0.0408	0.0056	0.0792	0.0056	0.0400	0.0400					
36.0	0.0620	0.0017	0.0062	0.0412	0.0069	0.0781	0.0097	0.0400	0.0400					
16.0	0.0622	0.0039	0.0073	0.0436	0.0115	0.0760	0.0145	0.0400	0.0400					
9.0	0.0621	0.0069	0.0090	0.0440	0.0121	0.0764	0.0189	0.0400	0.0400					
4.0	0.0593	0.0148	0.0100	0.0440	0.0130	0.0729	0.0217	0.0400	0.0400					
V _{model} [m ³]	V _{mean} [m ³]	σ _{V_{mean}} [m ³]	V _{50%,mean} [m ³]	σ _{V_{50%,mean}} [m ³]	V _{75%,mean} [m ³]	σ _{V_{75%,mean}} [m ³]	V _{25%,mean} [m ³]	σ _{V_{25%,mean}} [m ³]						
1000.0	0.0156	0.0011	0.0106	0.0038	0.0161	0.0008	0.0080	0.0000						
640.0	0.0155	0.0012	0.0104	0.0037	0.0163	0.0016	0.0080	0.0000						
360.0	0.0154	0.0015	0.0112	0.0039	0.0166	0.0021	0.0080	0.0000						
160.0	0.0155	0.0018	0.0111	0.0039	0.0170	0.0029	0.0080	0.0000						
90.0	0.0154	0.0023	0.0108	0.0038	0.0180	0.0043	0.0080	0.0000						
40.0	0.0148	0.0025	0.0102	0.0037	0.0173	0.0032	0.0080	0.0000						
V _{per}	T _{mean}		T _{50%}		T _{75%}		T _{25%}							
0.0080	1.9500		1.3250		2.0125		1.0000							



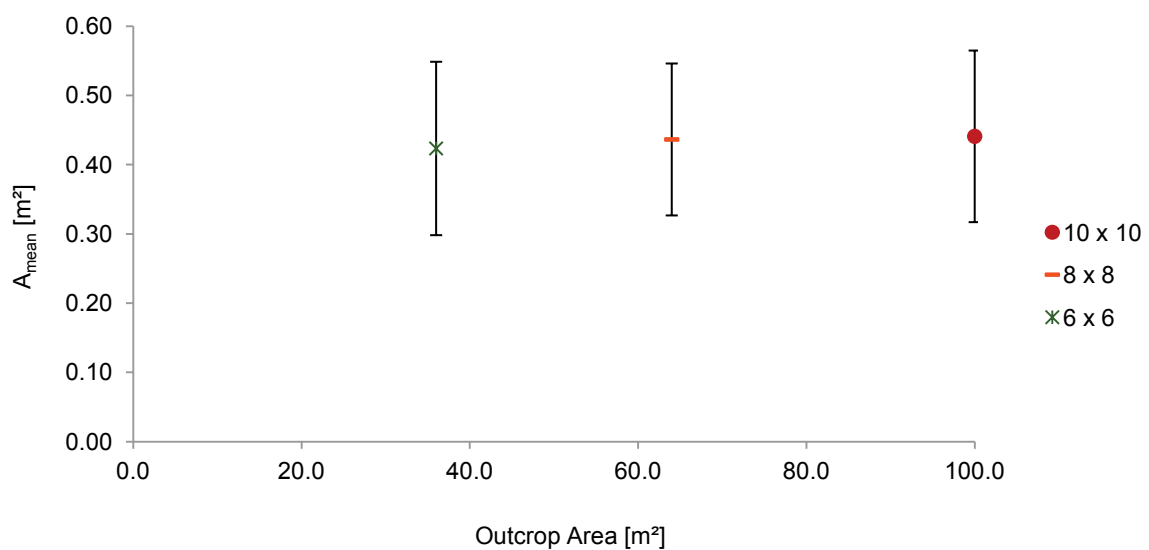
Test 6			z-rotation [°]			0.0			y-rotation [°]			0.0		
dd ₁ [°]	dip ₁ [°]	dd ₂ [°]	dip ₂ [°]	dd ₃ [°]	dip ₃ [°]	sp ₁ [m]	sp ₂ [m]	sp ₃ [m]	p ₁ [-]	p ₂ [-]	p ₃ [-]			
0.0	90.0	0.0	0.0	90.0	90.0	0.2	0.2	0.2	0.6	0.6	0.6			
A _{out} [m ²]	A _{mean} [m ²]	A _{mean/A_{out}} [-]	σ _{A_{mean}} [m ²]	A _{50%,mean} [m ²]	σ _{A_{50%,mean}} [m ²]	A _{75%,mean} [m ²]	σ _{A_{75%,mean}} [m ²]	A _{25%,mean} [m ²]	σ _{A_{25%,mean}} [m ²]					
100.0	0.1085	0.0011	0.0121	0.0804	0.0040	0.1289	0.0193	0.0416	0.0079					
64.0	0.1084	0.0017	0.0135	0.0812	0.0069	0.1304	0.0210	0.0418	0.0081					
36.0	0.1079	0.0030	0.0162	0.0800	0.0114	0.1291	0.0299	0.0435	0.0110					
16.0	0.1088	0.0068	0.0237	0.0814	0.0171	0.1273	0.0371	0.0470	0.0151					
9.0	0.1081	0.0120	0.0295	0.0814	0.0237	0.1259	0.0400	0.0488	0.0171					
4.0	n/a	n/a	n/a	n/a	n/a	n/a	n/a	n/a	n/a	n/a	n/a			
V _{model} [m ³]	V _{mean} [m ³]	σ _{V_{mean}} [m ³]	V _{50%,mean} [m ³]	σ _{V_{50%,mean}} [m ³]	V _{75%,mean} [m ³]	σ _{V_{75%,mean}} [m ³]	V _{25%,mean} [m ³]	σ _{V_{25%,mean}} [m ³]						
1000.0	0.0357	0.0040	0.0212	0.0045	0.0412	0.0077	0.0146	0.0030						
640.0	0.0356	0.0045	0.0214	0.0046	0.0405	0.0078	0.0139	0.0035						
360.0	0.0355	0.0054	0.0210	0.0048	0.0402	0.0082	0.0134	0.0038						
160.0	0.0357	0.0078	0.0216	0.0059	0.0405	0.0110	0.0134	0.0039						
90.0	0.0355	0.0097	0.0215	0.0070	0.0417	0.0130	0.0134	0.0046						
40.0	n/a	n/a	n/a	n/a	n/a	n/a	n/a	n/a	n/a	n/a	n/a			
V _{per}	T _{mean}		T _{50%}		T _{75%}		T _{25%}							
0.0080	4.4625		2.6500		5.1500		1.8250							



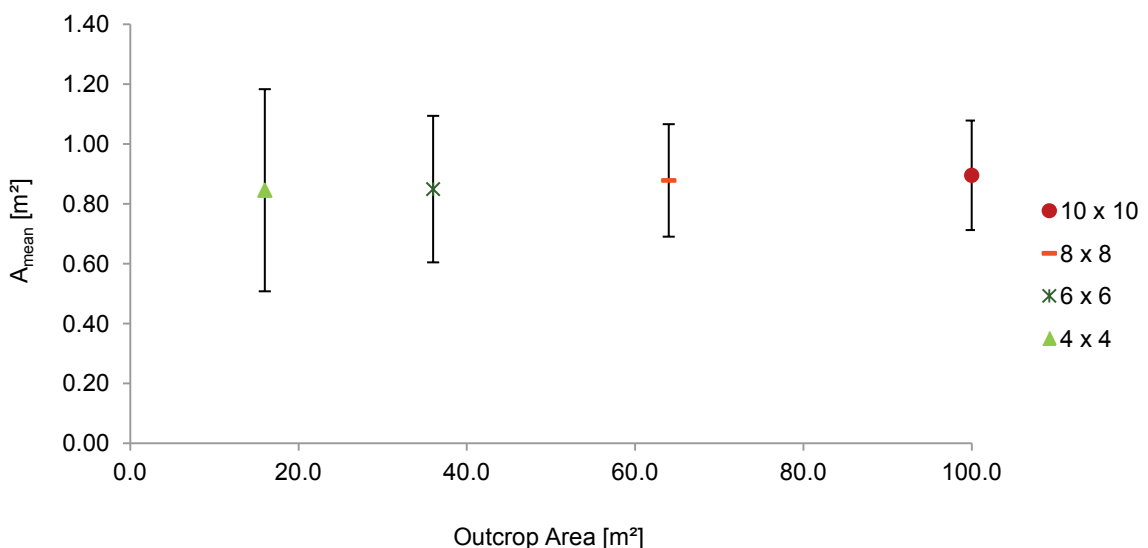
Test 7			z-rotation [°]			0.0			y-rotation [°]			0.0		
dd ₁ [°]	dip ₁ [°]	dd ₂ [°]	dip ₂ [°]	dd ₃ [°]	dip ₃ [°]	sp ₁ [m]	sp ₂ [m]	sp ₃ [m]	p ₁ [-]	p ₂ [-]	p ₃ [-]			
0.0	90.0	0.0	0.0	90.0	90.0	0.3	0.3	0.3	0.6	0.6	0.6			
A _{out} [m ²]	A _{mean} [m ²]	A _{mean} /A _{out} [-]	σ _{Amean} [m ²]	A _{50%,mean} [m ²]	σ _{A50%,mean} [m ²]	A _{75%,mean} [m ²]	σ _{A75%,mean} [m ²]	A _{25%,mean} [m ²]	σ _{A25%,mean} [m ²]					
100.0	0.2397	0.0024	0.0377	0.1791	0.0202	0.2774	0.0538	0.0918	0.0127					
64.0	0.2426	0.0038	0.0428	0.1809	0.0156	0.2873	0.0644	0.0954	0.0215					
36.0	0.2400	0.0067	0.0507	0.1804	0.0341	0.2824	0.0795	0.0963	0.0231					
16.0	0.2288	0.0143	0.0656	0.1732	0.0476	0.2646	0.0938	0.1004	0.0285					
9.0	0.2245	0.0249	0.0926	0.1791	0.0819	0.2610	0.1321	0.1210	0.0679					
4.0	n/a	n/a	n/a	n/a	n/a	n/a	n/a	n/a	n/a					
V _{model} [m ³]	V _{mean} [m ³]	σ _{Vmean} [m ³]	V _{50%,mean} [m ³]	σ _{V50%,mean} [m ³]	V _{75%,mean} [m ³]	σ _{V75%,mean} [m ³]	V _{25%,mean} [m ³]	σ _{V25%,mean} [m ³]						
1000.0	0.1173	0.0186	0.0686	0.0146	0.1331	0.0275	0.0462	0.0123						
640.0	0.1187	0.0209	0.0699	0.0168	0.1328	0.0273	0.0451	0.0128						
360.0	0.1174	0.0248	0.0702	0.0184	0.1353	0.0329	0.0456	0.0126						
160.0	0.1120	0.0327	0.0691	0.0224	0.1310	0.0384	0.0427	0.0145						
90.0	0.1099	0.0440	0.0737	0.0391	0.1295	0.0513	0.0436	0.0213						
40.0	n/a	n/a	n/a	n/a	n/a	n/a	n/a	n/a						
V _{per}	T_{mean}			T_{50%}			T_{75%}			T_{25%}				
0.0270	4.3444			2.5407			4.9296			1.7111				



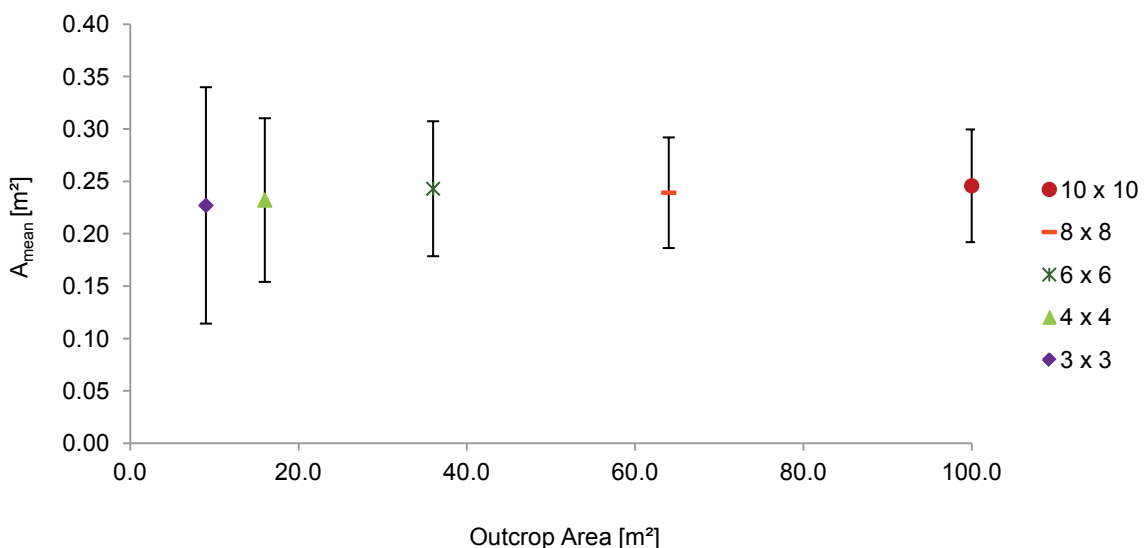
Test 8			z-rotation [°]			0.0			y-rotation [°]			0.0		
dd ₁ [°]	dip ₁ [°]	dd ₂ [°]	dip ₂ [°]	dd ₃ [°]	dip ₃ [°]	sp ₁ [m]	sp ₂ [m]	sp ₃ [m]	p ₁ [-]	p ₂ [-]	p ₃ [-]			
0.0	90.0	0.0	0.0	90.0	90.0	0.4	0.4	0.4	0.6	0.6	0.6			
A _{out} [m ²]	A _{mean} [m ²]	A _{mean/A_{out}} [-]	$\sigma_{A\text{mean}}$ [m ²]	A _{50%,mean} [m ²]	$\sigma_{A50\%,\text{mean}}$ [m ²]	A _{75%,mean} [m ²]	$\sigma_{A75\%,\text{mean}}$ [m ²]	A _{25%,mean} [m ²]	$\sigma_{A25\%,\text{mean}}$ [m ²]					
100.0	0.4410	0.0044	0.1239	0.3312	0.0917	0.5268	0.1668	0.1792	0.0523					
64.0	0.4365	0.0068	0.1097	0.3144	0.0806	0.5040	0.1502	0.1880	0.0598					
36.0	0.4235	0.0118	0.1252	0.3088	0.1067	0.4928	0.1841	0.2028	0.0740					
16.0	n/a	n/a	n/a	n/a	n/a	n/a	n/a	n/a	n/a	n/a	n/a			
9.0	n/a	n/a	n/a	n/a	n/a	n/a	n/a	n/a	n/a	n/a	n/a			
4.0	n/a	n/a	n/a	n/a	n/a	n/a	n/a	n/a	n/a	n/a	n/a			
V _{model} [m ³]	V _{mean} [m ³]	$\sigma_{V\text{mean}}$ [m ³]	V _{50%,mean} [m ³]	$\sigma_{V50\%,\text{mean}}$ [m ³]	V _{75%,mean} [m ³]	$\sigma_{V75\%,\text{mean}}$ [m ³]	V _{25%,mean} [m ³]	$\sigma_{V25\%,\text{mean}}$ [m ³]						
1000.0	0.2851	0.0801	0.1619	0.0502	0.3194	0.0921	0.1034	0.0311						
640.0	0.2822	0.0711	0.1686	0.0485	0.3232	0.1023	0.1056	0.0333						
360.0	0.2738	0.0813	0.1741	0.0576	0.3202	0.1009	0.1024	0.0375						
160.0	n/a	n/a	n/a	n/a	n/a	n/a	n/a	n/a	n/a	n/a	n/a			
90.0	n/a	n/a	n/a	n/a	n/a	n/a	n/a	n/a	n/a	n/a	n/a			
40.0	n/a	n/a	n/a	n/a	n/a	n/a	n/a	n/a	n/a	n/a	n/a			
V _{per}	T_{mean}			T_{50%}			T_{75%}			T_{25%}				
0.0640	4.4547			2.5297			4.9906			1.6156				



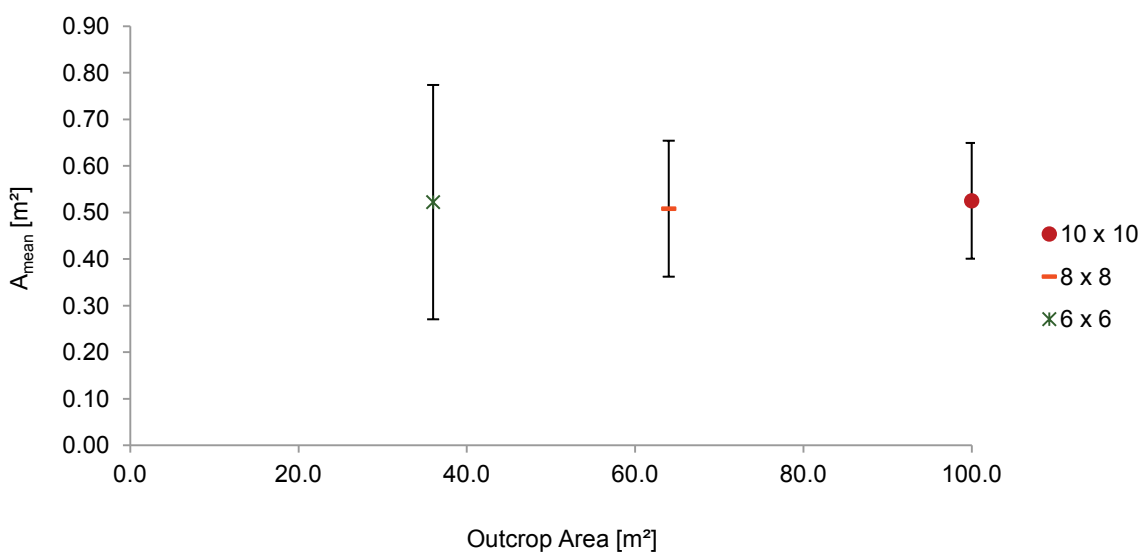
Test 9			z-rotation [°]			0.0			y-rotation [°]			0.0		
dd ₁ [°]	dip ₁ [°]	dd ₂ [°]	dip ₂ [°]	dd ₃ [°]	dip ₃ [°]	sp ₁ [m]	sp ₂ [m]	sp ₃ [m]	p ₁ [-]	p ₂ [-]	p ₃ [-]			
0.0	90.0	0.0	0.0	90.0	90.0	0.6	0.6	0.6	0.6	0.6	0.6			
A _{out} [m ²]	A _{mean} [m ²]	A _{mean} /A _{out} [-]	σ _{Amean} [m ²]	A _{50%,mean} [m ²]	σ _{A50%,mean} [m ²]	A _{75%,mean} [m ²]	σ _{A75%,mean} [m ²]	A _{25%,mean} [m ²]	σ _{A25%,mean} [m ²]					
100.0	0.8954	0.0090	0.1829	0.6732	0.1802	1.0431	0.2726	0.4113	0.1255					
64.0	0.8783	0.0137	0.1879	0.6840	0.2156	1.0161	0.2753	0.4068	0.1217					
36.0	0.8493	0.0236	0.2447	0.6588	0.2710	1.0152	0.3406	0.4536	0.1935					
16.0	0.8455	0.0528	0.3376	0.7110	0.3999	0.9891	0.4158	0.5013	0.3219					
9.0	n/a	n/a	n/a	n/a	n/a	n/a	n/a	n/a	n/a					
4.0	n/a	n/a	n/a	n/a	n/a	n/a	n/a	n/a	n/a					
V _{model} [m ³]	V _{mean} [m ³]	σ _{Vmean} [m ³]	V _{50%,mean} [m ³]	σ _{V50%,mean} [m ³]	V _{75%,mean} [m ³]	σ _{V75%,mean} [m ³]	V _{25%,mean} [m ³]	σ _{V25%,mean} [m ³]						
1000.0	0.8550	0.1790	0.5238	0.1359	1.0022	0.2288	0.3272	0.1080						
640.0	0.8382	0.1719	0.5357	0.1389	0.9871	0.2368	0.3326	0.1082						
360.0	0.8114	0.2294	0.5422	0.1797	0.9596	0.2967	0.3397	0.1378						
160.0	0.8070	0.3246	0.5724	0.2665	0.9812	0.4651	0.3505	0.2233						
90.0	n/a	n/a	n/a	n/a	n/a	n/a	n/a	n/a						
40.0	n/a	n/a	n/a	n/a	n/a	n/a	n/a	n/a						
V _{per}	T _{mean}			T _{50%}			T _{75%}			T _{25%}				
0.02160	3.9583			2.4250			4.6398			1.5148				



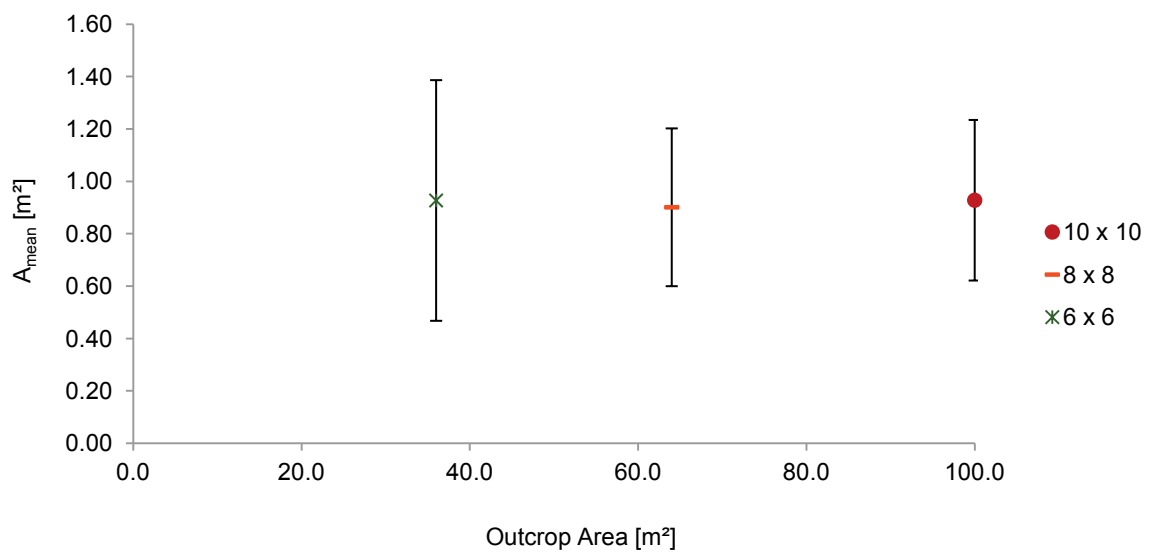
Test 10			z-rotation [°]			0.0			y-rotation [°]			0.0		
dd ₁ [°]	dip ₁ [°]	dd ₂ [°]	dip ₂ [°]	dd ₃ [°]	dip ₃ [°]	sp ₁ [m]	sp ₂ [m]	sp ₃ [m]	p ₁ [-]	p ₂ [-]	p ₃ [-]			
0.0	90.0	0.0	0.0	90.0	90.0	0.2	0.2	0.2	0.4	0.4	0.4			
A _{out} [m ²]	A _{mean} [m ²]	A _{mean} /A _{out} [-]		σ _{Amean} [m ²]	A _{50%,mean} [m ²]	σ _{A50%,mean} [m ²]	A _{75%,mean} [m ²]	σ _{A75%,mean} [m ²]	A _{25%,mean} [m ²]	σ _{A25%,mean} [m ²]				
100.0	0.2458	0.0025		0.0538	0.1540	0.0416	0.2940	0.0667	0.0844	0.0179				
64.0	0.2392	0.0037		0.0528	0.1500	0.0372	0.2923	0.0732	0.0842	0.0221				
36.0	0.2430	0.0068		0.0644	0.1574	0.0532	0.2901	0.0804	0.0891	0.0330				
16.0	0.2322	0.0145		0.0781	0.1536	0.0742	0.2763	0.1063	0.0873	0.0411				
9.0	0.2271	0.0252		0.1128	0.1532	0.0839	0.2704	0.1529	0.1016	0.0658				
4.0	n/a	n/a		n/a	n/a	n/a	n/a	n/a	n/a	n/a	n/a			
V _{model} [m ³]	V _{mean} [m ³]	σ _{Vmean} [m ³]		V _{50%,mean} [m ³]	σ _{V50%,mean} [m ³]	V _{75%,mean} [m ³]	σ _{V75%,mean} [m ³]	V _{25%,mean} [m ³]	σ _{V25%,mean} [m ³]					
1000.0	0.1188	0.0259		0.0578	0.0128	0.1297	0.0305	0.0276	0.0068					
640.0	0.1156	0.0254		0.0574	0.0141	0.1258	0.0309	0.0273	0.0067					
360.0	0.1177	0.0313		0.0606	0.0189	0.1303	0.0378	0.0285	0.0097					
160.0	0.1124	0.0389		0.0592	0.0250	0.1256	0.0498	0.0276	0.0112					
90.0	0.1098	0.0543		0.0606	0.0331	0.1265	0.0682	0.0309	0.0197					
40.0	n/a	n/a		n/a	n/a	n/a	n/a	n/a	n/a	n/a	n/a			
V _{per}	T _{mean}			T _{50%}			T _{75%}			T _{25%}				
0.0080	14.8500			7.2250			16.2125			3.4500				



Test 11			z-rotation [°]			0.0			y-rotation [°]			0.0		
dd ₁ [°]	dip ₁ [°]	dd ₂ [°]	dip ₂ [°]	dd ₃ [°]	dip ₃ [°]	sp ₁ [m]	sp ₂ [m]	sp ₃ [m]	p ₁ [-]	p ₂ [-]	p ₃ [-]			
0.0	90.0	0.0	0.0	90.0	90.0	0.3	0.3	0.3	0.4	0.4	0.4			
A _{out} [m ²]	A _{mean} [m ²]	A _{mean} /A _{out} [-]		σ _{Amean} [m ²]	A _{50%,mean} [m ²]	σ _{A50%,mean} [m ²]	A _{75%,mean} [m ²]	σ _{A75%,mean} [m ²]	A _{25%,mean} [m ²]	σ _{A25%,mean} [m ²]				
100.0	0.5251	0.0053		0.1243	0.3231	0.0859	0.6426	0.1940	0.1800	0.0437				
64.0	0.5082	0.0079		0.1460	0.3213	0.1084	0.6183	0.2373	0.1786	0.0656				
36.0	0.5223	0.0145		0.2516	0.3510	0.2670	0.6374	0.3595	0.1964	0.1370				
16.0	n/a	n/a		n/a	n/a	n/a	n/a	n/a	n/a	n/a	n/a			
9.0	n/a	n/a		n/a	n/a	n/a	n/a	n/a	n/a	n/a	n/a			
4.0	n/a	n/a		n/a	n/a	n/a	n/a	n/a	n/a	n/a	n/a			
V _{model} [m ³]	V _{mean} [m ³]	σ _{Vmean} [m ³]		V _{50%,mean} [m ³]	σ _{V50%,mean} [m ³]	V _{75%,mean} [m ³]	σ _{V75%,mean} [m ³]	V _{25%,mean} [m ³]	σ _{V25%,mean} [m ³]					
1000.0	0.3751	0.0884		0.1876	0.0501	0.4120	0.1029	0.0891	0.0222					
640.0	0.3624	0.1034		0.1856	0.0643	0.4041	0.1282	0.0874	0.0304					
360.0	0.3723	0.1771		0.1930	0.1090	0.4173	0.2143	0.0968	0.0775					
160.0	n/a	n/a		n/a	n/a	n/a	n/a	n/a	n/a	n/a	n/a			
90.0	n/a	n/a		n/a	n/a	n/a	n/a	n/a	n/a	n/a	n/a			
40.0	n/a	n/a		n/a	n/a	n/a	n/a	n/a	n/a	n/a	n/a			
V _{per}	T _{mean}			T _{50%}			T _{75%}			T _{25%}				
0.0270	13.8926			6.9481			15.2593			3.3000				



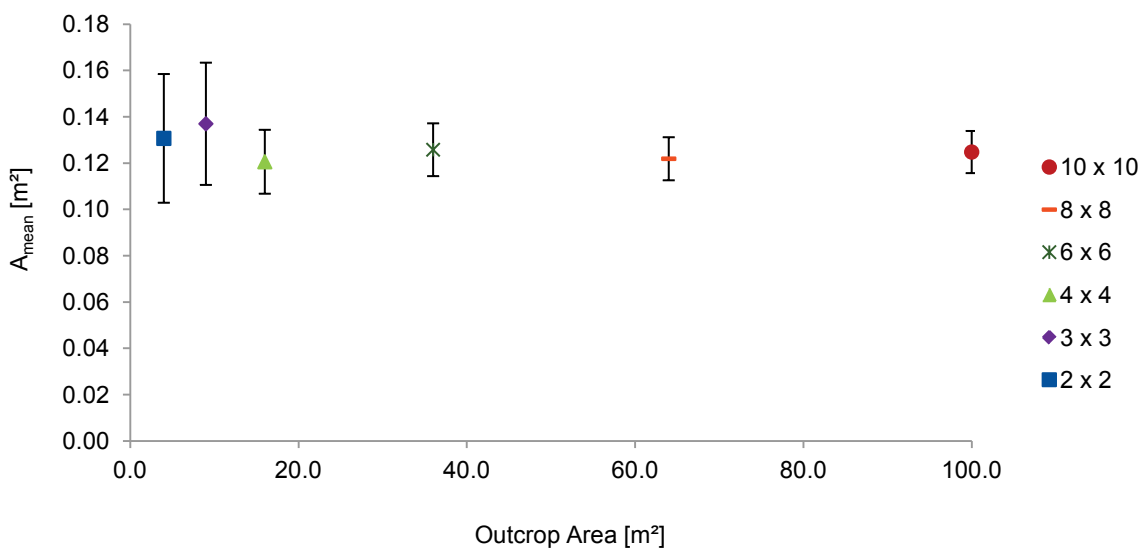
Test 12			z-rotation [°]			0.0			y-rotation [°]			0.0		
dd ₁ [°]	dip ₁ [°]	dd ₂ [°]	dip ₂ [°]	dd ₃ [°]	dip ₃ [°]	sp ₁ [m]	sp ₂ [m]	sp ₃ [m]	p ₁ [-]	p ₂ [-]	p ₃ [-]			
0.0	90.0	0.0	0.0	90.0	90.0	0.4	0.4	0.4	0.4	0.4	0.4			
A _{out} [m ²]	A _{mean} [m ²]	A _{mean} /A _{out} [-]		σ _{Amean} [m ²]	A _{50%,mean} [m ²]	σ _{A50%,mean} [m ²]	A _{75%,mean} [m ²]	σ _{A75%,mean} [m ²]	A _{25%,mean} [m ²]	σ _{A25%,mean} [m ²]				
100.0	0.9281	0.0093		0.3065	0.5904	0.2560	1.1080	0.4089	0.3272	0.1360				
64.0	0.9012	0.0141		0.3012	0.5944	0.2551	1.0760	0.4404	0.3264	0.1382				
36.0	0.9272	0.0258		0.4594	0.6024	0.3461	1.1476	0.7073	0.3424	0.1898				
16.0	n/a	n/a		n/a	n/a	n/a	n/a	n/a	n/a	n/a	n/a			
9.0	n/a	n/a		n/a	n/a	n/a	n/a	n/a	n/a	n/a	n/a			
4.0	n/a	n/a		n/a	n/a	n/a	n/a	n/a	n/a	n/a	n/a			
V _{model} [m ³]	V _{mean} [m ³]	σ _{Vmean} [m ³]		V _{50%,mean} [m ³]	σ _{V50%,mean} [m ³]	V _{75%,mean} [m ³]	σ _{V75%,mean} [m ³]	V _{25%,mean} [m ³]	σ _{V25%,mean} [m ³]					
1000.0	0.8582	0.2784		0.4307	0.1627	0.9390	0.3221	0.2085	0.1044					
640.0	0.8325	0.2701		0.4349	0.1702	0.9174	0.3357	0.2149	0.1008					
360.0	0.8598	0.4465		0.4656	0.3161	0.9869	0.5240	0.2302	0.1551					
160.0	n/a	n/a		n/a	n/a	n/a	n/a	n/a	n/a	n/a	n/a			
90.0	n/a	n/a		n/a	n/a	n/a	n/a	n/a	n/a	n/a	n/a			
40.0	n/a	n/a		n/a	n/a	n/a	n/a	n/a	n/a	n/a	n/a			
V _{per}	T _{mean}			T _{50%}			T _{75%}			T _{25%}				
0.0640	13.4094			6.7297			14.6719			3.2578				



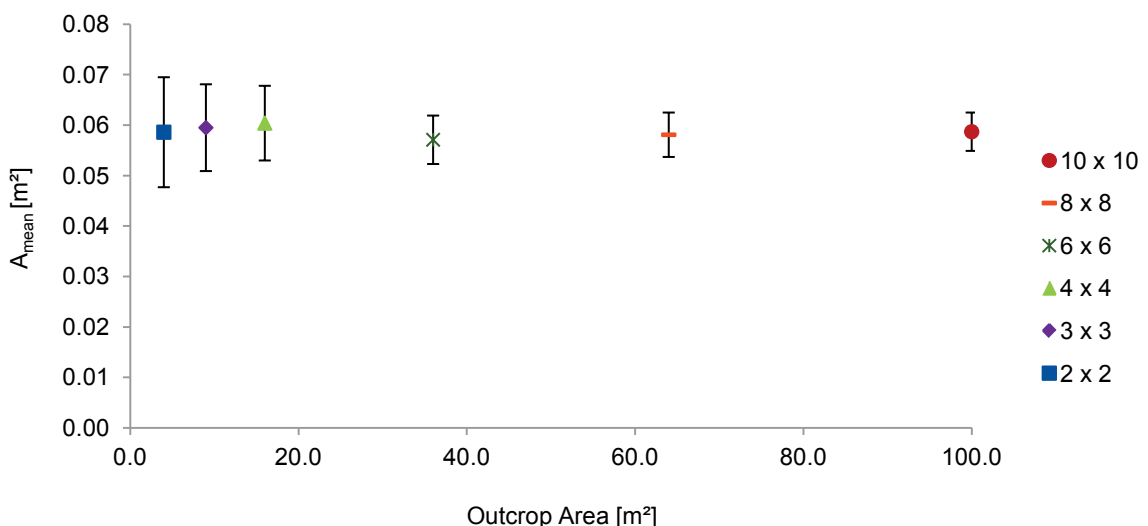
Test 13			z-rotation [°]			0.0			y-rotation [°]			0.0		
dd ₁ [°]	dip ₁ [°]	dd ₂ [°]	dip ₂ [°]	dd ₃ [°]	dip ₃ [°]	sp ₁ [m]	sp ₂ [m]	sp ₃ [m]	p ₁ [-]	p ₂ [-]	p ₃ [-]			
0.0	90.0	0.0	0.0	90.0	90.0	0.6	0.6	0.6	0.4	0.4	0.4			
A _{out} [m ²]	A _{mean} [m ²]	A _{mean} /A _{out} [-]	σ _{Amean} [m ²]	A _{50%,mean} [m ²]	σ _{A50%,mean} [m ²]	A _{75%,mean} [m ²]	σ _{A75%,mean} [m ²]	A _{25%,mean} [m ²]	σ _{A25%,mean} [m ²]					
100.0	2.0106	0.0201	0.8764	1.3608	0.6289	2.3364	0.8904	0.7434	0.3904					
64.0	n/a	n/a	n/a	n/a	n/a	n/a	n/a	n/a	n/a	n/a	n/a			
36.0	n/a	n/a	n/a	n/a	n/a	n/a	n/a	n/a	n/a	n/a	n/a			
16.0	n/a	n/a	n/a	n/a	n/a	n/a	n/a	n/a	n/a	n/a	n/a			
9.0	n/a	n/a	n/a	n/a	n/a	n/a	n/a	n/a	n/a	n/a	n/a			
4.0	n/a	n/a	n/a	n/a	n/a	n/a	n/a	n/a	n/a	n/a	n/a			
V _{model} [m ³]	V _{mean} [m ³]	σ _{Vmean} [m ³]	V _{50%,mean} [m ³]	σ _{V50%,mean} [m ³]	V _{75%,mean} [m ³]	σ _{V75%,mean} [m ³]	V _{25%,mean} [m ³]	σ _{V25%,mean} [m ³]						
1000.0	2.6946	1.1237	1.4386	0.5988	3.0672	1.2609	0.7182	0.3428						
640.0	n/a	n/a	n/a	n/a	n/a	n/a	n/a	n/a	n/a	n/a	n/a			
360.0	n/a	n/a	n/a	n/a	n/a	n/a	n/a	n/a	n/a	n/a	n/a			
160.0	n/a	n/a	n/a	n/a	n/a	n/a	n/a	n/a	n/a	n/a	n/a			
90.0	n/a	n/a	n/a	n/a	n/a	n/a	n/a	n/a	n/a	n/a	n/a			
40.0	n/a	n/a	n/a	n/a	n/a	n/a	n/a	n/a	n/a	n/a	n/a			
V _{per}	T _{mean}			T _{50%}			T _{75%}			T _{25%}				
0.2160	12.4750			6.6602			14.2000			3.3250				

Transformation factors invalid because limitation ratio has already been exceeded in the major outcrop area!

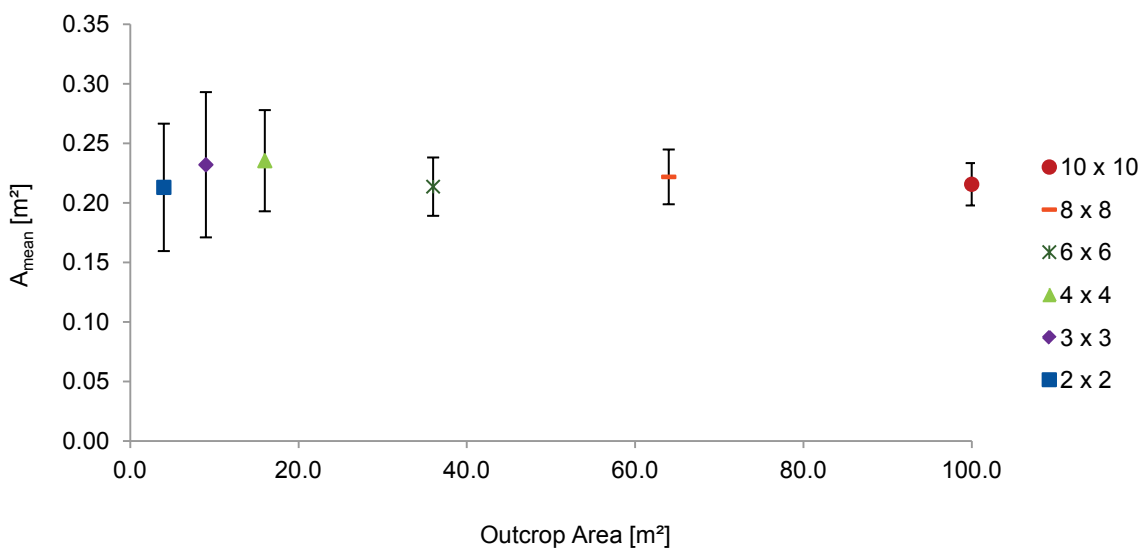
Test 14			z-rotation [°]			10.0			y-rotation [°]			0.0		
dd ₁ [°]	dip ₁ [°]	dd ₂ [°]	dip ₂ [°]	dd ₃ [°]	dip ₃ [°]	sp ₁ [m]	sp ₂ [m]	sp ₃ [m]	p ₁ [-]	p ₂ [-]	p ₃ [-]			
10.0	90.0	0.0	0.0	100.0	90.0	0.3	0.3	0.3	0.8	0.8	0.8			
A _{out} [m ²]	A _{mean} [m ²]	A _{mean} /A _{out} [-]	$\sigma_{A\text{mean}}$ [m ²]	A _{50%,mean} [m ²]	$\sigma_{A50\%,\text{mean}}$ [m ²]	A _{75%,mean} [m ²]	$\sigma_{A75\%,\text{mean}}$ [m ²]	A _{25%,mean} [m ²]	$\sigma_{A25\%,\text{mean}}$ [m ²]					
100.0	0.1248	0.0012	0.0091	0.0914	0.0000	0.1645	0.0302	0.0914	0.0000					
64.0	0.1219	0.0019	0.0093	0.0914	0.0000	0.1578	0.0352	0.0909	0.0037					
36.0	0.1258	0.0035	0.0114	0.0923	0.0052	0.1622	0.0367	0.0914	0.0000					
16.0	0.1206	0.0075	0.0138	0.0914	0.0000	0.1467	0.0403	0.0833	0.0132					
9.0	0.1370	0.0152	0.0264	0.1060	0.0324	0.1622	0.0559	0.0921	0.0069					
4.0	0.1307	0.0327	0.0278	0.1014	0.0287	0.1474	0.0556	0.0925	0.0094					
V _{model} [m ³]	V _{mean} [m ³]	$\sigma_{V\text{mean}}$ [m ³]	V _{50%,mean} [m ³]	$\sigma_{V50\%,\text{mean}}$ [m ³]	V _{75%,mean} [m ³]	$\sigma_{V75\%,\text{mean}}$ [m ³]	V _{25%,mean} [m ³]	$\sigma_{V25\%,\text{mean}}$ [m ³]						
1000.0	0.0517	0.0037	0.0362	0.0129	0.0543	0.0027	0.0270	0.0000						
640.0	0.0516	0.0041	0.0378	0.0133	0.0545	0.0038	0.0270	0.0000						
360.0	0.0514	0.0050	0.0367	0.0130	0.0548	0.0046	0.0270	0.0000						
160.0	0.0506	0.0065	0.0364	0.0129	0.0556	0.0073	0.0270	0.0000						
90.0	0.0502	0.0082	0.0373	0.0132	0.0575	0.0119	0.0275	0.0038						
40.0	0.0487	0.0092	0.0362	0.0129	0.0586	0.0139	0.0281	0.0053						
V _{per}	T _{mean}			T _{50%}			T _{75%}			T _{25%}				
0.0270	1.9148			1.3407			2.0111			1.0000				



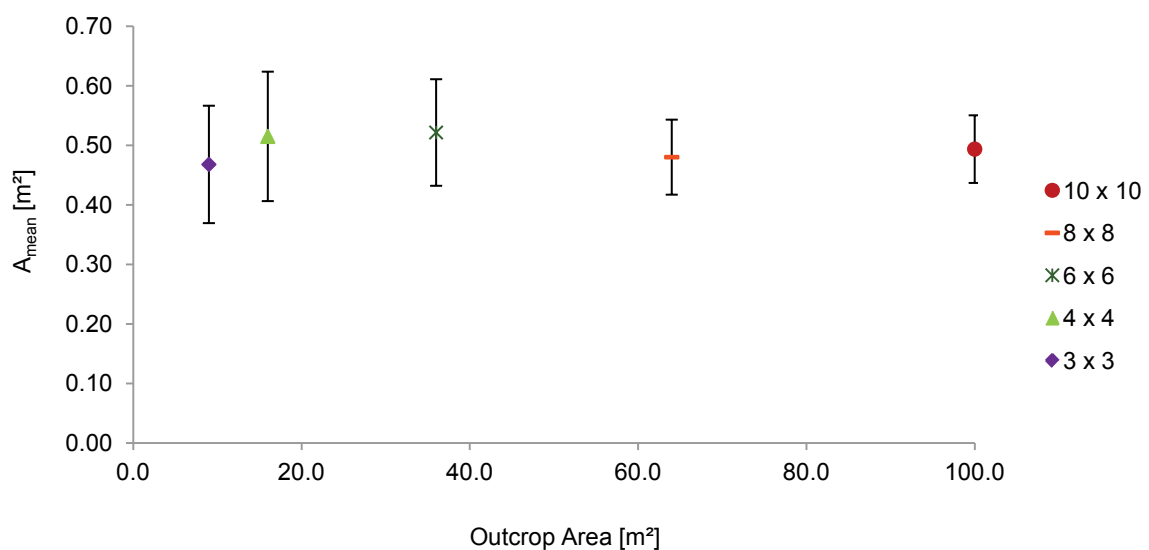
Test 17			z-rotation [°]			10.0		y-rotation [°]			0.0	
dd ₁ [°]	dip ₁ [°]	dd ₂ [°]	dip ₂ [°]	dd ₃ [°]	dip ₃ [°]	sp ₁ [m]	sp ₂ [m]	sp ₃ [m]	p ₁ [-]	p ₂ [-]	p ₃ [-]	
10.0	90.0	0.0	0.0	100.0	90.0	0.2	0.2	0.2	0.8	0.8	0.8	
A _{out} [m ²]	A _{mean} [m ²]	A _{mean} /A _{out} [-]	σ _{Amean} [m ²]	A _{50%,mean} [m ²]	σ _{A50%,mean} [m ²]	A _{75%,mean} [m ²]	σ _{A75%,mean} [m ²]	A _{25%,mean} [m ²]	σ _{A25%,mean} [m ²]			
100.0	0.0587	0.0006	0.0038	0.0406	0.0000	0.0785	0.0086	0.0406	0.0000			
64.0	0.0581	0.0009	0.0044	0.0406	0.0000	0.0755	0.0127	0.0406	0.0000			
36.0	0.0571	0.0016	0.0048	0.0408	0.0013	0.0740	0.0141	0.0406	0.0000			
16.0	0.0604	0.0038	0.0074	0.0421	0.0072	0.0753	0.0141	0.0406	0.0000			
9.0	0.0595	0.0066	0.0086	0.0421	0.0072	0.0707	0.0182	0.0406	0.0000			
4.0	0.0586	0.0147	0.0109	0.0463	0.0139	0.0680	0.0238	0.0413	0.0051			
V _{model} [m ³]	V _{mean} [m ³]	σ _{Vmean} [m ³]	V _{50%,mean} [m ³]	σ _{V50%,mean} [m ³]	V _{75%,mean} [m ³]	σ _{V75%,mean} [m ³]	V _{25%,mean} [m ³]	σ _{V25%,mean} [m ³]				
1000.0	0.0153	0.0011	0.0105	0.0037	0.0161	0.0008	0.0080	0.0000				
640.0	0.0153	0.0012	0.0106	0.0038	0.0162	0.0014	0.0080	0.0000				
360.0	0.0152	0.0014	0.0108	0.0038	0.0162	0.0014	0.0080	0.0000				
160.0	0.0151	0.0018	0.0108	0.0038	0.0166	0.0027	0.0080	0.0000				
90.0	0.0151	0.0022	0.0109	0.0038	0.0170	0.0033	0.0080	0.0000				
40.0	0.0150	0.0026	0.0106	0.0038	0.0170	0.0033	0.0080	0.0000				
V _{per}	T _{mean}		T _{50%}		T _{75%}		T _{25%}					
0.0080	1.9125		1.3125		2.0125		1.0000					



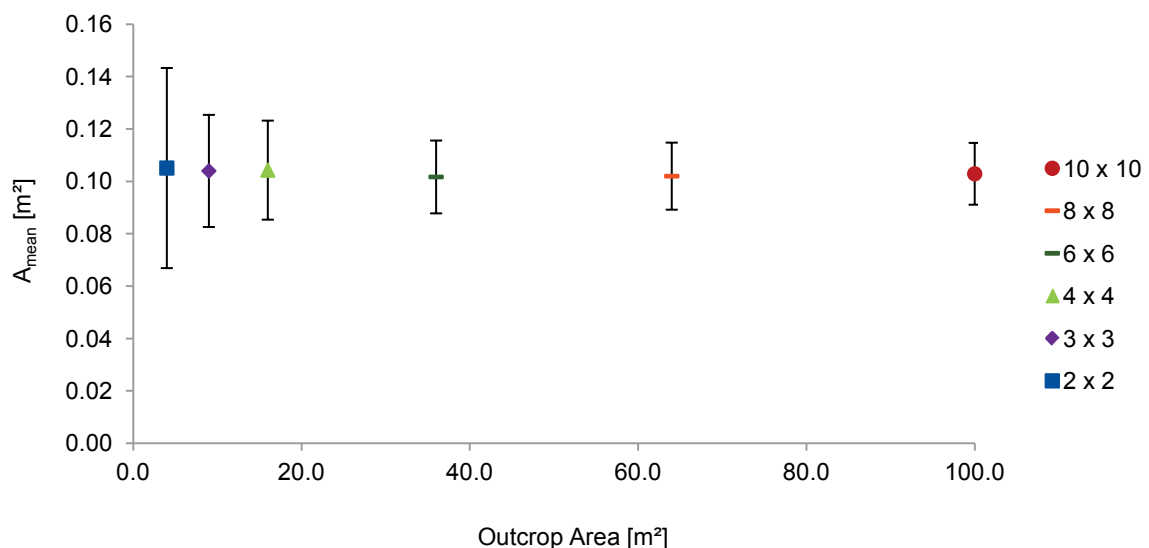
Test 18			z-rotation [°]			10.0			y-rotation [°]			0.0		
dd ₁ [°]	dip ₁ [°]	dd ₂ [°]	dip ₂ [°]	dd ₃ [°]	dip ₃ [°]	sp ₁ [m]	sp ₂ [m]	sp ₃ [m]	p ₁ [-]	p ₂ [-]	p ₃ [-]			
10.0	90.0	0.0	0.0	100.0	90.0	0.4	0.4	0.4	0.8	0.8	0.8			
A _{out} [m ²]	A _{mean} [m ²]	A _{mean} /A _{out} [-]	$\sigma_{A\text{mean}}$ [m ²]	A _{50%,mean} [m ²]	$\sigma_{A50\%,\text{mean}}$ [m ²]	A _{75%,mean} [m ²]	$\sigma_{A75\%,\text{mean}}$ [m ²]	A _{25%,mean} [m ²]	$\sigma_{A25\%,\text{mean}}$ [m ²]					
100.0	0.2156	0.0022	0.0178	0.1625	0.0000	0.2735	0.0685	0.1551	0.0183					
64.0	0.2218	0.0035	0.0230	0.1630	0.0053	0.2759	0.0686	0.1610	0.0053					
36.0	0.2136	0.0059	0.0245	0.1636	0.0077	0.2511	0.0710	0.1589	0.0130					
16.0	0.2354	0.0147	0.0425	0.1828	0.0570	0.2774	0.0936	0.1665	0.0242					
9.0	0.2320	0.0258	0.0610	0.1909	0.0725	0.2490	0.0957	0.1710	0.0362					
4.0	0.2130	0.0533	0.0535	0.1828	0.0521	0.2250	0.0873	0.1747	0.0410					
V _{model} [m ³]	V _{mean} [m ³]	$\sigma_{V\text{mean}}$ [m ³]	V _{50%,mean} [m ³]	$\sigma_{V50\%,\text{mean}}$ [m ³]	V _{75%,mean} [m ³]	$\sigma_{V75\%,\text{mean}}$ [m ³]	V _{25%,mean} [m ³]	$\sigma_{V25\%,\text{mean}}$ [m ³]						
1000.0	0.1218	0.0113	0.0883	0.0312	0.1318	0.0153	0.0640	0.0000						
640.0	0.1219	0.0134	0.0902	0.0316	0.1330	0.0170	0.0640	0.0000						
360.0	0.1201	0.0153	0.0845	0.0300	0.1350	0.0221	0.0640	0.0000						
160.0	0.1147	0.0180	0.0787	0.0271	0.1344	0.0249	0.0646	0.0064						
90.0	0.1116	0.0219	0.0810	0.0289	0.1342	0.0277	0.0659	0.0110						
40.0	0.1085	0.0258	0.0806	0.0317	0.1275	0.0392	0.0672	0.0140						
V _{per}	T _{mean}		T _{50%}		T _{75%}		T _{25%}							
0.0640	1.9031		1.3797		2.0594		1.0000							



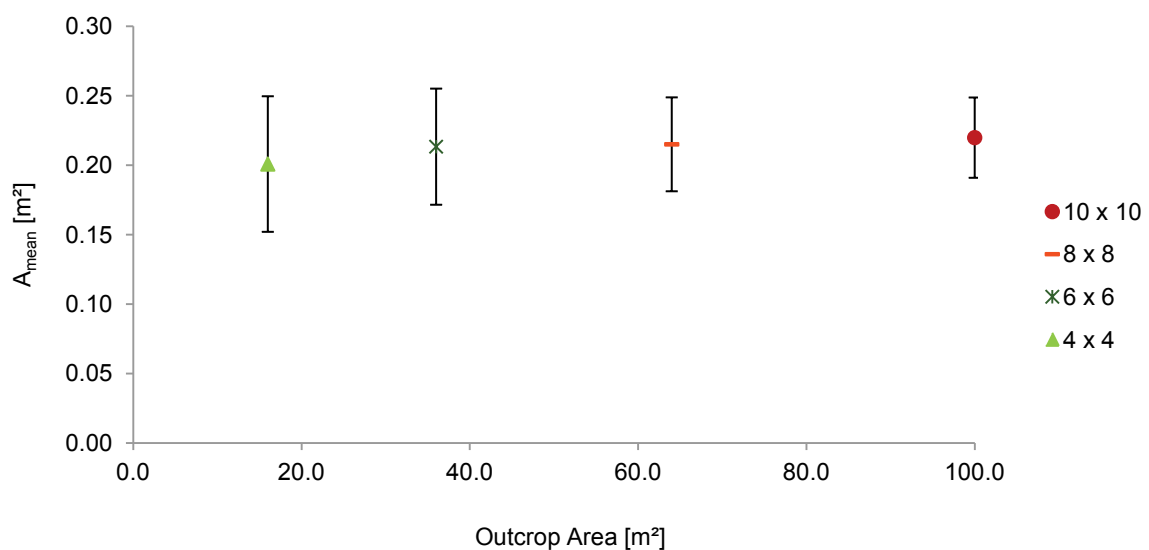
Test 19			z-rotation [°]			10.0			y-rotation [°]			0.0		
dd ₁ [°]	dip ₁ [°]	dd ₂ [°]	dip ₂ [°]	dd ₃ [°]	dip ₃ [°]	sp ₁ [m]	sp ₂ [m]	sp ₃ [m]	p ₁ [-]	p ₂ [-]	p ₃ [-]			
10.0	90.0	0.0	0.0	100.0	90.0	0.6	0.6	0.6	0.8	0.8	0.8			
A _{out} [m ²]	A _{mean} [m ²]	A _{mean/A_{out}} [-]	σ _{A_{mean}} [m ²]	A _{50%,mean} [m ²]	σ _{A_{50%,mean}} [m ²]	A _{75%,mean} [m ²]	σ _{A_{75%,mean}} [m ²]	A _{25%,mean} [m ²]	σ _{A_{25%,mean}} [m ²]					
100.0	0.4936	0.0049	0.0568	0.3704	0.0384	0.6072	0.1627	0.3629	0.0171					
64.0	0.4801	0.0075	0.0630	0.3680	0.0245	0.5772	0.1688	0.3336	0.0517					
36.0	0.5215	0.0145	0.0895	0.3966	0.0974	0.6077	0.2022	0.3656	0.0000					
16.0	0.5150	0.0322	0.1087	0.4076	0.1128	0.5739	0.2154	0.3692	0.0366					
9.0	0.4679	0.0520	0.0986	0.4131	0.1208	0.4962	0.1919	0.3720	0.0416					
4.0	n/a	n/a	n/a	n/a	n/a	n/a	n/a	n/a	n/a					
V _{model} [m ³]	V _{mean} [m ³]	σ _{V_{mean}} [m ³]	V _{50%,mean} [m ³]	σ _{V_{50%,mean}} [m ³]	V _{75%,mean} [m ³]	σ _{V_{75%,mean}} [m ³]	V _{25%,mean} [m ³]	σ _{V_{25%,mean}} [m ³]						
1000.0	0.4085	0.0530	0.2873	0.1021	0.4514	0.0621	0.2160	0.0000						
640.0	0.4027	0.0542	0.2873	0.1021	0.4536	0.0651	0.2160	0.0000						
360.0	0.3934	0.0640	0.2808	0.1030	0.4622	0.0813	0.2160	0.0000						
160.0	0.3834	0.0774	0.2894	0.1028	0.4531	0.0885	0.2203	0.0304						
90.0	0.3671	0.0814	0.2819	0.1040	0.4320	0.1141	0.2246	0.0425						
40.0	0.3299	0.0768	0.2884	0.1042	0.3569	0.1151	0.2387	0.0643						
V _{per}	T _{mean}		T _{50%}		T _{75%}		T _{25%}							
0.2160	1.8912		1.3301		2.0898		1.0000							



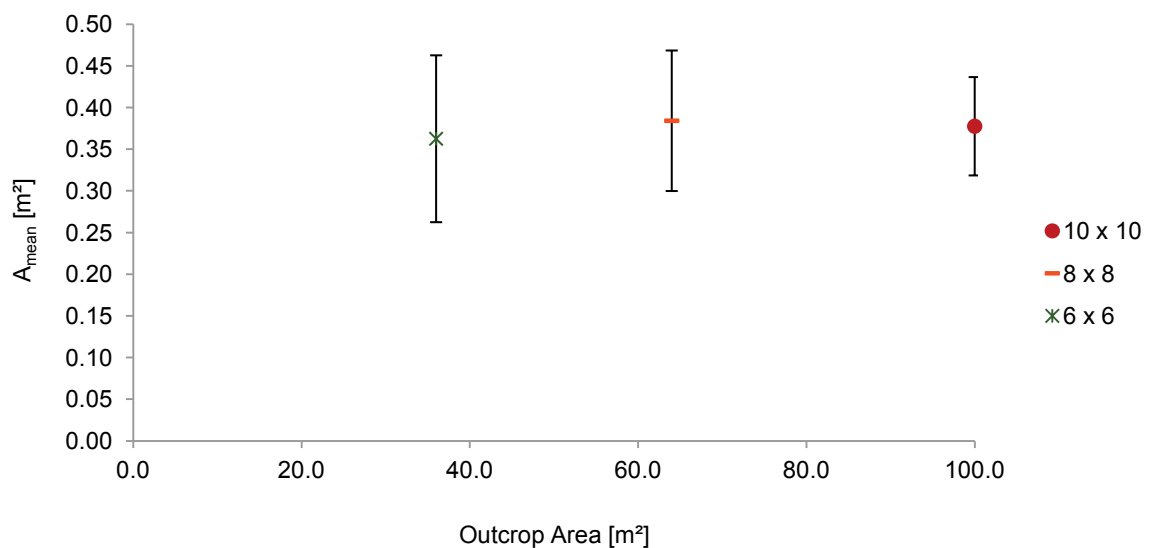
Test 20			z-rotation [°]			10.0		y-rotation [°]			0.0	
dd ₁ [°]	dip ₁ [°]	dd ₂ [°]	dip ₂ [°]	dd ₃ [°]	dip ₃ [°]	sp ₁ [m]	sp ₂ [m]	sp ₃ [m]	p ₁ [-]	p ₂ [-]	p ₃ [-]	
10.0	90.0	0.0	0.0	100.0	90.0	0.2	0.2	0.2	0.6	0.6	0.6	
A _{out} [m ²]	A _{mean} [m ²]	A _{mean} /A _{out} [-]	σ _{Amean} [m ²]	A _{50%,mean} [m ²]	σ _{A50%,mean} [m ²]	A _{75%,mean} [m ²]	σ _{A75%,mean} [m ²]	A _{25%,mean} [m ²]	σ _{A25%,mean} [m ²]			
100.0	0.1029	0.0010	0.0118	0.0792	0.0080	0.1231	0.0186	0.0407	0.0007			
64.0	0.1020	0.0016	0.0128	0.0781	0.0095	0.1212	0.0228	0.0408	0.0014			
36.0	0.1017	0.0028	0.0139	0.0775	0.0114	0.1189	0.0245	0.0419	0.0053			
16.0	0.1043	0.0065	0.0189	0.0785	0.0153	0.1218	0.0303	0.0462	0.0135			
9.0	0.1040	0.0116	0.0214	0.0783	0.0212	0.1223	0.0348	0.0472	0.0140			
4.0	0.1051	0.0263	0.0382	0.0802	0.0327	0.1208	0.0558	0.0551	0.0229			
V _{model} [m ³]	V _{mean} [m ³]	σ _{Vmean} [m ³]	V _{50%,mean} [m ³]	σ _{V50%,mean} [m ³]	V _{75%,mean} [m ³]	σ _{V75%,mean} [m ³]	V _{25%,mean} [m ³]	σ _{V25%,mean} [m ³]				
1000.0	0.0364	0.0043	0.0213	0.0041	0.0413	0.0073	0.0142	0.0034				
640.0	0.0366	0.0045	0.0210	0.0044	0.0411	0.0075	0.0140	0.0035				
360.0	0.0363	0.0051	0.0210	0.0049	0.0409	0.0075	0.0138	0.0036				
160.0	0.0362	0.0071	0.0208	0.0057	0.0409	0.0098	0.0134	0.0039				
90.0	0.0361	0.0089	0.0212	0.0061	0.0414	0.0121	0.0132	0.0040				
40.0	0.0342	0.0102	0.0205	0.0068	0.0398	0.0140	0.0127	0.0046				
V _{per}	T_{mean}		T_{50%}		T_{75%}		T_{25%}					
0.0080	4.5500		2.6625		5.1625		1.7750					



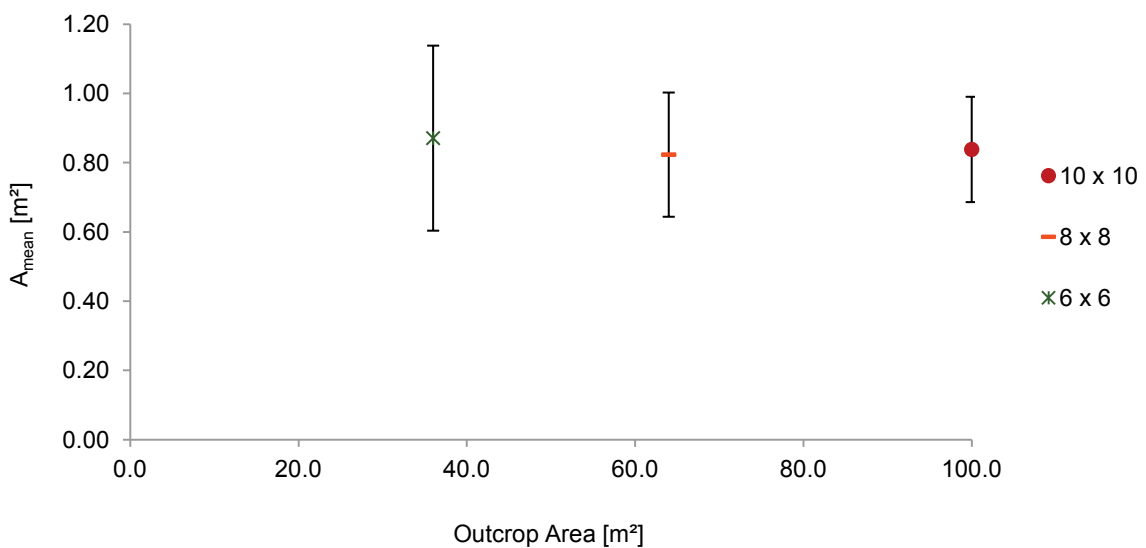
Test 21			z-rotation [°]			10.0			y-rotation [°]			0.0		
dd ₁ [°]	dip ₁ [°]	dd ₂ [°]	dip ₂ [°]	dd ₃ [°]	dip ₃ [°]	sp ₁ [m]	sp ₂ [m]	sp ₃ [m]	p ₁ [-]	p ₂ [-]	p ₃ [-]			
10.0	90.0	0.0	0.0	100.0	90.0	0.3	0.3	0.3	0.6	0.6	0.6			
A _{out} [m ²]	A _{mean} [m ²]	A _{mean} /A _{out} [-]	σ _{Amean} [m ²]	A _{50%,mean} [m ²]	σ _{A50%,mean} [m ²]	A _{75%,mean} [m ²]	σ _{A75%,mean} [m ²]	A _{25%,mean} [m ²]	σ _{A25%,mean} [m ²]					
100.0	0.2198	0.0022	0.0289	0.1708	0.0266	0.2628	0.0464	0.0924	0.0080					
64.0	0.2150	0.0034	0.0338	0.1579	0.0341	0.2534	0.0527	0.0929	0.0090					
36.0	0.2133	0.0059	0.0418	0.1606	0.0380	0.2501	0.0675	0.0944	0.0147					
16.0	0.2008	0.0126	0.0488	0.1469	0.0489	0.2380	0.0727	0.0941	0.0178					
9.0	n/a	n/a	n/a	n/a	n/a	n/a	n/a	n/a	n/a	n/a	n/a			
4.0	n/a	n/a	n/a	n/a	n/a	n/a	n/a	n/a	n/a	n/a	n/a			
V _{model} [m ³]	V _{mean} [m ³]	σ _{Vmean} [m ³]	V _{50%,mean} [m ³]	σ _{V50%,mean} [m ³]	V _{75%,mean} [m ³]	σ _{V75%,mean} [m ³]	V _{25%,mean} [m ³]	σ _{V25%,mean} [m ³]						
1000.0	0.1213	0.0196	0.0710	0.0161	0.1401	0.0294	0.0470	0.1190						
640.0	0.1207	0.0220	0.0699	0.0159	0.1365	0.0300	0.0454	0.0127						
360.0	0.1179	0.0243	0.0702	0.0184	0.1350	0.0312	0.0446	0.0129						
160.0	0.1124	0.0371	0.0672	0.0256	0.1280	0.0489	0.0402	0.0151						
90.0	0.1080	0.0431	0.0662	0.0278	0.1267	0.0568	0.0421	0.0218						
40.0	n/a	n/a	n/a	n/a	n/a	n/a	n/a	n/a						
V _{per}	T _{mean}			T _{50%}			T _{75%}			T _{25%}				
0.0270	4.4926			2.6296			5.1889			1.7407				



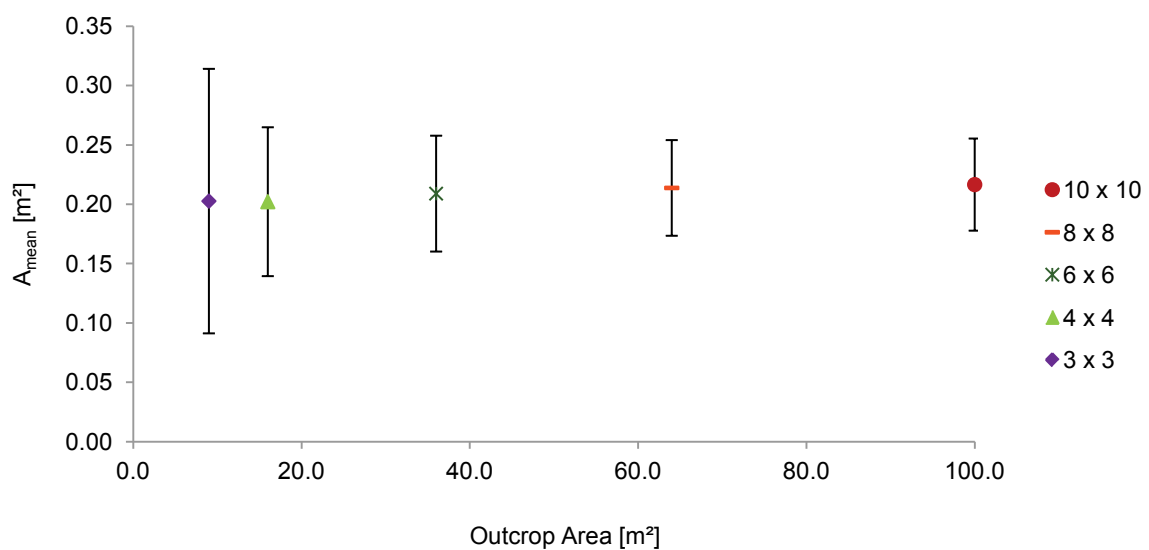
Test 22			z-rotation [°]			10.0		y-rotation [°]			0.0	
dd ₁ [°]	dip ₁ [°]	dd ₂ [°]	dip ₂ [°]	dd ₃ [°]	dip ₃ [°]	sp ₁ [m]	sp ₂ [m]	sp ₃ [m]	p ₁ [-]	p ₂ [-]	p ₃ [-]	
10.0	90.0	0.0	0.0	100.0	90.0	0.4	0.4	0.4	0.6	0.6	0.6	
A _{out} [m ²]	A _{mean} [m ²]	A _{mean} /A _{out} [-]	σ _{Amean} [m ²]	A _{50%,mean} [m ²]	σ _{A50%,mean} [m ²]	A _{75%,mean} [m ²]	σ _{A75%,mean} [m ²]	A _{25%,mean} [m ²]	σ _{A25%,mean} [m ²]			
100.0	0.3776	0.0038	0.0590	0.2768	0.0674	0.4476	0.0970	0.1646	0.0185			
64.0	0.3842	0.0060	0.0843	0.2788	0.0809	0.4469	0.1176	0.1690	0.0362			
36.0	0.3626	0.0101	0.1001	0.2657	0.0963	0.4303	0.1588	0.1707	0.0409			
16.0	n/a	n/a	n/a	n/a	n/a	n/a	n/a	n/a	n/a	n/a	n/a	
9.0	n/a	n/a	n/a	n/a	n/a	n/a	n/a	n/a	n/a	n/a	n/a	
4.0	n/a	n/a	n/a	n/a	n/a	n/a	n/a	n/a	n/a	n/a	n/a	
V _{model} [m ³]	V _{mean} [m ³]	σ _{Vmean} [m ³]	V _{50%,mean} [m ³]	σ _{V50%,mean} [m ³]	V _{75%,mean} [m ³]	σ _{V75%,mean} [m ³]	V _{25%,mean} [m ³]	σ _{V25%,mean} [m ³]				
1000.0	0.2813	0.0590	0.1651	0.0456	0.3174	0.0761	0.1011	0.0330				
640.0	0.2789	0.0718	0.1638	0.0501	0.3232	0.0977	0.1024	0.0364				
360.0	0.2729	0.0878	0.1651	0.0638	0.3230	0.1168	0.1019	0.0399				
160.0	0.2728	0.1598	0.1808	0.1274	0.3293	0.1950	0.1061	0.0681				
90.0	n/a	n/a	n/a	n/a	n/a	n/a	n/a	n/a				
40.0	n/a	n/a	n/a	n/a	n/a	n/a	n/a	n/a				
V _{per}	T _{mean}		T _{50%}		T _{75%}		T _{25%}					
0.0640	4.3953		2.5797		4.9594		1.5797					



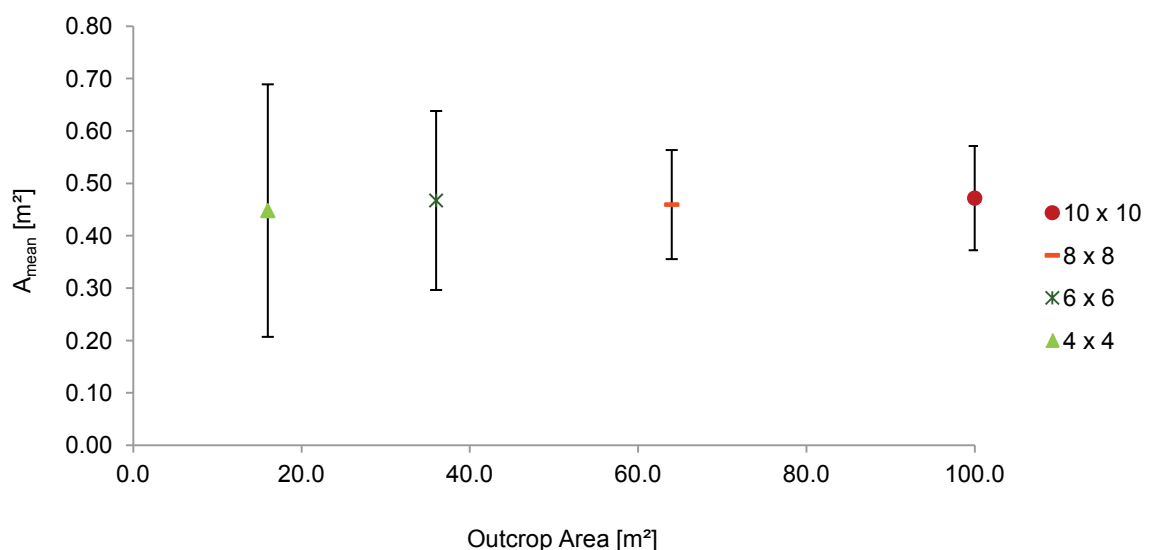
Test 23			z-rotation [°]			10.0			y-rotation [°]			0.0		
dd ₁ [°]	dip ₁ [°]	dd ₂ [°]	dip ₂ [°]	dd ₃ [°]	dip ₃ [°]	sp ₁ [m]	sp ₂ [m]	sp ₃ [m]	p ₁ [-]	p ₂ [-]	p ₃ [-]			
10.0	90.0	0.0	0.0	100.0	90.0	0.6	0.6	0.6	0.6	0.6	0.6			
A _{out} [m ²]	A _{mean} [m ²]	A _{mean} /A _{out} [-]	σ _{Amean} [m ²]	A _{50%,mean} [m ²]	σ _{A50%,mean} [m ²]	A _{75%,mean} [m ²]	σ _{A75%,mean} [m ²]	A _{25%,mean} [m ²]	σ _{A25%,mean} [m ²]					
100.0	0.8384	0.0084	0.1521	0.6089	0.1671	0.9941	0.2517	0.3853	0.0771					
64.0	0.8234	0.0129	0.1794	0.5863	0.1801	0.9875	0.2811	0.3777	0.0757					
36.0	0.8710	0.0242	0.2672	0.6470	0.2564	1.0235	0.4031	0.4588	0.1762					
16.0	n/a	n/a	n/a	n/a	n/a	n/a	n/a	n/a	n/a	n/a	n/a			
9.0	n/a	n/a	n/a	n/a	n/a	n/a	n/a	n/a	n/a	n/a	n/a			
4.0	n/a	n/a	n/a	n/a	n/a	n/a	n/a	n/a	n/a	n/a	n/a			
V _{model} [m ³]	V _{mean} [m ³]	σ _{Vmean} [m ³]	V _{50%,mean} [m ³]	σ _{V50%,mean} [m ³]	V _{75%,mean} [m ³]	σ _{V75%,mean} [m ³]	V _{25%,mean} [m ³]	σ _{V25%,mean} [m ³]						
1000.0	0.9147	0.2143	0.5443	0.1550	1.0498	0.2641	0.3272	0.1122						
640.0	0.8883	0.2285	0.5486	0.1827	1.0352	0.2737	0.3262	0.1209						
360.0	0.8763	0.3514	0.5746	0.2460	1.0735	0.4917	0.3440	0.1439						
160.0	n/a	n/a	n/a	n/a	n/a	n/a	n/a	n/a	n/a	n/a	n/a			
90.0	n/a	n/a	n/a	n/a	n/a	n/a	n/a	n/a	n/a	n/a	n/a			
40.0	n/a	n/a	n/a	n/a	n/a	n/a	n/a	n/a	n/a	n/a	n/a			
V _{per}	T _{mean}			T _{50%}			T _{75%}			T _{25%}				
0.2160	4.2347			2.5199			4.8602			1.5148				



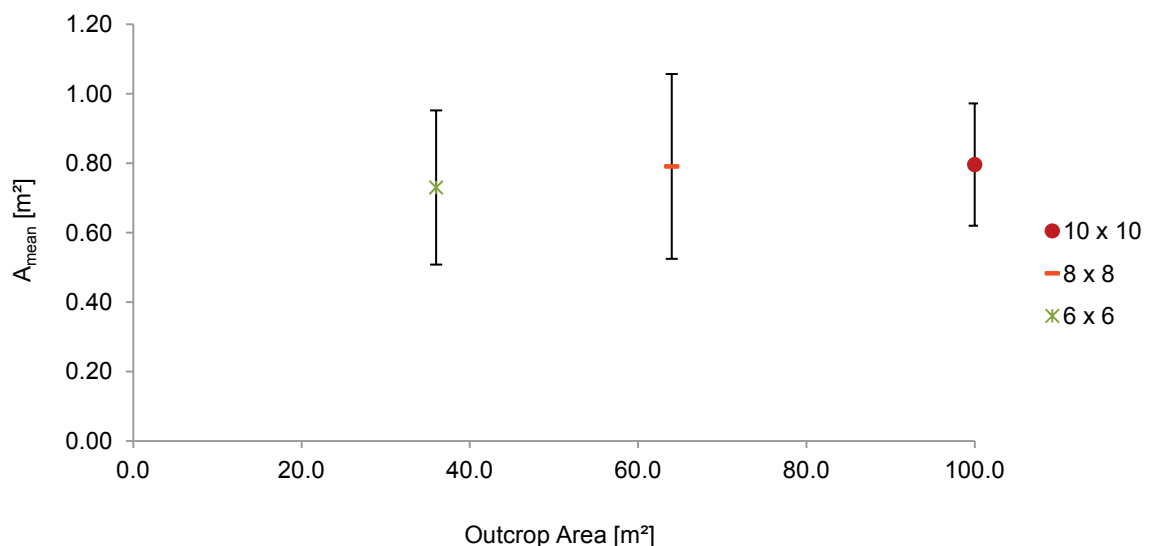
Test 24			z-rotation [°]			10.0			y-rotation [°]			0.0		
dd ₁ [°]	dip ₁ [°]	dd ₂ [°]	dip ₂ [°]	dd ₃ [°]	dip ₃ [°]	sp ₁ [m]	sp ₂ [m]	sp ₃ [m]	p ₁ [-]	p ₂ [-]	p ₃ [-]			
10.0	90.0	0.0	0.0	100.0	90.0	0.2	0.2	0.2	0.4	0.4	0.4			
A _{out} [m ²]	A _{mean} [m ²]	A _{mean} /A _{out} [-]	σ _{Amean} [m ²]	A _{50%,mean} [m ²]	σ _{A50%,mean} [m ²]	A _{75%,mean} [m ²]	σ _{A75%,mean} [m ²]	A _{25%,mean} [m ²]	σ _{A25%,mean} [m ²]					
100.0	0.2166	0.0022	0.0388	0.1342	0.0234	0.2594	0.0550	0.0756	0.0144					
64.0	0.2138	0.0033	0.0403	0.1345	0.0279	0.2568	0.0571	0.0750	0.0186					
36.0	0.2090	0.0058	0.0488	0.1325	0.0357	0.2529	0.0654	0.0721	0.0224					
16.0	0.2022	0.0126	0.0627	0.1315	0.0464	0.2413	0.0763	0.0770	0.0340					
9.0	0.2027	0.0225	0.1114	0.1338	0.0544	0.2513	0.1602	0.0796	0.0398					
4.0	n/a	n/a	n/a	n/a	n/a	n/a	n/a	n/a	n/a					
V _{model} [m ³]	V _{mean} [m ³]	σ _{Vmean} [m ³]	V _{50%,mean} [m ³]	σ _{V50%,mean} [m ³]	V _{75%,mean} [m ³]	σ _{V75%,mean} [m ³]	V _{25%,mean} [m ³]	σ _{V25%,mean} [m ³]						
1000.0	0.1149	0.0214	0.0561	0.0118	0.1252	0.0267	0.0263	0.0056						
640.0	0.1137	0.0236	0.0568	0.0123	0.1241	0.0292	0.0270	0.0064						
360.0	0.1133	0.0281	0.0564	0.0151	0.1242	0.0336	0.0271	0.0080						
160.0	0.1082	0.0350	0.0557	0.0202	0.1215	0.0437	0.0268	0.0106						
90.0	0.1034	0.0441	0.0562	0.0288	0.1186	0.0620	0.0264	0.0126						
40.0	0.0878	0.0318	0.0499	0.0236	0.0995	0.0410	0.0277	0.0168						
V _{per}	T _{mean}		T _{50%}		T _{75%}		T _{25%}							
0.0080	14.3625		7.0125		15.6500		3.2875							



Test 25			z-rotation [°]			10.0		y-rotation [°]			0.0	
dd ₁ [°]	dip ₁ [°]	dd ₂ [°]	dip ₂ [°]	dd ₃ [°]	dip ₃ [°]	sp ₁ [m]	sp ₂ [m]	sp ₃ [m]	p ₁ [-]	p ₂ [-]	p ₃ [-]	
10.0	90.0	0.0	0.0	100.0	90.0	0.3	0.3	0.3	0.4	0.4	0.4	
A _{out} [m ²]	A _{mean} [m ²]	A _{mean} /A _{out} [-]	$\sigma_{A\text{mean}}$ [m ²]	A _{50%,mean} [m ²]	$\sigma_{A\text{50%,mean}}$ [m ²]	A _{75%,mean} [m ²]	$\sigma_{A\text{75%,mean}}$ [m ²]	A _{25%,mean} [m ²]	$\sigma_{A\text{25%,mean}}$ [m ²]			
100.0	0.4719	0.0047	0.0995	0.2890	0.0703	0.5559	0.1210	0.1553	0.0477			
64.0	0.4596	0.0072	0.1041	0.2783	0.0745	0.5488	0.1322	0.1475	0.0460			
36.0	0.4674	0.0130	0.1708	0.3023	0.1340	0.5609	0.2712	0.1600	0.0733			
16.0	0.4481	0.0280	0.2410	0.3131	0.1883	0.5194	0.2902	0.1798	0.1135			
9.0	n/a	n/a	n/a	n/a	n/a	n/a	n/a	n/a	n/a			
4.0	n/a	n/a	n/a	n/a	n/a	n/a	n/a	n/a	n/a			
V _{model} [m ³]	V _{mean} [m ³]	$\sigma_{V\text{mean}}$ [m ³]	V _{50%,mean} [m ³]	$\sigma_{V\text{50%,mean}}$ [m ³]	V _{75%,mean} [m ³]	$\sigma_{V\text{75%,mean}}$ [m ³]	V _{25%,mean} [m ³]	$\sigma_{V\text{25%,mean}}$ [m ³]				
1000.0	0.4719	0.0047	0.0995	0.2890	0.0703	0.5559	0.1210	0.1553				
640.0	0.4596	0.0072	0.1041	0.2783	0.0745	0.5488	0.1322	0.1475				
360.0	0.4674	0.0130	0.1708	0.3023	0.1340	0.5609	0.2712	0.1600				
160.0	0.4481	0.0280	0.2410	0.3131	0.1883	0.5194	0.2902	0.1798				
90.0	n/a	n/a	n/a	n/a	n/a	n/a	n/a	n/a				
40.0	n/a	n/a	n/a	n/a	n/a	n/a	n/a	n/a				
V _{per}	T_{mean}		T_{50%}		T_{75%}		T_{25%}					
0.0270	17.4778		3.6852		2.6037		4.4815					



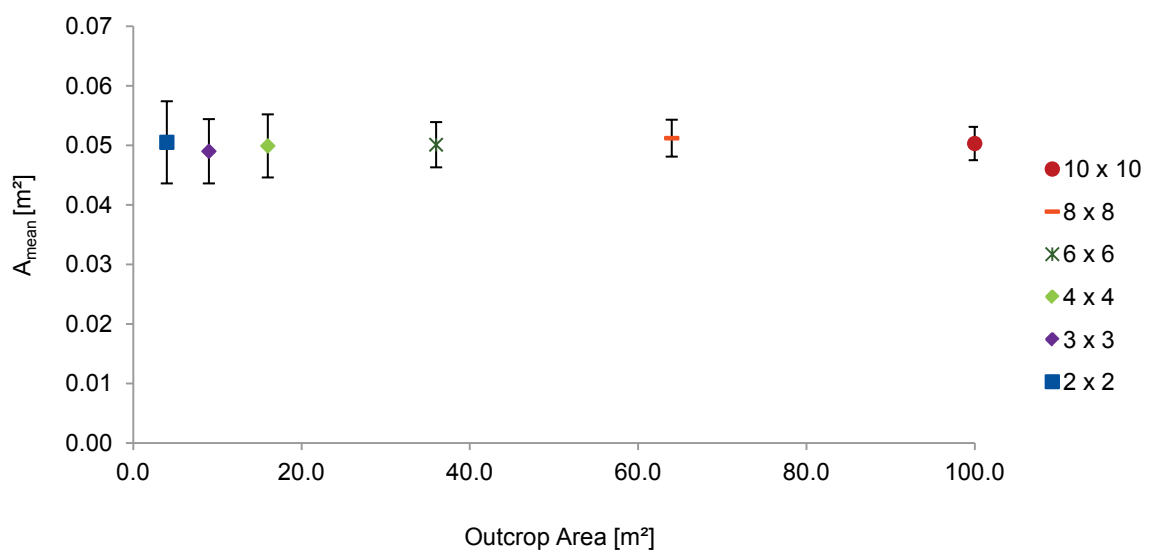
Test 26			z-rotation [°]			10.0			y-rotation [°]			0.0		
dd ₁ [°]	dip ₁ [°]	dd ₂ [°]	dip ₂ [°]	dd ₃ [°]	dip ₃ [°]	sp ₁ [m]	sp ₂ [m]	sp ₃ [m]	p ₁ [-]	p ₂ [-]	p ₃ [-]			
10.0	90.0	0.0	0.0	100.0	90.0	0.4	0.4	0.4	0.4	0.4	0.4			
A _{out} [m ²]	A _{mean} [m ²]	A _{mean} /A _{out} [-]	σ _{Amean} [m ²]	A _{50%,mean} [m ²]	σ _{A50%,mean} [m ²]	A _{75%,mean} [m ²]	σ _{A75%,mean} [m ²]	A _{25%,mean} [m ²]	σ _{A25%,mean} [m ²]					
100.0	0.7959	0.0080	0.1761	0.4817	0.1202	0.9486	0.2461	0.2670	0.0766					
64.0	0.7906	0.0124	0.2661	0.4978	0.1750	0.9473	0.3546	0.2784	0.1059					
36.0	0.7299	0.0203	0.2220	0.4734	0.1695	0.9048	0.3245	0.2694	0.1190					
16.0	n/a	n/a	n/a	n/a	n/a	n/a	n/a	n/a	n/a					
9.0	n/a	n/a	n/a	n/a	n/a	n/a	n/a	n/a	n/a					
4.0	n/a	n/a	n/a	n/a	n/a	n/a	n/a	n/a	n/a					
V _{model} [m ³]	V _{mean} [m ³]	σ _{Vmean} [m ³]	V _{50%,mean} [m ³]	σ _{V50%,mean} [m ³]	V _{75%,mean} [m ³]	σ _{V75%,mean} [m ³]	V _{25%,mean} [m ³]	σ _{V25%,mean} [m ³]						
1000.0	0.8340	0.2205	0.4262	0.1136	0.9237	0.2422	0.2138	0.0645						
640.0	0.8089	0.2688	0.4186	0.1357	0.9277	0.3120	0.2080	0.0683						
360.0	0.7887	0.3824	0.4282	0.2204	0.9115	0.4154	0.2147	0.1182						
160.0	n/a	n/a	n/a	n/a	n/a	n/a	n/a	n/a						
90.0	n/a	n/a	n/a	n/a	n/a	n/a	n/a	n/a						
40.0	n/a	n/a	n/a	n/a	n/a	n/a	n/a	n/a						
V _{per}	T _{mean}			T _{50%}			T _{75%}			T _{25%}				
0.0640	13.0313			6.6594			14.4328			3.3406				



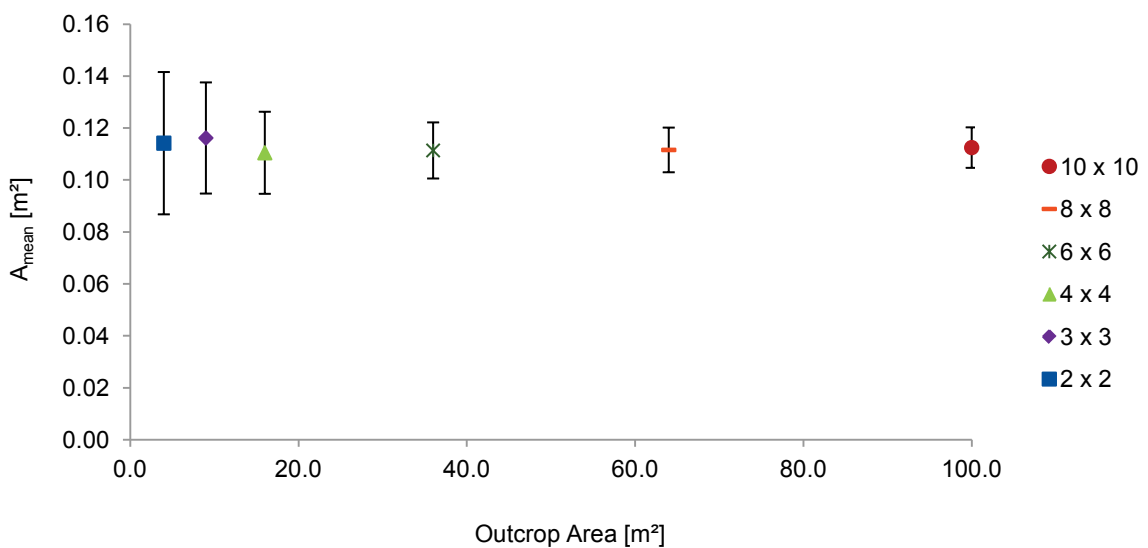
Test 27			z-rotation [°]			10.0		y-rotation [°]			0.0	
dd ₁ [°]	dip ₁ [°]	dd ₂ [°]	dip ₂ [°]	dd ₃ [°]	dip ₃ [°]	sp ₁ [m]	sp ₂ [m]	sp ₃ [m]	p ₁ [-]	p ₂ [-]	p ₃ [-]	
10.0	90.0	0.0	0.0	100.0	90.0	0.6	0.6	0.6	0.4	0.4	0.4	
A _{out} [m ²]	A _{mean} [m ²]	A _{mean} /A _{out} [-]	σ _{Amean} [m ²]	A _{50%,mean} [m ²]	σ _{A50%,mean} [m ²]	A _{75%,mean} [m ²]	σ _{A75%,mean} [m ²]	A _{25%,mean} [m ²]	σ _{A25%,mean} [m ²]			
100.0	1.6807	0.0168	0.5285	1.1595	0.4761	2.0923	0.8114	0.6382	0.2810			
64.0	1.7005	0.0266	0.5731	1.1579	0.4247	2.2077	0.9333	0.6437	0.2662			
36.0	n/a	n/a	n/a	n/a	n/a	n/a	n/a	n/a	n/a	n/a	n/a	
16.0	n/a	n/a	n/a	n/a	n/a	n/a	n/a	n/a	n/a	n/a	n/a	
9.0	n/a	n/a	n/a	n/a	n/a	n/a	n/a	n/a	n/a	n/a	n/a	
4.0	n/a	n/a	n/a	n/a	n/a	n/a	n/a	n/a	n/a	n/a	n/a	
V _{model} [m ³]	V _{mean} [m ³]	σ _{Vmean} [m ³]	V _{50%,mean} [m ³]	σ _{V50%,mean} [m ³]	V _{75%,mean} [m ³]	σ _{V75%,mean} [m ³]	V _{25%,mean} [m ³]	σ _{V25%,mean} [m ³]				
1000.0	2.4905	0.8377	1.3673	0.5726	2.8652	1.1734	0.7160	0.3415				
640.0	2.4508	0.9123	1.4105	0.6220	2.8366	1.2139	0.6950	0.2985				
360.0	2.3022	1.4174	1.4947	1.0260	2.7729	1.6235	0.8159	0.5980				
160.0	n/a	n/a	n/a	n/a	n/a	n/a	n/a	n/a	n/a	n/a	n/a	
90.0	n/a	n/a	n/a	n/a	n/a	n/a	n/a	n/a	n/a	n/a	n/a	
40.0	n/a	n/a	n/a	n/a	n/a	n/a	n/a	n/a	n/a	n/a	n/a	
V _{per}	T _{mean}		T _{50%}		T _{75%}		T _{25%}					
0.2160	11.5301		6.3301		13.2648		3.3148					

Transformation factors invalid because limitation ratio has already been exceeded in the major outcrop area!

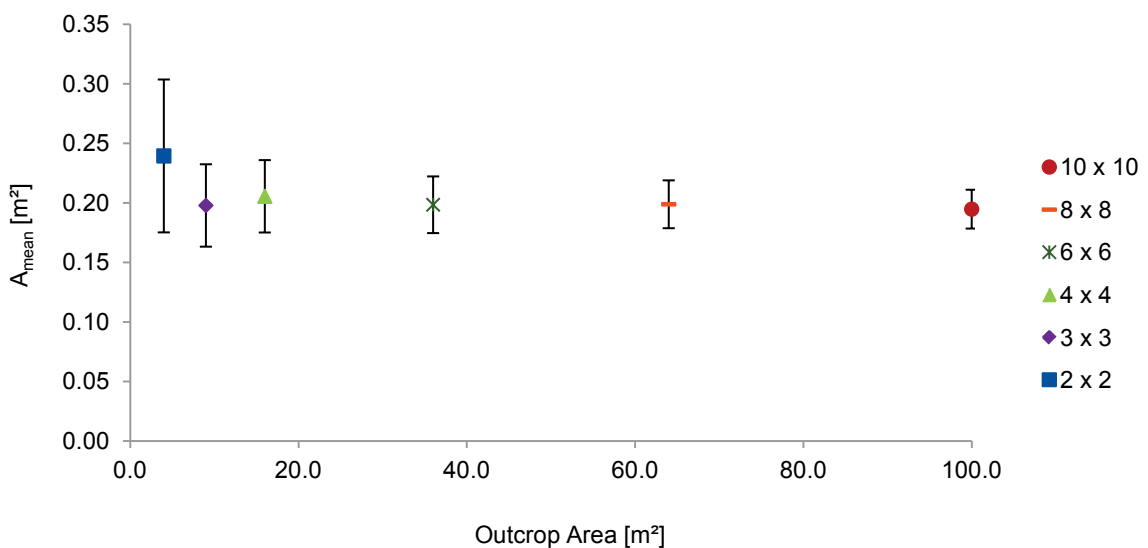
Test 28			z-rotation [°]			22.5			y-rotation [°]			0.0		
dd ₁ [°]	dip ₁ [°]	dd ₂ [°]	dip ₂ [°]	dd ₃ [°]	dip ₃ [°]	sp ₁ [m]	sp ₂ [m]	sp ₃ [m]	p ₁ [-]	p ₂ [-]	p ₃ [-]			
22.5	90.0	0.0	0.0	112.5	90.0	0.2	0.2	0.2	0.8	0.8	0.8			
A _{out} [m ²]	A _{mean} [m ²]	A _{mean/A_{out}} [-]	σ _{A_{mean}} [m ²]	A _{50%,mean} [m ²]	σ _{A_{50%,mean}} [m ²]	A _{75%,mean} [m ²]	σ _{A_{75%,mean}} [m ²]	A _{25%,mean} [m ²]	σ _{A_{25%,mean}} [m ²]					
100.0	0.0503	0.0005	0.0028	0.0433	0.0000	0.0559	0.0109	0.0302	0.0015					
64.0	0.0512	0.0008	0.0031	0.0433	0.0000	0.0562	0.0121	0.0318	0.0023					
36.0	0.0501	0.0014	0.0038	0.0433	0.0000	0.0560	0.0124	0.0311	0.0030					
16.0	0.0499	0.0031	0.0053	0.0433	0.0000	0.0577	0.0152	0.0307	0.0043					
9.0	0.0490	0.0054	0.0054	0.0433	0.0000	0.0573	0.0157	0.0300	0.0057					
4.0	0.0505	0.0126	0.0069	0.0443	0.0062	0.0581	0.0171	0.0330	0.0081					
V _{model} [m ³]	V _{mean} [m ³]	σ _{V_{mean}} [m ³]	V _{50%,mean} [m ³]	σ _{V_{50%,mean}} [m ³]	V _{75%,mean} [m ³]	σ _{V_{75%,mean}} [m ³]	V _{25%,mean} [m ³]	σ _{V_{25%,mean}} [m ³]						
1000.0	0.0153	0.0009	0.0103	0.0036	0.0160	0.0000	0.0080	0.0000						
640.0	0.0152	0.0010	0.0101	0.0035	0.0160	0.0000	0.0080	0.0000						
360.0	0.0152	0.0011	0.0099	0.0034	0.0160	0.0000	0.0080	0.0000						
160.0	0.0150	0.0012	0.0098	0.0034	0.0162	0.0011	0.0080	0.0000						
90.0	0.0148	0.0013	0.0098	0.0033	0.0162	0.0011	0.0080	0.0000						
40.0	0.0144	0.0014	0.0097	0.0033	0.0160	0.0000	0.0080	0.0000						
V _{per}	T _{mean}		T _{50%}		T _{75%}		T _{25%}							
0.0080	1.9125		1.2875		2.0000		1.0000							



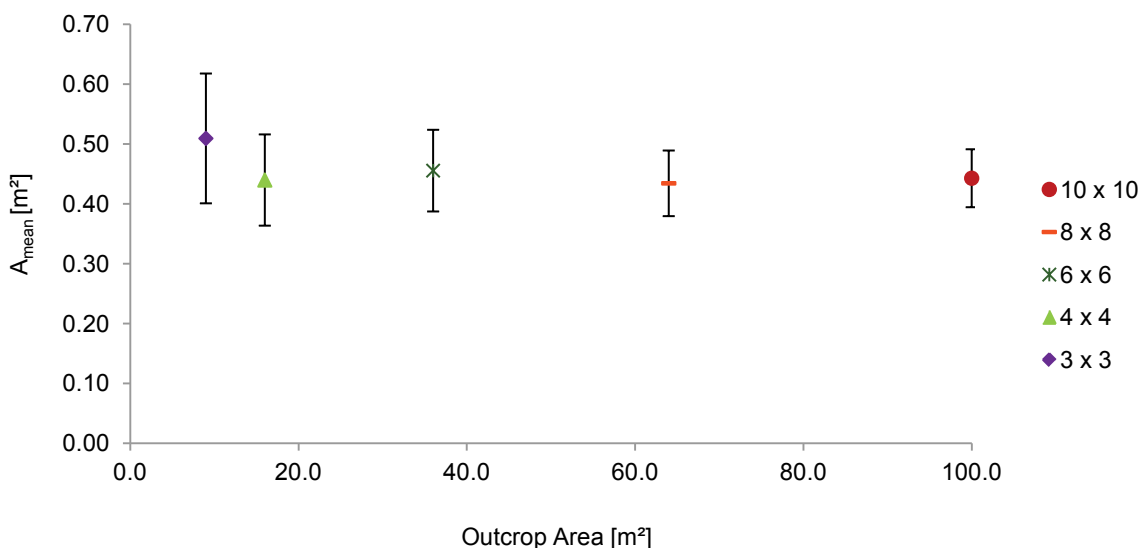
Test 29			z-rotation [°]			22.5			y-rotation [°]			0.0		
dd ₁ [°]	dip ₁ [°]	dd ₂ [°]	dip ₂ [°]	dd ₃ [°]	dip ₃ [°]	sp ₁ [m]	sp ₂ [m]	sp ₃ [m]	p ₁ [-]	p ₂ [-]	p ₃ [-]			
22.5	90.0	0.0	0.0	112.5	90.0	0.3	0.3	0.3	0.8	0.8	0.8			
A _{out} [m ²]	A _{mean} [m ²]	A _{mean} /A _{out} [-]	σ _{Amean} [m ²]	A _{50%,mean} [m ²]	σ _{A50%,mean} [m ²]	A _{75%,mean} [m ²]	σ _{A75%,mean} [m ²]	A _{25%,mean} [m ²]	σ _{A25%,mean} [m ²]					
100.0	0.1125	0.0011	0.0078	0.0974	0.0000	0.1254	0.0276	0.0656	0.0076					
64.0	0.1116	0.0017	0.0086	0.0974	0.0000	0.1254	0.0274	0.0671	0.0068					
36.0	0.1114	0.0031	0.0108	0.0977	0.0024	0.1254	0.0303	0.0688	0.0102					
16.0	0.1105	0.0069	0.0158	0.0981	0.0058	0.1269	0.0353	0.0663	0.0139					
9.0	0.1162	0.0129	0.0214	0.1004	0.0099	0.1270	0.0380	0.0769	0.0190					
4.0	0.1142	0.0286	0.0274	0.1017	0.0155	0.1302	0.0496	0.0753	0.0229					
V _{model} [m ³]	V _{mean} [m ³]	σ _{Vmean} [m ³]	V _{50%,mean} [m ³]	σ _{V50%,mean} [m ³]	V _{75%,mean} [m ³]	σ _{V75%,mean} [m ³]	V _{25%,mean} [m ³]	σ _{V25%,mean} [m ³]						
1000.0	0.0516	0.0038	0.0346	0.0122	0.0545	0.0038	0.0270	0.0000						
640.0	0.0515	0.0042	0.0356	0.0127	0.0545	0.0038	0.0270	0.0000						
360.0	0.0512	0.0046	0.0346	0.0122	0.0548	0.0046	0.0270	0.0000						
160.0	0.0503	0.0051	0.0348	0.0123	0.0551	0.0053	0.0270	0.0000						
90.0	0.0492	0.0054	0.0343	0.0120	0.0554	0.0059	0.0270	0.0000						
40.0	0.0474	0.0055	0.0340	0.0119	0.0545	0.0038	0.0270	0.0000						
V _{per}	T _{mean}			T _{50%}			T _{75%}			T _{25%}				
0.0270	1.9111			1.2815			2.0185			1.0000				



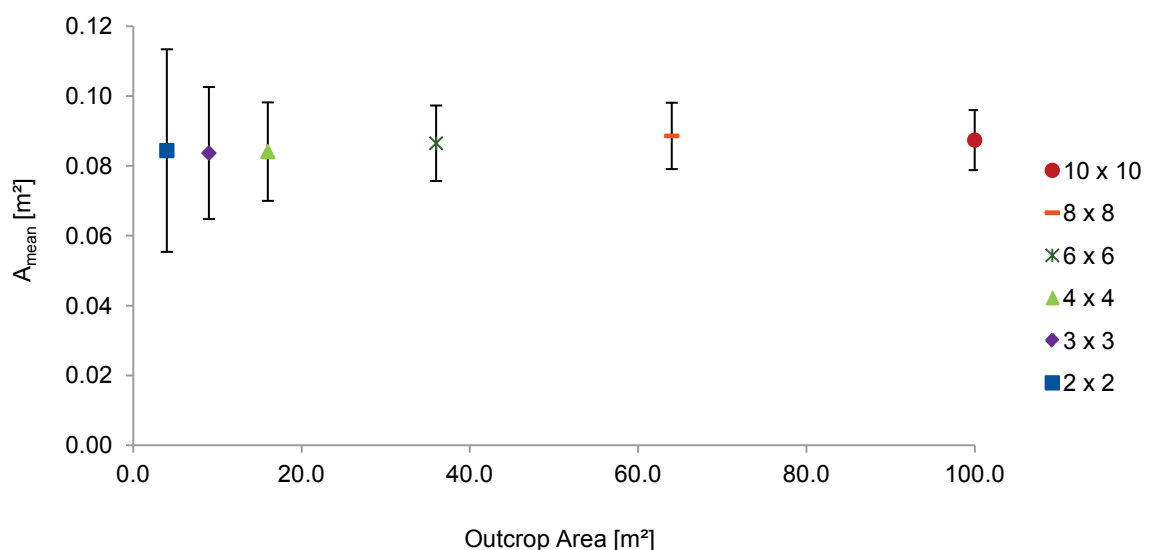
Test 30			z-rotation [°]			22.5			y-rotation [°]			0.0		
dd ₁ [°]	dip ₁ [°]	dd ₂ [°]	dip ₂ [°]	dd ₃ [°]	dip ₃ [°]	sp ₁ [m]	sp ₂ [m]	sp ₃ [m]	p ₁ [-]	p ₂ [-]	p ₃ [-]			
22.5	90.0	0.0	0.0	112.5	90.0	0.4	0.4	0.4	0.8	0.8	0.8			
A _{out} [m ²]	A _{mean} [m ²]	A _{mean} /A _{out} [-]	σ _{Amean} [m ²]	A _{50%,mean} [m ²]	σ _{A50%,mean} [m ²]	A _{75%,mean} [m ²]	σ _{A75%,mean} [m ²]	A _{25%,mean} [m ²]	σ _{A25%,mean} [m ²]					
100.0	0.1947	0.0019	0.0163	0.1732	0.0000	0.2249	0.0485	0.1113	0.0102					
64.0	0.1988	0.0031	0.0201	0.1732	0.0000	0.2358	0.0589	0.1203	0.0172					
36.0	0.1984	0.0055	0.0238	0.1743	0.0062	0.2287	0.0608	0.1172	0.0247					
16.0	0.2055	0.0128	0.0304	0.1773	0.0252	0.2369	0.0670	0.1347	0.0330					
9.0	0.1978	0.0220	0.0346	0.1755	0.0334	0.2282	0.0761	0.1274	0.0398					
4.0	0.2394	0.0599	0.0642	0.1992	0.0609	0.2541	0.0966	0.1896	0.0468					
V _{model} [m ³]	V _{mean} [m ³]	σ _{Vmean} [m ³]	V _{50%,mean} [m ³]	σ _{V50%,mean} [m ³]	V _{75%,mean} [m ³]	σ _{V75%,mean} [m ³]	V _{25%,mean} [m ³]	σ _{V25%,mean} [m ³]						
1000.0	0.1213	0.0110	0.0801	0.0277	0.1325	0.0164	0.0640	0.0000						
640.0	0.1217	0.0130	0.0832	0.0293	0.1338	0.0205	0.0640	0.0000						
360.0	0.1215	0.0156	0.0857	0.0304	0.1350	0.0221	0.0646	0.0064						
160.0	0.1206	0.0188	0.0858	0.0318	0.1389	0.0274	0.0646	0.0064						
90.0	0.1173	0.0189	0.0848	0.0313	0.1382	0.0269	0.0659	0.0110						
40.0	0.1098	0.0188	0.0813	0.0296	0.1325	0.0228	0.0656	0.0095						
V _{per}	T _{mean}			T _{50%}			T _{75%}			T _{25%}				
0.0640	1.8953			1.2516			2.0703			1.0000				



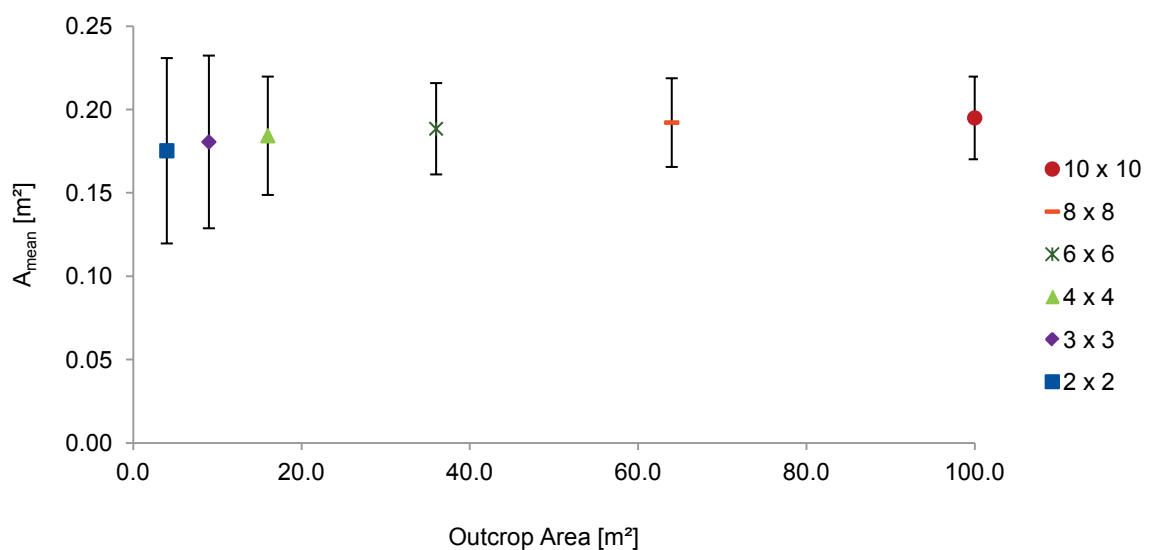
Test 31			z-rotation [°]			22.5			y-rotation [°]			0.0		
dd ₁ [°]	dip ₁ [°]	dd ₂ [°]	dip ₂ [°]	dd ₃ [°]	dip ₃ [°]	sp ₁ [m]	sp ₂ [m]	sp ₃ [m]	p ₁ [-]	p ₂ [-]	p ₃ [-]			
22.5	90.0	0.0	0.0	112.5	90.0	0.6	0.6	0.6	0.8	0.8	0.8			
A _{out} [m ²]	A _{mean} [m ²]	A _{mean} /A _{out} [-]	σ _{Amean} [m ²]	A _{50%,mean} [m ²]	σ _{A50%,mean} [m ²]	A _{75%,mean} [m ²]	σ _{A75%,mean} [m ²]	A _{25%,mean} [m ²]	σ _{A25%,mean} [m ²]					
100.0	0.4428	0.0044	0.0484	0.3903	0.0067	0.5075	0.1318	0.2746	0.0554					
64.0	0.4343	0.0068	0.0548	0.3919	0.0198	0.4884	0.1301	0.2672	0.0563					
36.0	0.4555	0.0127	0.0682	0.3975	0.0390	0.5012	0.1482	0.3094	0.0762					
16.0	0.4398	0.0275	0.0762	0.3978	0.0571	0.5093	0.1680	0.2939	0.0827					
9.0	0.5093	0.0566	0.1084	0.4364	0.1211	0.5377	0.1803	0.4043	0.0697					
4.0	n/a	n/a	n/a	n/a	n/a	n/a	n/a	n/a	n/a					
V _{model} [m ³]	V _{mean} [m ³]	σ _{Vmean} [m ³]	V _{50%,mean} [m ³]	σ _{V50%,mean} [m ³]	V _{75%,mean} [m ³]	σ _{V75%,mean} [m ³]	V _{25%,mean} [m ³]	σ _{V25%,mean} [m ³]						
1000.0	0.4014	0.0579	0.2743	0.0964	0.4601	0.0792	0.2160	0.0000						
640.0	0.3996	0.0616	0.2743	0.0964	0.4601	0.0792	0.2182	0.0216						
360.0	0.3920	0.0643	0.2743	0.0964	0.4601	0.0792	0.2182	0.0216						
160.0	0.3813	0.0675	0.2711	0.0989	0.4601	0.0792	0.2225	0.0370						
90.0	0.3592	0.0632	0.2560	0.0836	0.4423	0.0884	0.2225	0.0370						
40.0	0.3151	0.0650	0.2549	0.0834	0.3537	0.1352	0.2263	0.0425						
V _{per}	T _{mean}		T _{50%}		T _{75%}		T _{25%}							
0.2160	1.8583		1.2699		2.1301		1.0000							



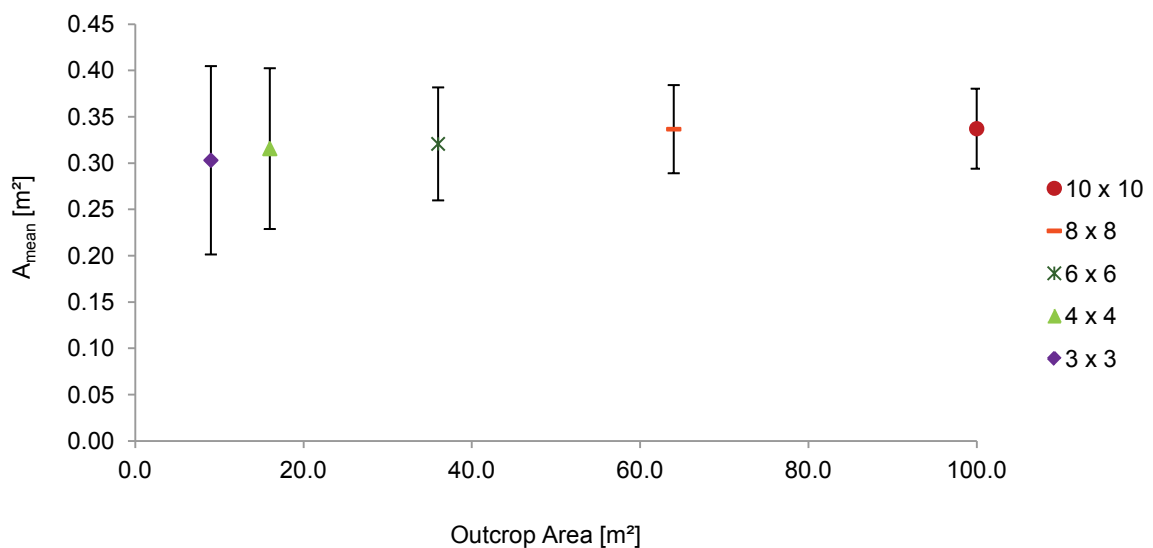
Test 32			z-rotation [°]			22.5			y-rotation [°]			0.0		
dd ₁ [°]	dip ₁ [°]	dd ₂ [°]	dip ₂ [°]	dd ₃ [°]	dip ₃ [°]	sp ₁ [m]	sp ₂ [m]	sp ₃ [m]	p ₁ [-]	p ₂ [-]	p ₃ [-]			
22.5	90.0	0.0	0.0	112.5	90.0	0.2	0.2	0.2	0.6	0.6	0.6			
A _{out} [m ²]	A _{mean} [m ²]	A _{mean} /A _{out} [-]	σ _{Amean} [m ²]	A _{50%,mean} [m ²]	σ _{A50%,mean} [m ²]	A _{75%,mean} [m ²]	σ _{A75%,mean} [m ²]	A _{25%,mean} [m ²]	σ _{A25%,mean} [m ²]					
100.0	0.0874	0.0009	0.0086	0.0606	0.0125	0.1009	0.0147	0.0427	0.0020					
64.0	0.0886	0.0014	0.0095	0.0633	0.0136	0.1041	0.0166	0.0430	0.0013					
36.0	0.0865	0.0024	0.0108	0.0601	0.0147	0.1005	0.0164	0.0421	0.0029					
16.0	0.0841	0.0053	0.0141	0.0595	0.0156	0.1003	0.0189	0.0409	0.0037					
9.0	0.0837	0.0093	0.0189	0.0598	0.0176	0.1045	0.0259	0.0412	0.0058					
4.0	0.0844	0.0211	0.0290	0.0654	0.0259	0.1032	0.0434	0.0455	0.0142					
V _{model} [m ³]	V _{mean} [m ³]	σ _{Vmean} [m ³]	V _{50%,mean} [m ³]	σ _{V50%,mean} [m ³]	V _{75%,mean} [m ³]	σ _{V75%,mean} [m ³]	V _{25%,mean} [m ³]	σ _{V25%,mean} [m ³]						
1000.0	0.0356	0.0044	0.0211	0.0045	0.0410	0.0076	0.0144	0.0032						
640.0	0.0353	0.0048	0.0208	0.0047	0.0407	0.0081	0.0140	0.0035						
360.0	0.0348	0.0053	0.0207	0.0047	0.0399	0.0082	0.0136	0.0037						
160.0	0.0339	0.0056	0.0202	0.0051	0.0382	0.0082	0.0129	0.0039						
90.0	0.0327	0.0057	0.0198	0.0048	0.0373	0.0084	0.0123	0.0040						
40.0	0.0304	0.0054	0.0189	0.0049	0.0351	0.0073	0.0115	0.0040						
V _{per}	T _{mean}		T _{50%}		T _{75%}		T _{25%}							
0.0080	4.4500		2.6375		5.1250		1.8000							



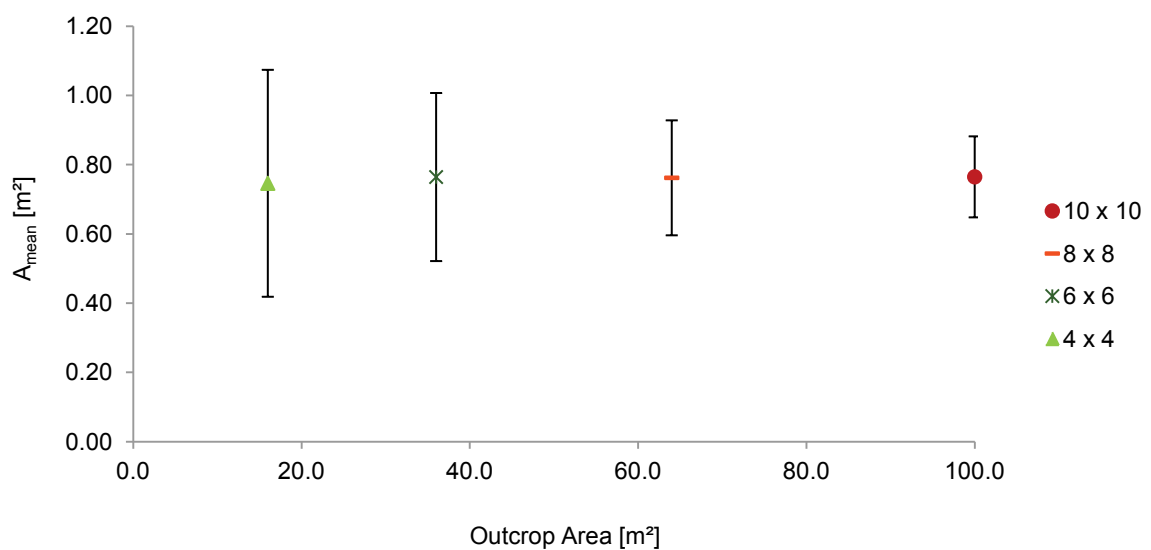
Test 33		z-rotation [°]			22.5		y-rotation [°]			0.0	
dd ₁ [°]	dip ₁ [°]	dd ₂ [°]	dip ₂ [°]	dd ₃ [°]	dip ₃ [°]	sp ₁ [m]	sp ₂ [m]	sp ₃ [m]	p ₁ [-]	p ₂ [-]	p ₃ [-]
22.5	90.0	0.0	0.0	112.5	90.0	0.3	0.3	0.3	0.6	0.6	0.6
A _{out} [m ²]	A _{mean} [m ²]	A _{mean} /A _{out} [-]	σ _{Amean} [m ²]	A _{50%,mean} [m ²]	σ _{A50%,mean} [m ²]	A _{75%,mean} [m ²]	σ _{A75%,mean} [m ²]	A _{25%,mean} [m ²]	σ _{A25%,mean} [m ²]		
100.0	0.1950	0.0020	0.0248	0.1330	0.0303	0.2228	0.0339	0.0954	0.0054		
64.0	0.1922	0.0030	0.0266	0.1294	0.0309	0.2222	0.0375	0.0938	0.0082		
36.0	0.1885	0.0052	0.0274	0.1293	0.0350	0.2211	0.0381	0.0901	0.0106		
16.0	0.1843	0.0115	0.0355	0.1313	0.0388	0.2234	0.0516	0.0894	0.0184		
9.0	0.1806	0.0201	0.0518	0.1364	0.0542	0.2146	0.0688	0.0971	0.0325		
4.0	0.1753	0.0438	0.0556	0.1403	0.0610	0.2063	0.0811	0.1022	0.0420		
V _{model} [m ³]	V _{mean} [m ³]	σ _{Vmean} [m ³]	V _{50%,mean} [m ³]	σ _{V50%,mean} [m ³]	V _{75%,mean} [m ³]	σ _{V75%,mean} [m ³]	V _{25%,mean} [m ³]	σ _{V25%,mean} [m ³]			
1000.0	0.1197	0.0192	0.0688	0.0177	0.1353	0.0308	0.0448	0.0129			
640.0	0.1185	0.0212	0.0683	0.0174	0.1341	0.0327	0.0443	0.0130			
360.0	0.1165	0.0219	0.0686	0.0178	0.1336	0.0306	0.0421	0.0135			
160.0	0.1122	0.0245	0.0672	0.0189	0.1310	0.0343	0.0413	0.0135			
90.0	0.1042	0.0255	0.0651	0.0180	0.1213	0.0335	0.0400	0.0146			
40.0	0.0891	0.0196	0.0598	0.0137	0.1029	0.0239	0.0375	0.0136			
V _{per}	T _{mean}		T _{50%}		T _{75%}		T _{25%}				
0.0270	4.4333		2.5481		5.0111		1.6593				



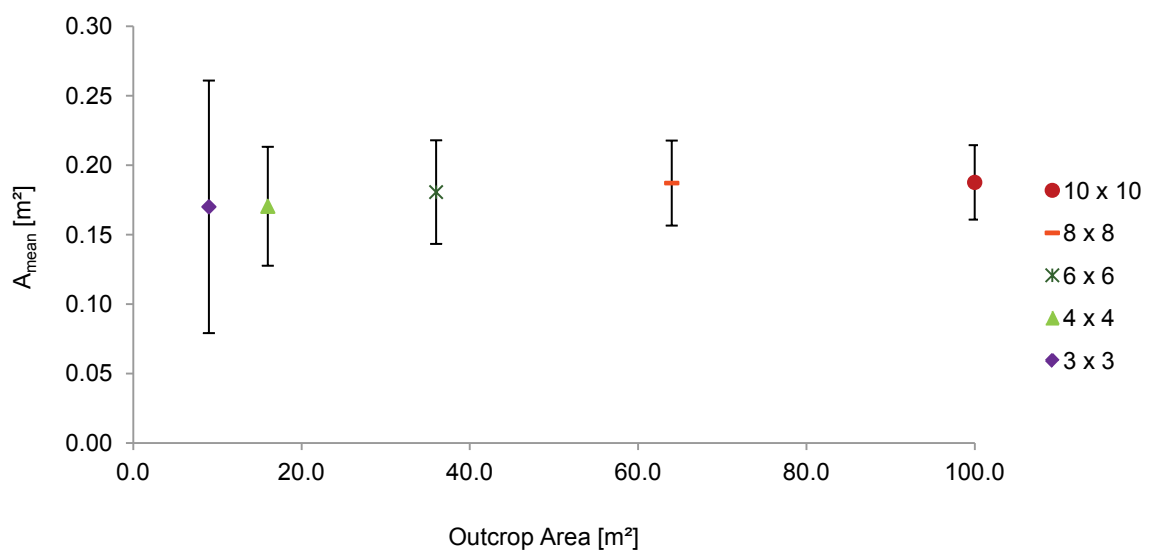
Test 34			z-rotation [°]			22.5			y-rotation [°]			0.0		
dd ₁ [°]	dip ₁ [°]	dd ₂ [°]	dip ₂ [°]	dd ₃ [°]	dip ₃ [°]	sp ₁ [m]	sp ₂ [m]	sp ₃ [m]	p ₁ [-]	p ₂ [-]	p ₃ [-]			
22.5	90.0	0.0	0.0	112.5	90.0	0.4	0.4	0.4	0.6	0.6	0.6			
A _{out} [m ²]	A _{mean} [m ²]	A _{mean} /A _{out} [-]	σ _{Amean} [m ²]	A _{50%,mean} [m ²]	σ _{A50%,mean} [m ²]	A _{75%,mean} [m ²]	σ _{A75%,mean} [m ²]	A _{25%,mean} [m ²]	σ _{A25%,mean} [m ²]					
100.0	0.3372	0.0034	0.0432	0.2326	0.0535	0.4008	0.0627	0.1598	0.0166					
64.0	0.3367	0.0053	0.0476	0.2417	0.0661	0.4038	0.0733	0.1609	0.0189					
36.0	0.3208	0.0089	0.0610	0.2323	0.0707	0.3894	0.0759	0.1568	0.0247					
16.0	0.3157	0.0197	0.0868	0.2312	0.0765	0.3791	0.1361	0.1699	0.0482					
9.0	0.3031	0.0337	0.1017	0.2405	0.1058	0.3471	0.1320	0.1728	0.0692					
4.0	n/a	n/a	n/a	n/a	n/a	n/a	n/a	n/a	n/a					
V _{model} [m ³]	V _{mean} [m ³]	σ _{Vmean} [m ³]	V _{50%,mean} [m ³]	σ _{V50%,mean} [m ³]	V _{75%,mean} [m ³]	σ _{V75%,mean} [m ³]	V _{25%,mean} [m ³]	σ _{V25%,mean} [m ³]						
1000.0	0.2779	0.0490	0.1686	0.0439	0.3162	0.0726	0.1074	0.0312						
640.0	0.2784	0.0536	0.1664	0.0436	0.3193	0.0758	0.1062	0.0330						
360.0	0.2747	0.0614	0.1651	0.0491	0.3090	0.0808	0.1037	0.0338						
160.0	0.2580	0.0694	0.1622	0.0509	0.2989	0.1004	0.1009	0.0364						
90.0	0.2375	0.0725	0.1568	0.0510	0.2802	0.1001	0.0992	0.0400						
40.0	0.1893	0.0671	0.1430	0.0580	0.2219	0.0825	0.0936	0.0465						
V _{per}	T _{mean}		T _{50%}		T _{75%}		T _{25%}							
0.0640	4.3422		2.6344		4.9406		1.6781							



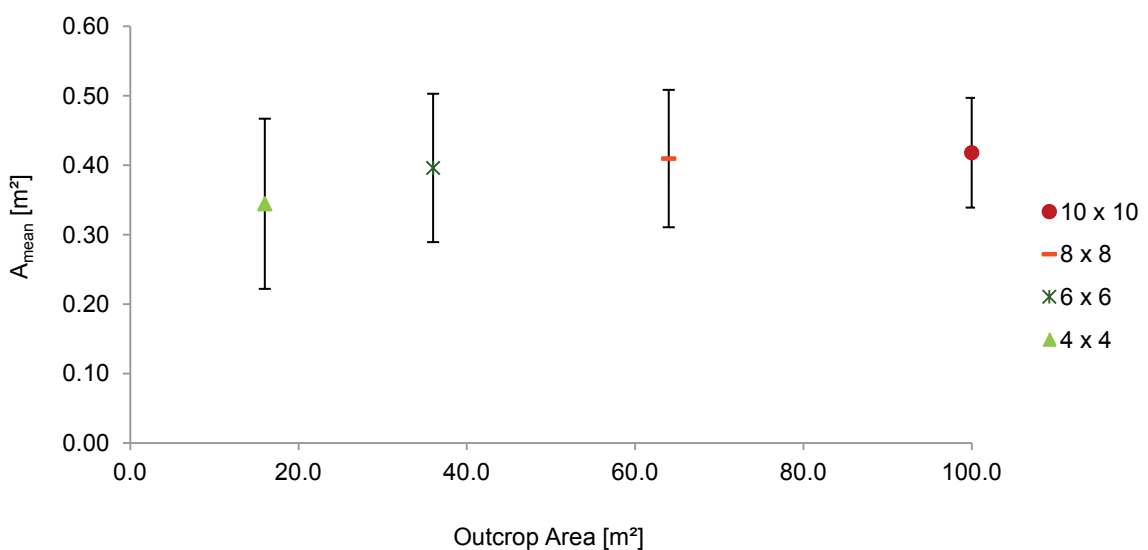
Test 35			z-rotation [°]			22.5			y-rotation [°]			0.0		
dd ₁ [°]	dip ₁ [°]	dd ₂ [°]	dip ₂ [°]	dd ₃ [°]	dip ₃ [°]	sp ₁ [m]	sp ₂ [m]	sp ₃ [m]	p ₁ [-]	p ₂ [-]	p ₃ [-]			
22.5	90.0	0.0	0.0	112.5	90.0	0.6	0.6	0.6	0.6	0.6	0.6			
A _{out} [m ²]	A _{mean} [m ²]	A _{mean} /A _{out} [-]	σ _{Amean} [m ²]	A _{50%,mean} [m ²]	σ _{A50%,mean} [m ²]	A _{75%,mean} [m ²]	σ _{A75%,mean} [m ²]	A _{25%,mean} [m ²]	σ _{A25%,mean} [m ²]					
100.0	0.7650	0.0077	0.1170	0.5414	0.1441	0.9014	0.1682	0.3618	0.0575					
64.0	0.7622	0.0119	0.1660	0.5516	0.1615	0.9189	0.2514	0.3518	0.0784					
36.0	0.7645	0.0212	0.2427	0.5695	0.1753	0.8807	0.2990	0.3948	0.1145					
16.0	0.7464	0.0467	0.3277	0.6182	0.3441	0.8680	0.3563	0.4664	0.3356					
9.0	n/a	n/a	n/a	n/a	n/a	n/a	n/a	n/a	n/a					
4.0	n/a	n/a	n/a	n/a	n/a	n/a	n/a	n/a	n/a					
V _{model} [m ³]	V _{mean} [m ³]	σ _{Vmean} [m ³]	V _{50%,mean} [m ³]	σ _{V50%,mean} [m ³]	V _{75%,mean} [m ³]	σ _{V75%,mean} [m ³]	V _{25%,mean} [m ³]	σ _{V25%,mean} [m ³]						
1000.0	0.9227	0.2058	0.5594	0.1620	1.0406	0.2617	0.3521	0.1092						
640.0	0.9059	0.2578	0.5378	0.1750	1.0562	0.3668	0.3569	0.1311						
360.0	0.8667	0.2643	0.5476	0.2183	1.0093	0.3986	0.3521	0.1754						
160.0	n/a	n/a	n/a	n/a	n/a	n/a	n/a	n/a						
90.0	n/a	n/a	n/a	n/a	n/a	n/a	n/a	n/a						
40.0	n/a	n/a	n/a	n/a	n/a	n/a	n/a	n/a						
V _{per}	T _{mean}			T _{50%}			T _{75%}			T _{25%}				
0.2160	4.2718			2.5898			4.8176			1.6301				



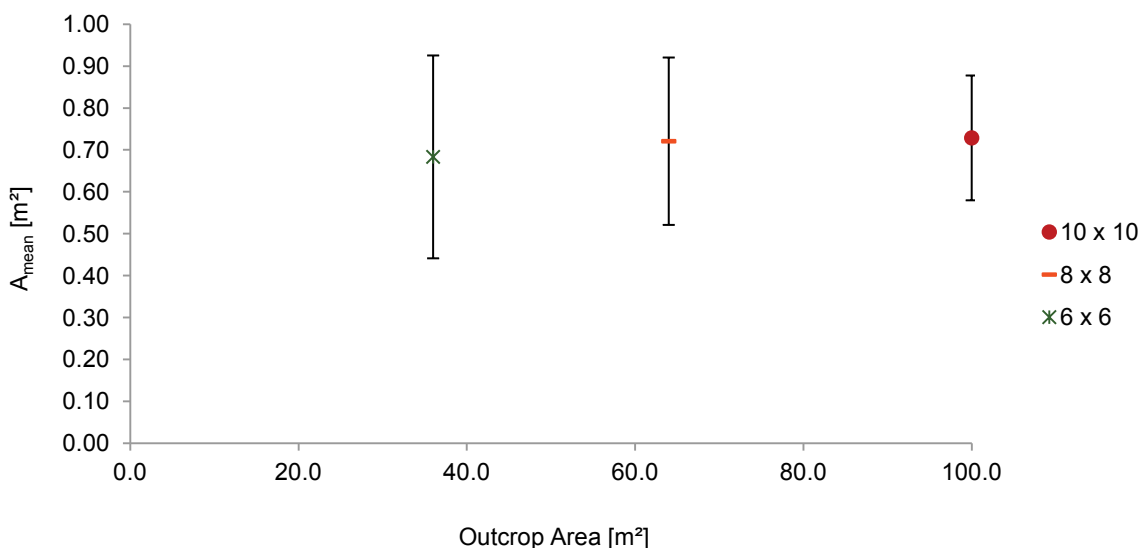
Test 36			z-rotation [°]			22.5			y-rotation [°]			0.0		
dd ₁ [°]	dip ₁ [°]	dd ₂ [°]	dip ₂ [°]	dd ₃ [°]	dip ₃ [°]	sp ₁ [m]	sp ₂ [m]	sp ₃ [m]	p ₁ [-]	p ₂ [-]	p ₃ [-]			
22.5	90.0	0.0	0.0	112.5	90.0	0.2	0.2	0.2	0.4	0.4	0.4			
A _{out} [m ²]	A _{mean} [m ²]	A _{mean} /A _{out} [-]	σ _{Amean} [m ²]	A _{50%,mean} [m ²]	σ _{A50%,mean} [m ²]	A _{75%,mean} [m ²]	σ _{A75%,mean} [m ²]	A _{25%,mean} [m ²]	σ _{A25%,mean} [m ²]					
100.0	0.1876	0.0019	0.0268	0.1134	0.0198	0.2268	0.0342	0.0573	0.0129					
64.0	0.1871	0.0029	0.0306	0.1141	0.0215	0.2258	0.0365	0.0590	0.0147					
36.0	0.1806	0.0050	0.0373	0.1111	0.0231	0.2191	0.0446	0.0571	0.0152					
16.0	0.1704	0.0107	0.0428	0.1078	0.0298	0.2033	0.0513	0.0566	0.0177					
9.0	0.1700	0.0189	0.0909	0.1183	0.0679	0.2100	0.1252	0.0652	0.0489					
4.0	n/a	n/a	n/a	n/a	n/a	n/a	n/a	n/a	n/a					
V _{model} [m ³]	V _{mean} [m ³]	σ _{Vmean} [m ³]	V _{50%,mean} [m ³]	σ _{V50%,mean} [m ³]	V _{75%,mean} [m ³]	σ _{V75%,mean} [m ³]	V _{25%,mean} [m ³]	σ _{V25%,mean} [m ³]						
1000.0	0.1137	0.0208	0.0556	0.0108	0.1229	0.0255	0.0268	0.0056						
640.0	0.1111	0.0222	0.0544	0.0114	0.1212	0.0268	0.0261	0.0057						
360.0	0.1080	0.0238	0.0539	0.0121	0.1201	0.0294	0.0255	0.0073						
160.0	0.1001	0.0244	0.0515	0.0140	0.1106	0.0308	0.0252	0.008.						
90.0	0.0934	0.0274	0.0498	0.0173	0.1046	0.0347	0.0241	0.0091						
40.0	0.0748	0.0228	0.0426	0.0152	0.0869	0.0281	0.0226	0.0104						
V _{per}	T _{mean}		T _{50%}		T _{75%}		T _{25%}							
0.0080	14.2125		6.9500		15.3625		3.3500							



Test 37			z-rotation [°]			22.5			y-rotation [°]			0.0		
dd ₁ [°]	dip ₁ [°]	dd ₂ [°]	dip ₂ [°]	dd ₃ [°]	dip ₃ [°]	sp ₁ [m]	sp ₂ [m]	sp ₃ [m]	p ₁ [-]	p ₂ [-]	p ₃ [-]			
22.5	90.0	0.0	0.0	112.5	90.0	0.3	0.3	0.3	0.4	0.4	0.4			
A _{out} [m ²]	A _{mean} [m ²]	A _{mean} /A _{out} [-]	σ _{Amean} [m ²]	A _{50%,mean} [m ²]	σ _{A50%,mean} [m ²]	A _{75%,mean} [m ²]	σ _{A75%,mean} [m ²]	A _{25%,mean} [m ²]	σ _{A25%,mean} [m ²]					
100.0	0.4179	0.0042	0.0790	0.2466	0.0542	0.4921	0.0991	0.1264	0.0339					
64.0	0.4095	0.0064	0.0989	0.2492	0.0651	0.4895	0.1195	0.1330	0.0399					
36.0	0.3960	0.0110	0.1068	0.2492	0.0745	0.4738	0.1346	0.1352	0.0502					
16.0	0.3444	0.0215	0.1225	0.2422	0.0938	0.4273	0.1510	0.1379	0.0616					
9.0	n/a	n/a	n/a	n/a	n/a	n/a	n/a	n/a	n/a					
4.0	n/a	n/a	n/a	n/a	n/a	n/a	n/a	n/a	n/a					
V _{model} [m ³]	V _{mean} [m ³]	σ _{Vmean} [m ³]	V _{50%,mean} [m ³]	σ _{V50%,mean} [m ³]	V _{75%,mean} [m ³]	σ _{V75%,mean} [m ³]	V _{25%,mean} [m ³]	σ _{V25%,mean} [m ³]						
1000.0	0.3748	0.0906	0.1804	0.0413	0.4067	0.1055	0.0850	0.0222						
640.0	0.3707	0.1139	0.1758	0.0460	0.4025	0.1318	0.0832	0.0239						
360.0	0.3469	0.1103	0.1744	0.0568	0.3840	0.1443	0.0817	0.0274						
160.0	0.3069	0.1249	0.1670	0.0724	0.3514	0.1605	0.0874	0.0404						
90.0	0.2505	0.0844	0.1457	0.0655	0.2922	0.1197	0.0811	0.0378						
40.0	n/a	n/a	n/a	n/a	n/a	n/a	n/a	n/a						
V _{per}	T _{mean}			T _{50%}			T _{75%}			T _{25%}				
0.0270	13.8815			6.6815			15.0630			3.1481				



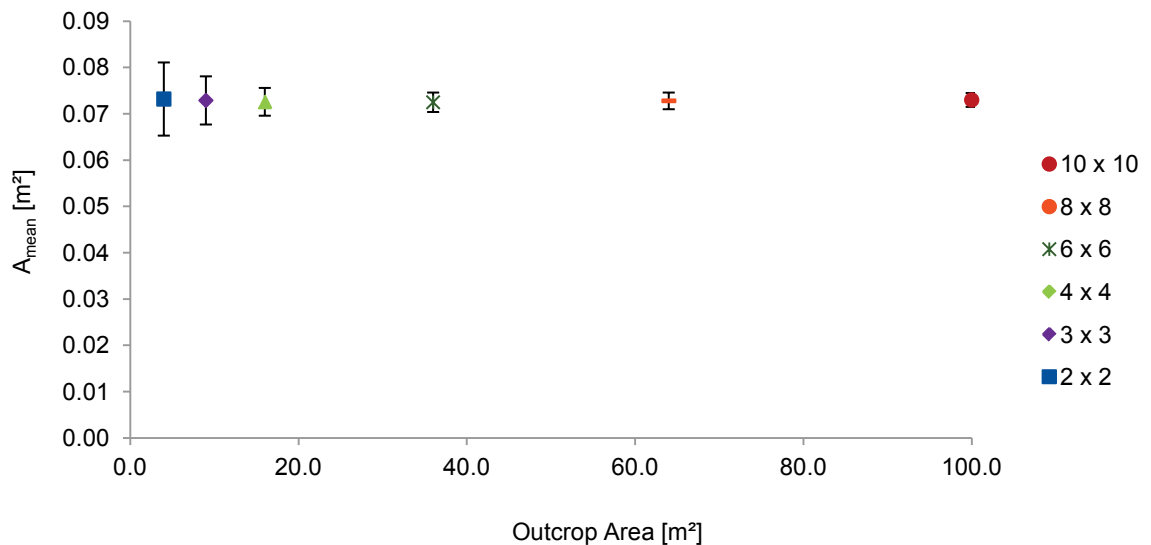
Test 38			z-rotation [°]			22.5			y-rotation [°]			0.0		
dd ₁ [°]	dip ₁ [°]	dd ₂ [°]	dip ₂ [°]	dd ₃ [°]	dip ₃ [°]	sp ₁ [m]	sp ₂ [m]	sp ₃ [m]	p ₁ [-]	p ₂ [-]	p ₃ [-]			
22.5	90.0	0.0	0.0	112.5	90.0	0.4	0.4	0.4	0.4	0.4	0.4			
A _{out} [m ²]	A _{mean} [m ²]	A _{mean} /A _{out} [-]	$\sigma_{A\text{mean}}$ [m ²]	A _{50%,mean} [m ²]	$\sigma_{A50\%,\text{mean}}$ [m ²]	A _{75%,mean} [m ²]	$\sigma_{A75\%,\text{mean}}$ [m ²]	A _{25%,mean} [m ²]	$\sigma_{A25\%,\text{mean}}$ [m ²]					
100.0	0.7288	0.0073	0.1489	0.4356	0.0923	0.8705	0.1854	0.2241	0.0688					
64.0	0.7209	0.0113	0.1997	0.4450	0.1365	0.8820	0.2996	0.2417	0.0979					
36.0	0.6835	0.0190	0.2420	0.4602	0.2287	0.8524	0.3518	0.2450	0.1344					
16.0	n/a	n/a	n/a	n/a	n/a	n/a	n/a	n/a	n/a					
9.0	n/a	n/a	n/a	n/a	n/a	n/a	n/a	n/a	n/a					
4.0	n/a	n/a	n/a	n/a	n/a	n/a	n/a	n/a	n/a					
V _{model} [m ³]	V _{mean} [m ³]	$\sigma_{V\text{mean}}$ [m ³]	V _{50%,mean} [m ³]	$\sigma_{V50\%,\text{mean}}$ [m ³]	V _{75%,mean} [m ³]	$\sigma_{V75\%,\text{mean}}$ [m ³]	V _{25%,mean} [m ³]	$\sigma_{V25\%,\text{mean}}$ [m ³]						
1000.0	0.8243	0.1831	0.4080	0.1047	0.9071	0.2060	0.1969	0.0572						
640.0	0.8155	0.2398	0.4025	0.1124	0.9001	0.2629	0.1947	0.0607						
360.0	0.7457	0.2350	0.3968	0.1564	0.8455	0.3164	0.1958	0.0733						
160.0	n/a	n/a	n/a	n/a	n/a	n/a	n/a	n/a						
90.0	n/a	n/a	n/a	n/a	n/a	n/a	n/a	n/a						
40.0	n/a	n/a	n/a	n/a	n/a	n/a	n/a	n/a						
V _{per}	T _{mean}			T _{50%}			T _{75%}			T _{25%}				
0.0640	12.8797			6.3750			14.1734			3.0766				



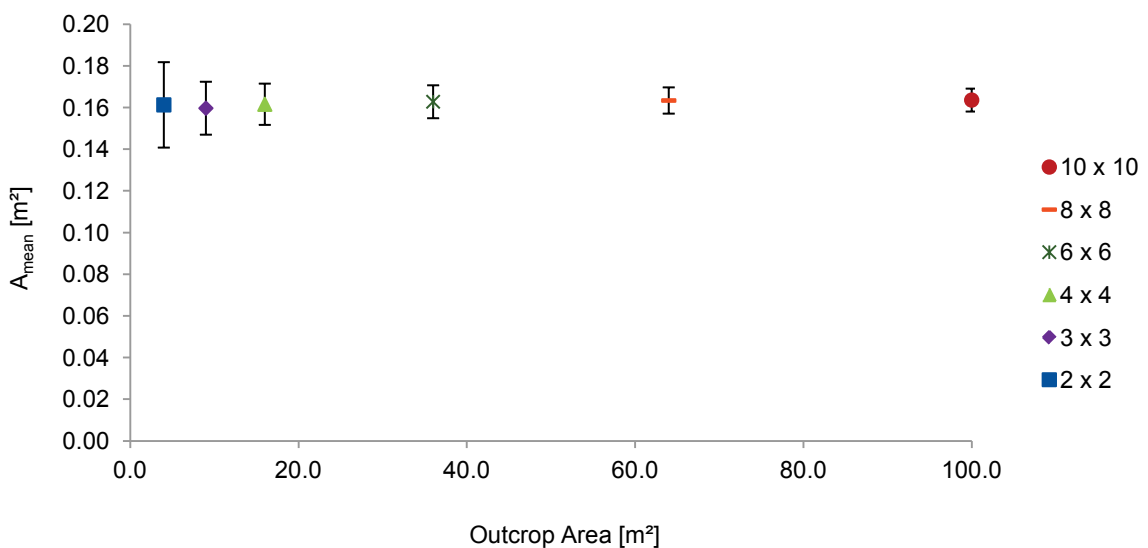
Test 39			z-rotation [°]			22.5			y-rotation [°]			0.0		
dd ₁ [°]	dip ₁ [°]	dd ₂ [°]	dip ₂ [°]	dd ₃ [°]	dip ₃ [°]	sp ₁ [m]	sp ₂ [m]	sp ₃ [m]	p ₁ [-]	p ₂ [-]	p ₃ [-]			
22.5	90.0	0.0	0.0	112.5	90.0	0.6	0.6	0.6	0.4	0.4	0.4			
A _{out} [m ²]	A _{mean} [m ²]	A _{mean} /A _{out} [-]	σ _{Amean} [m ²]	A _{50%,mean} [m ²]	σ _{A50%,mean} [m ²]	A _{75%,mean} [m ²]	σ _{A75%,mean} [m ²]	A _{25%,mean} [m ²]	σ _{A25%,mean} [m ²]					
100.0	1.5952	0.0160	0.5143	1.0307	0.3286	1.9241	0.6863	0.5503	0.2033					
64.0	1.4682	0.0229	0.5225	1.0382	0.3841	1.7361	0.6824	0.5849	0.2580					
36.0	n/a	n/a	n/a	n/a	n/a	n/a	n/a	n/a	n/a					
16.0	n/a	n/a	n/a	n/a	n/a	n/a	n/a	n/a	n/a					
9.0	n/a	n/a	n/a	n/a	n/a	n/a	n/a	n/a	n/a					
4.0	n/a	n/a	n/a	n/a	n/a	n/a	n/a	n/a	n/a					
V _{model} [m ³]	V _{mean} [m ³]	σ _{Vmean} [m ³]	V _{50%,mean} [m ³]	σ _{V50%,mean} [m ³]	V _{75%,mean} [m ³]	σ _{V75%,mean} [m ³]	V _{25%,mean} [m ³]	σ _{V25%,mean} [m ³]						
1000.0	2.6586	1.1373	1.4180	0.6593	3.0251	1.3699	0.7225	0.3647						
640.0	2.5960	1.2317	1.4623	0.8881	3.0056	1.9344	0.7625	0.5359						
360.0	n/a	n/a	n/a	n/a	n/a	n/a	n/a	n/a						
160.0	n/a	n/a	n/a	n/a	n/a	n/a	n/a	n/a						
90.0	n/a	n/a	n/a	n/a	n/a	n/a	n/a	n/a						
40.0	n/a	n/a	n/a	n/a	n/a	n/a	n/a	n/a						
V _{per}	T _{mean}			T _{50%}			T _{75%}			T _{25%}				
0.2160	12.3083			6.5648			14.0051			3.3449				

Transformation factors invalid because limitation ratio has already been exceeded in the major outcrop area!

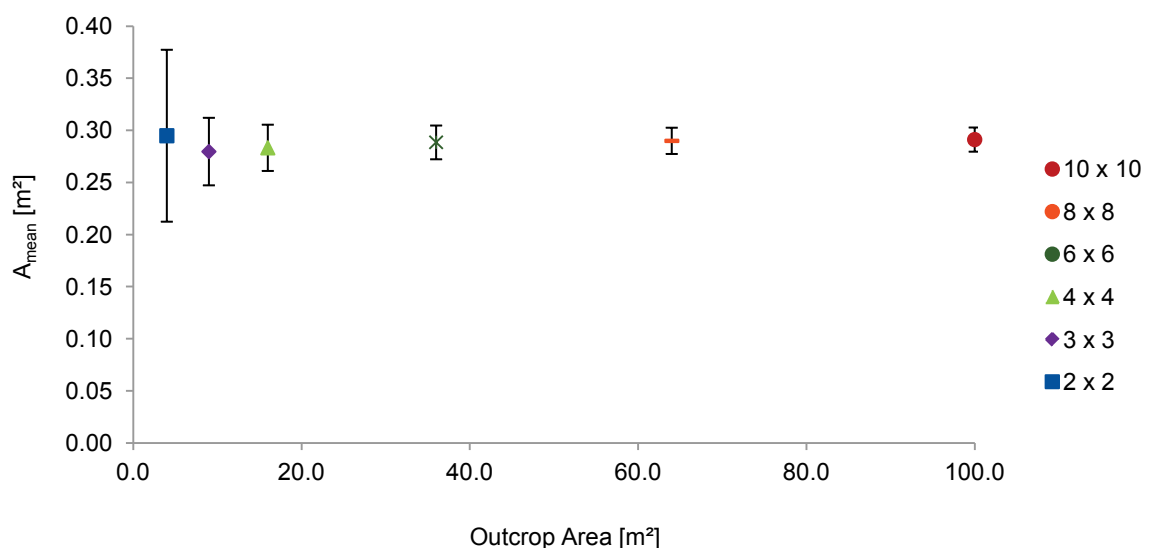
Test 40			z-rotation [°]			45.0			y-rotation [°]			0.0		
dd ₁ [°]	dip ₁ [°]	dd ₂ [°]	dip ₂ [°]	dd ₃ [°]	dip ₃ [°]	sp ₁ [m]	sp ₂ [m]	sp ₃ [m]	p ₁ [-]	p ₂ [-]	p ₃ [-]			
45.0	90.0	0.0	0.0	135.0	90.0	0.2	0.2	0.2	0.8	0.8	0.8			
A _{out} [m ²]	A _{mean} [m ²]	A _{mean} /A _{out} [-]	$\sigma_{A\text{mean}}$ [m ²]	A _{50%,mean} [m ²]	$\sigma_{A50\%,\text{mean}}$ [m ²]	A _{75%,mean} [m ²]	$\sigma_{A75\%,\text{mean}}$ [m ²]	A _{25%,mean} [m ²]	$\sigma_{A25\%,\text{mean}}$ [m ²]					
100.0	0.0730	0.0007	0.0015	0.0566	0.0000	0.0600	0.0135	0.0566	0.0000					
64.0	0.0728	0.0011	0.0018	0.0566	0.0000	0.0622	0.0171	0.0566	0.0000					
36.0	0.0725	0.0020	0.0021	0.0566	0.0000	0.0645	0.0197	0.0566	0.0000					
16.0	0.0726	0.0045	0.0030	0.0566	0.0000	0.0670	0.0218	0.0566	0.0000					
9.0	0.0729	0.0081	0.0052	0.0566	0.0000	0.0727	0.0250	0.0566	0.0000					
4.0	0.0732	0.0183	0.0079	0.0566	0.0000	0.0759	0.0255	0.0566	0.0000					
V _{model} [m ³]	V _{mean} [m ³]	$\sigma_{V\text{mean}}$ [m ³]	V _{50%,mean} [m ³]	$\sigma_{V50\%,\text{mean}}$ [m ³]	V _{75%,mean} [m ³]	$\sigma_{V75\%,\text{mean}}$ [m ³]	V _{25%,mean} [m ³]	$\sigma_{V25\%,\text{mean}}$ [m ³]						
1000.0	0.0153	0.0012	0.0098	0.0033	0.0163	0.0016	0.0080	0.0000						
640.0	0.0152	0.0012	0.0098	0.0033	0.0163	0.0016	0.0080	0.0000						
360.0	0.0152	0.0013	0.0098	0.0033	0.0163	0.0016	0.0080	0.0000						
160.0	0.0150	0.0014	0.0100	0.0035	0.0163	0.0016	0.0080	0.0000						
90.0	0.0148	0.0014	0.0098	0.0033	0.0163	0.0016	0.0080	0.0000						
40.0	0.0135	0.0014	0.0082	0.0014	0.0163	0.0016	0.0080	0.0000						
V _{per}	T _{mean}		T _{50%}		T _{75%}		T _{25%}							
0.0080	1.9125		1.2250		2.0375		1.0000							



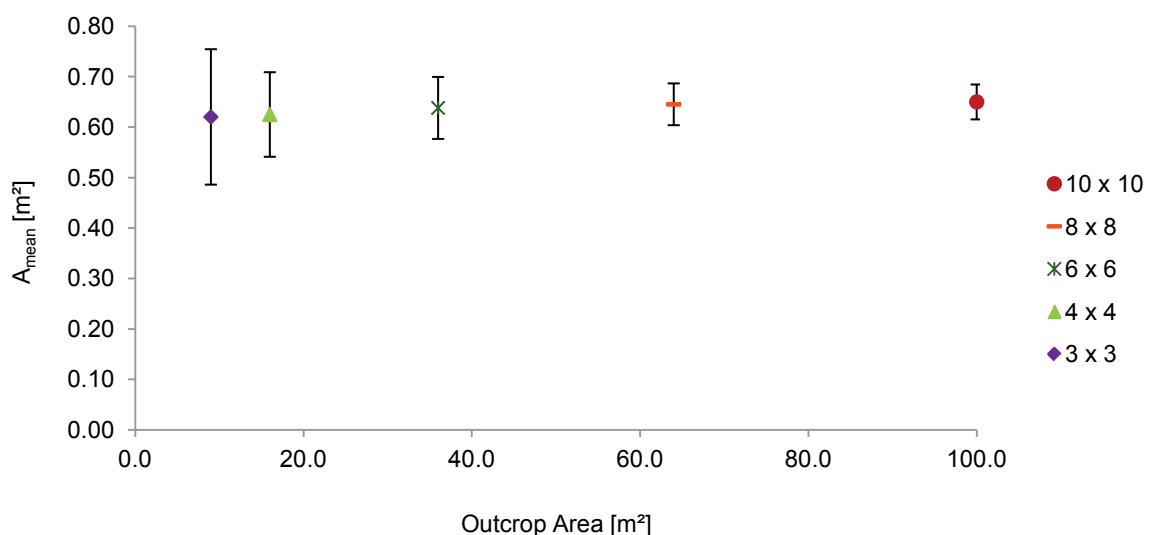
Test 41			z-rotation [°]			45.0			y-rotation [°]			0.0		
dd ₁ [°]	dip ₁ [°]	dd ₂ [°]	dip ₂ [°]	dd ₃ [°]	dip ₃ [°]	sp ₁ [m]	sp ₂ [m]	sp ₃ [m]	p ₁ [-]	p ₂ [-]	p ₃ [-]			
45.0	90.0	0.0	0.0	135.0	90.0	0.3	0.3	0.3	0.8	0.8	0.8			
A _{out} [m ²]	A _{mean} [m ²]	A _{mean} /A _{out} [-]	σ _{Amean} [m ²]	A _{50%,mean} [m ²]	σ _{A50%,mean} [m ²]	A _{75%,mean} [m ²]	σ _{A75%,mean} [m ²]	A _{25%,mean} [m ²]	σ _{A25%,mean} [m ²]					
100.0	0.1636	0.0016	0.0055	0.1273	0.0000	0.1406	0.0387	0.1273	0.0000					
64.0	0.1634	0.0026	0.0063	0.1273	0.0000	0.1429	0.0411	0.1273	0.0000					
36.0	0.1628	0.0045	0.0079	0.1273	0.0000	0.1480	0.0469	0.1273	0.0000					
16.0	0.1616	0.0101	0.0099	0.1273	0.0000	0.1566	0.0525	0.1273	0.0000					
9.0	0.1597	0.0177	0.0127	0.1273	0.0000	0.1502	0.0472	0.1273	0.0000					
4.0	0.1613	0.0403	0.0205	0.1298	0.0179	0.1674	0.0577	0.1273	0.0000					
V _{model} [m ³]	V _{mean} [m ³]	σ _{Vmean} [m ³]	V _{50%,mean} [m ³]	σ _{V50%,mean} [m ³]	V _{75%,mean} [m ³]	σ _{V75%,mean} [m ³]	V _{25%,mean} [m ³]	σ _{V25%,mean} [m ³]						
1000.0	0.0518	0.0050	0.0364	0.0129	0.0556	0.0064	0.0270	0.0000						
640.0	0.0516	0.0053	0.0348	0.0123	0.0559	0.0069	0.0270	0.0000						
360.0	0.0514	0.0056	0.0346	0.0122	0.0559	0.0069	0.0270	0.0000						
160.0	0.0505	0.0056	0.0338	0.0118	0.0559	0.0069	0.0272	0.0027						
90.0	0.0495	0.0056	0.0327	0.0111	0.0554	0.0059	0.0273	0.0027						
40.0	0.0471	0.0051	0.0305	0.0091	0.0551	0.0053	0.0273	0.0027						
V _{per}	T _{mean}		T _{50%}		T _{75%}		T _{25%}							
0.0270	1.9185		1.3481		2.0593		1.0000							



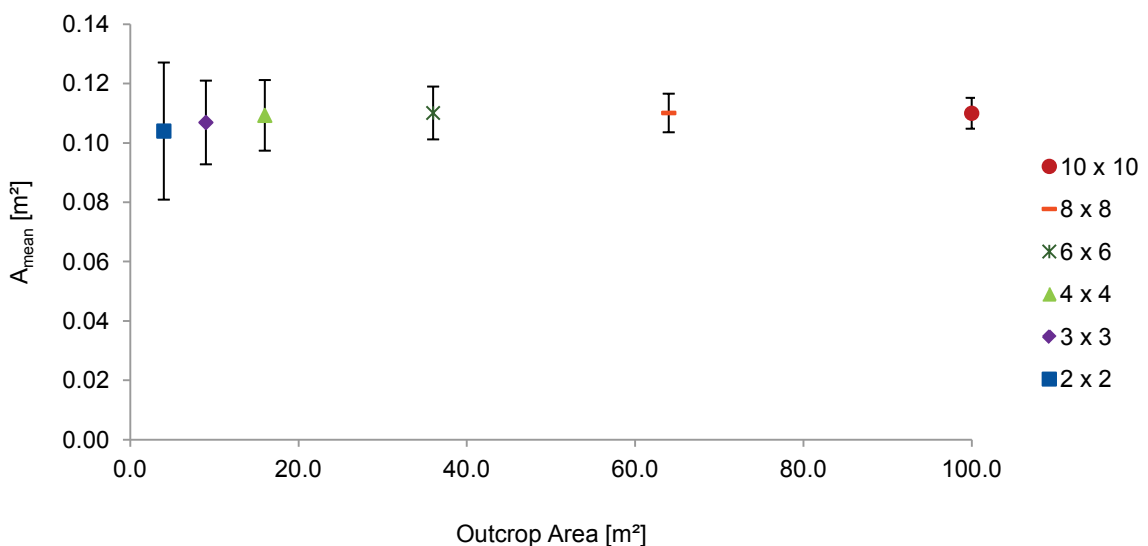
Test 42			z-rotation [°]			45.0			y-rotation [°]			0.0		
dd ₁ [°]	dip ₁ [°]	dd ₂ [°]	dip ₂ [°]	dd ₃ [°]	dip ₃ [°]	sp ₁ [m]	sp ₂ [m]	sp ₃ [m]	p ₁ [-]	p ₂ [-]	p ₃ [-]			
45.0	90.0	0.0	0.0	135.0	90.0	0.4	0.4	0.4	0.8	0.8	0.8			
A _{out} [m ²]	A _{mean} [m ²]	A _{mean} /A _{out} [-]	σ _{Amean} [m ²]	A _{50%,mean} [m ²]	σ _{A50%,mean} [m ²]	A _{75%,mean} [m ²]	σ _{A75%,mean} [m ²]	A _{25%,mean} [m ²]	σ _{A25%,mean} [m ²]					
100.0	0.2912	0.0029	0.0116	0.2263	0.0000	0.2738	0.0926	0.2263	0.0000					
64.0	0.2900	0.0045	0.0126	0.2263	0.0000	0.2670	0.0874	0.2263	0.0000					
36.0	0.2885	0.0080	0.0162	0.2263	0.0000	0.2789	0.0942	0.2263	0.0000					
16.0	0.2833	0.0177	0.0222	0.2263	0.0000	0.2664	0.0852	0.2262	0.0000					
9.0	0.2797	0.0311	0.0324	0.2263	0.0000	0.2840	0.0944	0.2263	0.0000					
4.0	0.2949	0.0737	0.0825	0.2512	0.0797	0.3173	0.1211	0.2421	0.0737					
V _{model} [m ³]	V _{mean} [m ³]	σ _{Vmean} [m ³]	V _{50%,mean} [m ³]	σ _{V50%,mean} [m ³]	V _{75%,mean} [m ³]	σ _{V75%,mean} [m ³]	V _{25%,mean} [m ³]	σ _{V25%,mean} [m ³]						
1000.0	0.1205	0.0115	0.0787	0.0271	0.1312	0.0140	0.0640	0.0000						
640.0	0.1201	0.0122	0.0800	0.0279	0.1331	0.0175	0.0640	0.0000						
360.0	0.1186	0.0128	0.0794	0.0275	0.1312	0.0140	0.0640	0.0000						
160.0	0.1163	0.0139	0.0768	0.0257	0.1325	0.0164	0.0640	0.0000						
90.0	0.1134	0.0147	0.0768	0.0257	0.1331	0.0175	0.0640	0.0000						
40.0	0.1059	0.0137	0.0704	0.0188	0.1280	0.0223	0.0640	0.0000						
V _{per}	T _{mean}		T _{50%}		T _{75%}		T _{25%}							
0.0640	1.8828		1.2297		2.0500		1.0000							



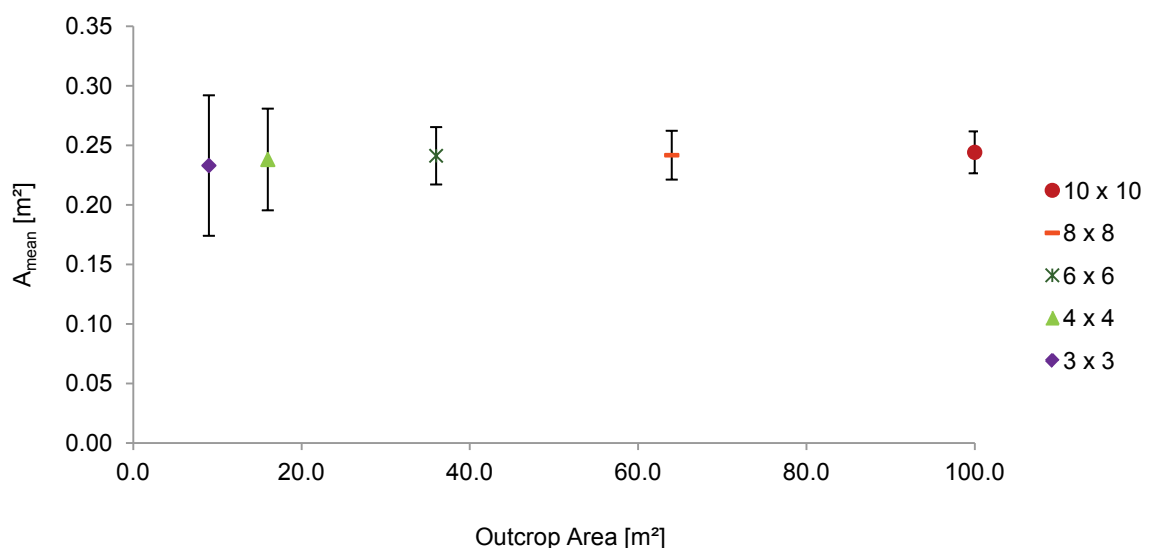
Test 43			z-rotation [°]			45.0			y-rotation [°]			0.0		
dd ₁ [°]	dip ₁ [°]	dd ₂ [°]	dip ₂ [°]	dd ₃ [°]	dip ₃ [°]	sp ₁ [m]	sp ₂ [m]	sp ₃ [m]	p ₁ [-]	p ₂ [-]	p ₃ [-]			
45.0	90.0	0.0	0.0	135.0	90.0	0.6	0.6	0.6	0.8	0.8	0.8			
A _{out} [m ²]	A _{mean} [m ²]	A _{mean} /A _{out} [-]	σ _{Amean} [m ²]	A _{50%,mean} [m ²]	σ _{A50%,mean} [m ²]	A _{75%,mean} [m ²]	σ _{A75%,mean} [m ²]	A _{25%,mean} [m ²]	σ _{A25%,mean} [m ²]					
100.0	0.6500	0.0065	0.0346	0.5091	0.0000	0.6186	0.2079	0.5091	0.0000					
64.0	0.6453	0.0101	0.0414	0.5091	0.0000	0.6186	0.2063	0.5091	0.0000					
36.0	0.6381	0.0177	0.0614	0.5142	0.0509	0.6135	0.1993	0.5091	0.0000					
16.0	0.6251	0.0391	0.0838	0.5218	0.0757	0.6173	0.2128	0.5091	0.0000					
9.0	0.6203	0.0689	0.1342	0.5575	0.1433	0.6402	0.2284	0.5333	0.0881					
4.0	n/a	n/a	n/a	n/a	n/a	n/a	n/a	n/a	n/a					
V _{model} [m ³]	V _{mean} [m ³]	σ _{Vmean} [m ³]	V _{50%,mean} [m ³]	σ _{V50%,mean} [m ³]	V _{75%,mean} [m ³]	σ _{V75%,mean} [m ³]	V _{25%,mean} [m ³]	σ _{V25%,mean} [m ³]						
1000.0	0.4107	0.0574	0.2743	0.0964	0.4644	0.0888	0.2182	0.0216						
640.0	0.4074	0.0618	0.2765	0.0975	0.4687	0.0974	0.2182	0.0216						
360.0	0.3986	0.0634	0.2743	0.0964	0.4676	0.0906	0.2182	0.0216						
160.0	0.3813	0.0633	0.2678	0.0914	0.4514	0.0758	0.2182	0.0216						
90.0	0.3622	0.0586	0.2603	0.0856	0.4304	0.0784	0.2182	0.0216						
40.0	0.3153	0.0565	0.2581	0.0853	0.3542	0.1131	0.2257	0.0430						
V _{per}	T _{mean}		T _{50%}		T _{75%}		T _{25%}							
0.2160	1.9014		1.2699		2.1500		1.0102							



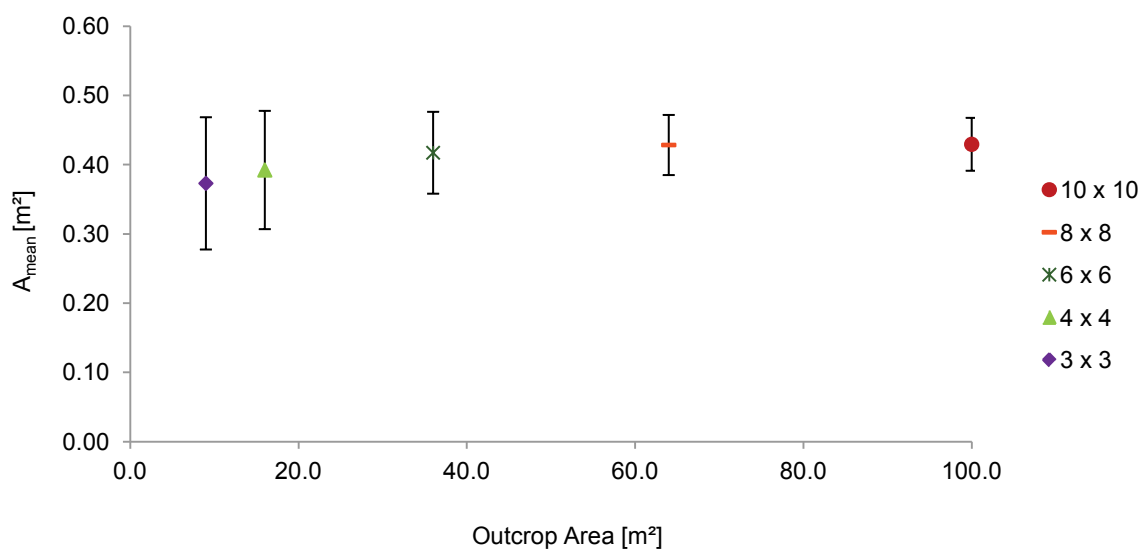
Test 44			z-rotation [°]			45.0			y-rotation [°]			0.0		
dd ₁ [°]	dip ₁ [°]	dd ₂ [°]	dip ₂ [°]	dd ₃ [°]	dip ₃ [°]	sp ₁ [m]	sp ₂ [m]	sp ₃ [m]	p ₁ [-]	p ₂ [-]	p ₃ [-]			
45.0	90.0	0.0	0.0	135.0	90.0	0.2	0.2	0.2	0.6	0.6	0.6			
A _{out} [m ²]	A _{mean} [m ²]	A _{mean} /A _{out} [-]	σ _{Amean} [m ²]	A _{50%,mean} [m ²]	σ _{A50%,mean} [m ²]	A _{75%,mean} [m ²]	σ _{A75%,mean} [m ²]	A _{25%,mean} [m ²]	σ _{A25%,mean} [m ²]					
100.0	0.1100	0.0011	0.0052	0.0775	0.0272	0.1143	0.0080	0.0566	0.0000					
64.0	0.1101	0.0017	0.0065	0.0783	0.0275	0.1171	0.0145	0.0566	0.0000					
36.0	0.1101	0.0031	0.0089	0.0772	0.0272	0.1185	0.0163	0.0566	0.0000					
16.0	0.1093	0.0068	0.0119	0.0758	0.0266	0.1233	0.0214	0.0566	0.0000					
9.0	0.1069	0.0119	0.0141	0.0755	0.0270	0.1230	0.0212	0.0566	0.0000					
4.0	0.1040	0.0260	0.0231	0.0769	0.0284	0.1243	0.0325	0.0594	0.0142					
V _{model} [m ³]	V _{mean} [m ³]	σ _{Vmean} [m ³]	V _{50%,mean} [m ³]	σ _{V50%,mean} [m ³]	V _{75%,mean} [m ³]	σ _{V75%,mean} [m ³]	V _{25%,mean} [m ³]	σ _{V25%,mean} [m ³]						
1000.0	0.0352	0.0042	0.0201	0.0043	0.0397	0.0073	0.0135	0.0037						
640.0	0.0350	0.0044	0.0200	0.0043	0.0389	0.0072	0.0133	0.0038						
360.0	0.0344	0.0045	0.0197	0.0042	0.0379	0.0072	0.0127	0.0040						
160.0	0.0332	0.0046	0.0188	0.0040	0.0366	0.0070	0.0120	0.0040						
90.0	0.0316	0.0041	0.0185	0.0037	0.0353	0.0062	0.0114	0.0040						
40.0	0.0279	0.0037	0.0169	0.0025	0.0325	0.0048	0.0093	0.0029						
V _{per}	T_{mean}			T_{50%}			T_{75%}			T_{25%}				
0.0080	4.4000			2.5125			4.9625			1.6875				



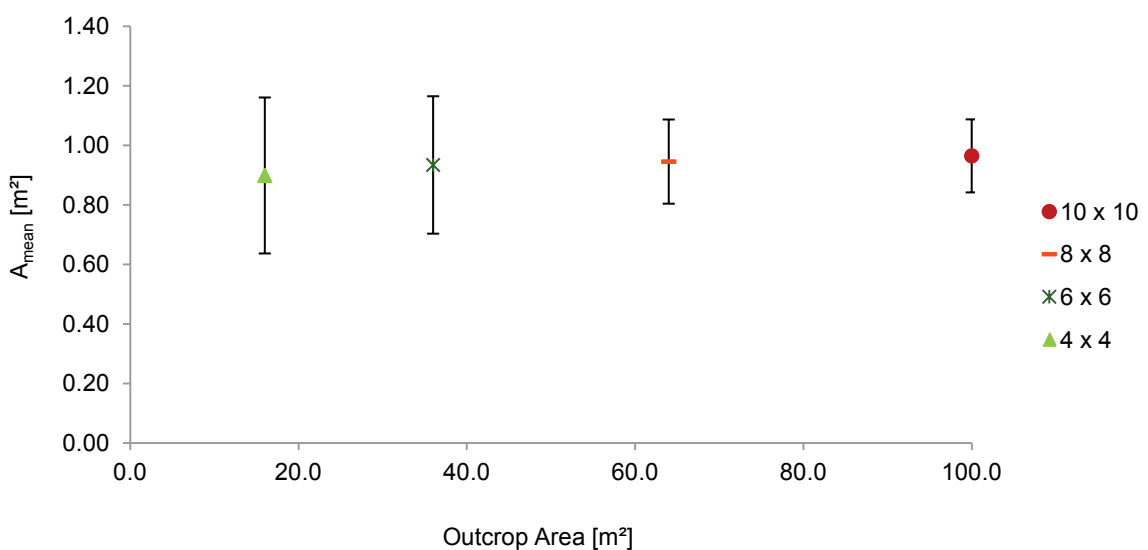
Test 45			z-rotation [°]			45.0			y-rotation [°]			0.0		
dd ₁ [°]	dip ₁ [°]	dd ₂ [°]	dip ₂ [°]	dd ₃ [°]	dip ₃ [°]	sp ₁ [m]	sp ₂ [m]	sp ₃ [m]	p ₁ [-]	p ₂ [-]	p ₃ [-]			
45.0	90.0	0.0	0.0	135.0	90.0	0.3	0.3	0.3	0.6	0.6	0.6			
A _{out} [m ²]	A _{mean} [m ²]	A _{mean} /A _{out} [-]	σ _{Amean} [m ²]	A _{50%,mean} [m ²]	σ _{A50%,mean} [m ²]	A _{75%,mean} [m ²]	σ _{A75%,mean} [m ²]	A _{25%,mean} [m ²]	σ _{A25%,mean} [m ²]					
100.0	0.2441	0.0024	0.0176	0.1642	0.0580	0.2635	0.0326	0.1273	0.0000					
64.0	0.2417	0.0038	0.0205	0.1623	0.0568	0.2673	0.0384	0.1273	0.0000					
36.0	0.2412	0.0067	0.0241	0.1718	0.0610	0.2670	0.0367	0.1273	0.0000					
16.0	0.2381	0.0149	0.0427	0.1725	0.0588	0.2765	0.0611	0.1273	0.0000					
9.0	0.2330	0.0259	0.0590	0.1725	0.0635	0.2721	0.0935	0.1343	0.0281					
4.0	n/a	n/a	n/a	n/a	n/a	n/a	n/a	n/a	n/a					
V _{model} [m ³]	V _{mean} [m ³]	σ _{Vmean} [m ³]	V _{50%,mean} [m ³]	σ _{V50%,mean} [m ³]	V _{75%,mean} [m ³]	σ _{V75%,mean} [m ³]	V _{25%,mean} [m ³]	σ _{V25%,mean} [m ³]						
1000.0	0.1180	0.0181	0.0688	0.0155	0.1339	0.0266	0.0446	0.0129						
640.0	0.1163	0.0191	0.0672	0.0161	0.1313	0.0264	0.0443	0.0130						
360.0	0.1139	0.0186	0.0662	0.0165	0.1285	0.0261	0.0432	0.0133						
160.0	0.1077	0.0181	0.0651	0.0159	0.1200	0.0245	0.0407	0.0135						
90.0	0.1008	0.0172	0.0616	0.0139	0.1165	0.0220	0.0381	0.0132						
40.0	0.0864	0.0148	0.0591	0.0119	0.1067	0.0192	0.0355	0.0123						
V _{per}	T _{mean}			T _{50%}			T _{75%}			T _{25%}				
0.0270	4.3704			2.5481			4.9593			1.6519				



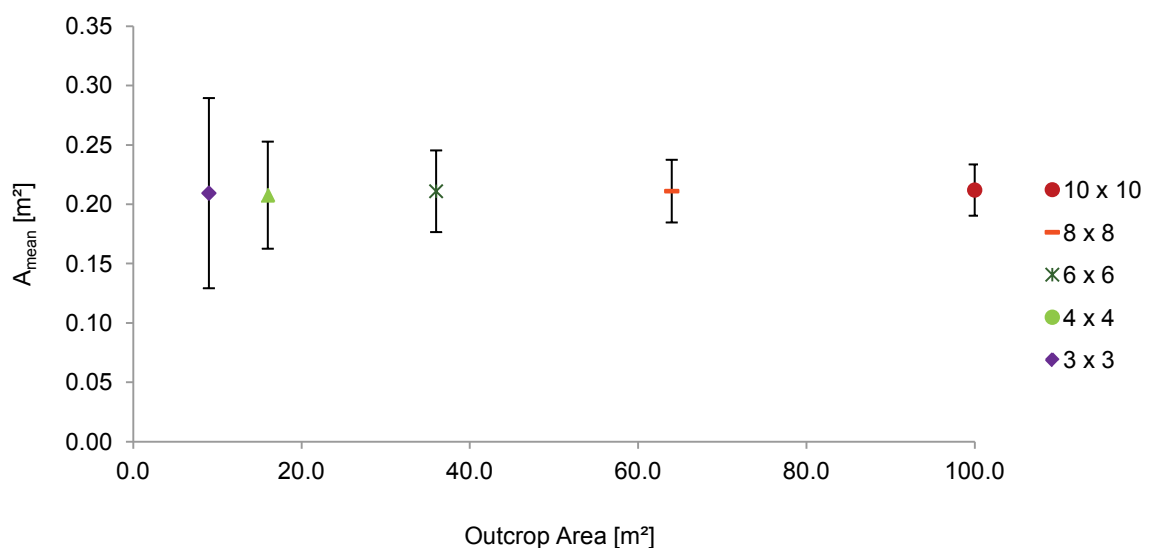
Test 46		z-rotation [°]			45.0		y-rotation [°]			0.0	
dd ₁ [°]	dip ₁ [°]	dd ₂ [°]	dip ₂ [°]	dd ₃ [°]	dip ₃ [°]	sp ₁ [m]	sp ₂ [m]	sp ₃ [m]	p ₁ [-]	p ₂ [-]	p ₃ [-]
45.0	90.0	0.0	0.0	135.0	90.0	0.4	0.4	0.4	0.6	0.6	0.6
A _{out} [m ²]	A _{mean} [m ²]	A _{mean} /A _{out} [-]	σ _{Amean} [m ²]	A _{50%,mean} [m ²]	σ _{A50%,mean} [m ²]	A _{75%,mean} [m ²]	σ _{A75%,mean} [m ²]	A _{25%,mean} [m ²]	σ _{A25%,mean} [m ²]		
100.0	0.4295	0.0043	0.0382	0.2919	0.1019	0.4656	0.0520	0.2263	0.0000		
64.0	0.4285	0.0067	0.0434	0.3077	0.1068	0.4695	0.0554	0.2263	0.0000		
36.0	0.4173	0.0116	0.0591	0.2930	0.1018	0.4803	0.0726	0.2263	0.0000		
16.0	0.3924	0.0245	0.0854	0.2851	0.0944	0.4616	0.1253	0.2308	0.0318		
9.0	0.3731	0.0415	0.0955	0.2862	0.1035	0.4475	0.1522	0.2410	0.0506		
4.0	n/a	n/a	n/a	n/a	n/a	n/a	n/a	n/a	n/a		
V _{model} [m ³]	V _{mean} [m ³]	σ _{Vmean} [m ³]	V _{50%,mean} [m ³]	σ _{V50%,mean} [m ³]	V _{75%,mean} [m ³]	σ _{V75%,mean} [m ³]	V _{25%,mean} [m ³]	σ _{V25%,mean} [m ³]			
1000.0	0.2741	0.0450	0.1594	0.0380	0.3056	0.0647	0.1075	0.0300			
640.0	0.2713	0.0475	0.1562	0.0389	0.3053	0.0668	0.1037	0.0312			
360.0	0.2608	0.0480	0.1549	0.0377	0.2970	0.0614	0.0960	0.0322			
160.0	0.2385	0.0447	0.1472	0.0322	0.2797	0.0665	0.0939	0.0318			
90.0	0.2162	0.0407	0.1405	0.0284	0.2530	0.0583	0.0875	0.0309			
40.0	0.1673	0.0329	0.1286	0.0322	0.2003	0.5690	0.0826	0.0287			
V _{per}	T_{mean}		T_{50%}		T_{75%}		T_{25%}				
0.0640	4.2828		2.4906		4.7750		1.6797				



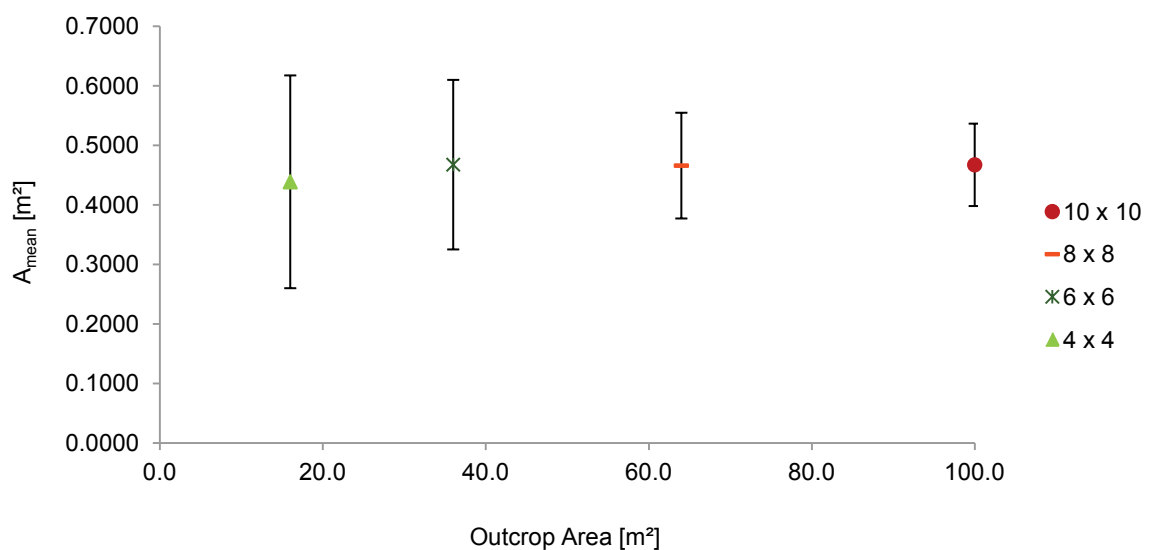
Test 47			z-rotation [°]			45.0			y-rotation [°]			0.0		
dd ₁ [°]	dip ₁ [°]	dd ₂ [°]	dip ₂ [°]	dd ₃ [°]	dip ₃ [°]	sp ₁ [m]	sp ₂ [m]	sp ₃ [m]	p ₁ [-]	p ₂ [-]	p ₃ [-]			
45.0	90.0	0.0	0.0	135.0	90.0	0.6	0.6	0.6	0.6	0.6	0.6			
A _{out} [m ²]	A _{mean} [m ²]	A _{mean} /A _{out} [-]	$\sigma_{A\text{mean}}$ [m ²]	A _{50%,mean} [m ²]	$\sigma_{A50\%,\text{mean}}$ [m ²]	A _{75%,mean} [m ²]	$\sigma_{A75\%,\text{mean}}$ [m ²]	A _{25%,mean} [m ²]	$\sigma_{A25\%,\text{mean}}$ [m ²]					
100.0	0.9645	0.0096	0.1227	0.7051	0.2423	1.0742	0.1506	0.5091	0.0000					
64.0	0.9453	0.0148	0.1414	0.6975	0.2417	1.1048	0.2085	0.5142	0.0509					
36.0	0.9340	0.0259	0.2308	0.6975	0.2574	1.1608	0.3514	0.5422	0.1235					
16.0	0.8987	0.0562	0.2620	0.7255	0.3223	1.0195	0.3529	0.6084	0.1885					
9.0	n/a	n/a	n/a	n/a	n/a	n/a	n/a	n/a	n/a					
4.0	n/a	n/a	n/a	n/a	n/a	n/a	n/a	n/a	n/a					
V _{model} [m ³]	V _{mean} [m ³]	$\sigma_{V\text{mean}}$ [m ³]	V _{50%,mean} [m ³]	$\sigma_{V50\%,\text{mean}}$ [m ³]	V _{75%,mean} [m ³]	$\sigma_{V75\%,\text{mean}}$ [m ³]	V _{25%,mean} [m ³]	$\sigma_{V25\%,\text{mean}}$ [m ³]						
1000.0	0.9428	0.2675	0.5746	0.1822	1.0751	0.3234	0.3445	0.1186						
640.0	0.9287	0.3143	0.5746	0.2042	1.0962	0.4445	0.3370	0.1243						
360.0	0.8877	0.3267	0.5616	0.2437	1.0098	0.3891	0.3305	0.1303						
160.0	0.7696	0.3036	0.5368	0.3361	0.9175	0.4225	0.3370	0.1868						
90.0	0.6214	0.2242	0.4936	0.2319	0.7339	0.3017	0.3294	0.1995						
40.0	n/a	n/a	n/a	n/a	n/a	n/a	n/a	n/a						
V _{per}	T _{mean}			T _{50%}			T _{75%}			T _{25%}				
0.2160	4.3648			2.6602			4.9773			1.5949				



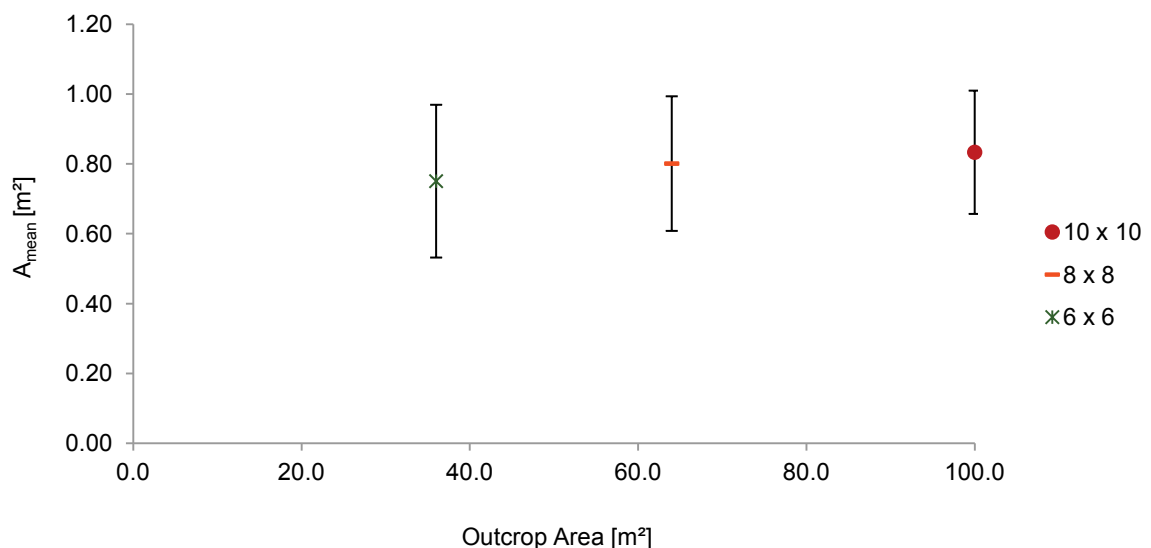
Test 48			z-rotation [°]			45.0			y-rotation [°]			0.0		
dd ₁ [°]	dip ₁ [°]	dd ₂ [°]	dip ₂ [°]	dd ₃ [°]	dip ₃ [°]	sp ₁ [m]	sp ₂ [m]	sp ₃ [m]	p ₁ [-]	p ₂ [-]	p ₃ [-]			
45.0	90.0	0.0	0.0	135.0	90.0	0.2	0.2	0.2	0.4	0.4	0.4			
A _{out} [m ²]	A _{mean} [m ²]	A _{mean} /A _{out} [-]	σ _{Amean} [m ²]	A _{50%,mean} [m ²]	σ _{A50%,mean} [m ²]	A _{75%,mean} [m ²]	σ _{A75%,mean} [m ²]	A _{25%,mean} [m ²]	σ _{A25%,mean} [m ²]					
100.0	0.2120	0.0021	0.0216	0.1273	0.0243	0.2469	0.0336	0.0735	0.0254					
64.0	0.2111	0.0033	0.0264	0.1278	0.0259	0.2498	0.0393	0.0733	0.0255					
36.0	0.2110	0.0059	0.0344	0.1310	0.0283	0.2495	0.0410	0.0765	0.0264					
16.0	0.2077	0.0130	0.0451	0.1338	0.0355	0.2476	0.0629	0.0805	0.0288					
9.0	0.2094	0.0233	0.0801	0.1471	0.0619	0.2510	0.1016	0.0846	0.0388					
4.0	n/a	n/a	n/a	n/a	n/a	n/a	n/a	n/a	n/a					
V _{model} [m ³]	V _{mean} [m ³]	σ _{Vmean} [m ³]	V _{50%,mean} [m ³]	σ _{V50%,mean} [m ³]	V _{75%,mean} [m ³]	σ _{V75%,mean} [m ³]	V _{25%,mean} [m ³]	σ _{V25%,mean} [m ³]						
1000.0	0.1150	0.0189	0.0551	0.0087	0.1239	0.0210	0.0265	0.0048						
640.0	0.1133	0.0201	0.0541	0.0089	0.1218	0.0234	0.0266	0.0049						
360.0	0.1091	0.0206	0.0535	0.0096	0.1189	0.0250	0.0253	0.0049						
160.0	0.1022	0.0221	0.0510	0.0105	0.1116	0.0263	0.0242	0.0068						
90.0	0.0923	0.0205	0.0474	0.0113	0.1033	0.0264	0.0233	0.0074						
40.0	0.0724	0.0194	0.0400	0.0134	0.0842	0.0268	0.0198	0.0073						
V _{per}	T _{mean}		T _{50%}		T _{75%}		T _{25%}							
0.0080	14.3750		6.8875		15.4875		3.3125							



Test 49			z-rotation [°]			45.0			y-rotation [°]			0.0		
dd ₁ [°]	dip ₁ [°]	dd ₂ [°]	dip ₂ [°]	dd ₃ [°]	dip ₃ [°]	sp ₁ [m]	sp ₂ [m]	sp ₃ [m]	p ₁ [-]	p ₂ [-]	p ₃ [-]			
45.0	90.0	0.0	0.0	135.0	90.0	0.3	0.3	0.3	0.4	0.4	0.4			
A _{out} [m ²]	A _{mean} [m ²]	A _{mean} /A _{out} [-]	σ _{Amean} [m ²]	A _{50%,mean} [m ²]	σ _{A50%,mean} [m ²]	A _{75%,mean} [m ²]	σ _{A75%,mean} [m ²]	A _{25%,mean} [m ²]	σ _{A25%,mean} [m ²]					
100.0	0.4672	0.0047	0.0692	0.2972	0.0634	0.5575	0.1002	0.1798	0.0627					
64.0	0.4659	0.0073	0.0888	0.2978	0.6320	0.5584	0.1207	0.1779	0.0619					
36.0	0.4675	0.0130	0.1424	0.3036	0.0990	0.5651	0.1631	0.1884	0.0848					
16.0	0.4387	0.0274	0.1787	0.3144	0.1505	0.5416	0.2317	0.1931	0.0993					
9.0	n/a	n/a	n/a	n/a	n/a	n/a	n/a	n/a	n/a					
4.0	n/a	n/a	n/a	n/a	n/a	n/a	n/a	n/a	n/a					
V _{model} [m ³]	V _{mean} [m ³]	σ _{Vmean} [m ³]	V _{50%,mean} [m ³]	σ _{V50%,mean} [m ³]	V _{75%,mean} [m ³]	σ _{V75%,mean} [m ³]	V _{25%,mean} [m ³]	σ _{V25%,mean} [m ³]						
1000.0	0.3770	0.0858	0.1913	0.0459	0.4176	0.1020	0.0907	0.0225						
640.0	0.3647	0.0841	0.1871	0.0443	0.4046	0.0986	0.0894	0.0236						
360.0	0.3480	0.0859	0.1797	0.0501	0.3883	0.1105	0.0859	0.0239						
160.0	0.3001	0.0705	0.1671	0.0522	0.3457	0.0992	0.0829	0.0323						
90.0	0.2563	0.0747	0.1504	0.0611	0.3035	0.1019	0.0786	0.0332						
40.0	0.1834	0.0841	0.1245	0.0769	0.2297	0.1283	0.0730	0.0519						
V _{per}	T _{mean}		T _{50%}		T _{75%}		T _{25%}							
0.0270	13.9630		7.0852		15.4667		3.3593							



Test 50			z-rotation [°]			45.0			y-rotation [°]			0.0		
dd ₁ [°]	dip ₁ [°]	dd ₂ [°]	dip ₂ [°]	dd ₃ [°]	dip ₃ [°]	sp ₁ [m]	sp ₂ [m]	sp ₃ [m]	p ₁ [-]	p ₂ [-]	p ₃ [-]			
45.0	90.0	0.0	0.0	135.0	90.0	0.4	0.4	0.4	0.4	0.4	0.4			
A _{out} [m ²]	A _{mean} [m ²]	A _{mean} /A _{out} [-]	σ _{Amean} [m ²]	A _{50%,mean} [m ²]	σ _{A50%,mean} [m ²]	A _{75%,mean} [m ²]	σ _{A75%,mean} [m ²]	A _{25%,mean} [m ²]	σ _{A25%,mean} [m ²]					
100.0	0.8334	0.0083	0.1765	0.5397	0.1315	1.0239	0.2449	0.3106	0.1127					
64.0	0.8010	0.0125	0.1927	0.5453	0.1451	0.9900	0.2590	0.3202	0.1121					
36.0	0.7507	0.0209	0.2187	0.5329	0.1891	0.9464	0.3550	0.3247	0.1313					
16.0	n/a	n/a	n/a	n/a	n/a	n/a	n/a	n/a	n/a	n/a	n/a			
9.0	n/a	n/a	n/a	n/a	n/a	n/a	n/a	n/a	n/a	n/a	n/a			
4.0	n/a	n/a	n/a	n/a	n/a	n/a	n/a	n/a	n/a	n/a	n/a			
V _{model} [m ³]	V _{mean} [m ³]	σ _{Vmean} [m ³]	V _{50%,mean} [m ³]	σ _{V50%,mean} [m ³]	V _{75%,mean} [m ³]	σ _{V75%,mean} [m ³]	V _{25%,mean} [m ³]	σ _{V25%,mean} [m ³]						
1000.0	0.8394	0.1998	0.4330	0.1141	0.9350	0.2342	0.2080	0.0614						
640.0	0.7981	0.1955	0.4240	0.1174	0.9099	0.2276	0.2066	0.0660						
360.0	0.7522	0.1953	0.4141	0.1279	0.8667	0.2471	0.2042	0.0678						
160.0	0.6390	0.2341	0.3811	0.1652	0.7350	0.2996	0.1955	0.0781						
90.0	0.4753	0.1683	0.3158	0.1353	0.5917	0.2773	0.1762	0.0956						
40.0	n/a	n/a	n/a	n/a	n/a	n/a	n/a	n/a						
V _{per}	T _{mean}			T _{50%}			T _{75%}			T _{25%}				
0.0640	13.1156			6.7656			14.6094			3.2500				



Test 51			z-rotation [°]			45.0			y-rotation [°]			0.0		
dd ₁ [°]	dip ₁ [°]	dd ₂ [°]	dip ₂ [°]	dd ₃ [°]	dip ₃ [°]	sp ₁ [m]	sp ₂ [m]	sp ₃ [m]	p ₁ [-]	p ₂ [-]	p ₃ [-]			
45.0	90.0	0.0	0.0	135.0	90.0	0.6	0.6	0.6	0.4	0.4	0.4			
A _{out} [m ²]	A _{mean} [m ²]	A _{mean} /A _{out} [-]	σ _{Amean} [m ²]	A _{50%,mean} [m ²]	σ _{A50%,mean} [m ²]	A _{75%,mean} [m ²]	σ _{A75%,mean} [m ²]	A _{25%,mean} [m ²]	σ _{A25%,mean} [m ²]					
100.0	1.7429	0.0174	0.4175	1.2117	0.3899	2.0848	0.6629	0.7255	0.2959					
64.0	1.5938	0.0249	0.4283	1.1888	0.4110	1.9372	0.6587	0.7764	0.3401					
36.0	n/a	n/a	n/a	n/a	n/a	n/a	n/a	n/a	n/a					
16.0	n/a	n/a	n/a	n/a	n/a	n/a	n/a	n/a	n/a					
9.0	n/a	n/a	n/a	n/a	n/a	n/a	n/a	n/a	n/a					
4.0	n/a	n/a	n/a	n/a	n/a	n/a	n/a	n/a	n/a					
V _{model} [m ³]	V _{mean} [m ³]	σ _{Vmean} [m ³]	V _{50%,mean} [m ³]	σ _{V50%,mean} [m ³]	V _{75%,mean} [m ³]	σ _{V75%,mean} [m ³]	V _{25%,mean} [m ³]	σ _{V25%,mean} [m ³]						
1000.0	2.5954	1.1227	1.4418	0.7326	3.0116	1.5849	0.7231	0.3721						
640.0	2.4619	1.1848	1.4310	0.7705	2.9365	1.4740	0.7063	0.3681						
360.0	2.1790	1.2636	1.3241	0.9099	2.5288	1.5334	0.7387	0.5187						
160.0	n/a	n/a	n/a	n/a	n/a	n/a	n/a	n/a						
90.0	n/a	n/a	n/a	n/a	n/a	n/a	n/a	n/a						
40.0	n/a	n/a	n/a	n/a	n/a	n/a	n/a	n/a						
V _{per}	T _{mean}			T _{50%}			T _{75%}			T _{25%}				
0.2160	12.0157			6.6750			13.9426			3.3477				

Transformation factors invalid because limitation ratio has already been exceeded in the major outcrop area!